LiDARPheno: A Low-Cost LiDAR-Based 3D Scanning System For Plant Morphological Trait Characterization

A Thesis Submitted to the College of

Graduate and Postdoctoral Studies

In Partial Fulfillment of the Requirements

For the Degree of Master of Science

In the Department of Electrical and Computer Engineering

University of Saskatchewan

Saskatoon, SK, Canada

By

KARIMALI PANJVANI

Permission to Use

In presenting this thesis in partial fulfillment of the requirements for a Postgraduate degree from the University of Saskatchewan, I agree that the Libraries of this University may make it freely available for inspection. I further agree that permission for copying of this thesis in any manner, in whole or in part, for scholarly purposes may be granted by the professor or professors who supervised my thesis work or, in their absence, by the Head of the Department or the Dean of the College in which my thesis work was done. It is understood that any copying or publication or use of this thesis or parts thereof for financial gain shall not be allowed without my written permission. It is also understood that due recognition shall be given to me and to the University of Saskatchewan in any scholarly use which may be made of any material in my thesis.

Requests for permission to copy or to make other uses of materials in this thesis/dissertation in whole or part should be addressed to:

Head of the Department of Electrical and Computer Engineering
57 Campus Drive
University of Saskatchewan
Saskatoon, Saskatchewan S7N 5A9
Canada

OR

Dean
College of Graduate and Postdoctoral Studies
University of Saskatchewan
116 Thorvaldson Building, 110 Science Place
Saskatoon, Saskatchewan S7N 5C9
Canada

Disclaimer

Reference in this thesis to any specific commercial products, process, or service by trade name, trademark, manufacturer, or otherwise, does not constitute or imply its endorsement, recommendation, or favoring by the University of Saskatchewan. The views and opinions of the author expressed herein do not state or reflect those of the University of Saskatchewan and shall not be used for advertising or product endorsement purposes.

Abstract

The ever-growing world population brings the challenge for food security in the current world. The gene modification tools have opened a new era for fast-paced research on new crop identification and development. However, the bottleneck in the plant phenotyping technology restricts the alignment in Geno-pheno development as phenotyping is the key for the identification of potential crop for improved yield and resistance to the changing environment. Various attempts to making the plant phenotyping a “high-throughput” have been made while utilizing the existing sensors and technology. However, the demand for ‘good’ phenotypic information for linkage to the genome in understanding the gene-environment interactions is still a bottleneck in the plant phenotyping technologies. Moreover, the available technologies and instruments are inaccessible, expensive and sometimes bulky.

This thesis work attempts to address some of the critical problems, such as exploration and development of a low-cost LiDAR-based platform for phenotyping the plants in-lab and in-field. A low-cost LiDAR-based system design, LiDARPheno, is introduced in this thesis work to assess the feasibility of the inexpensive LiDAR sensor in the leaf trait (length, width, and area) extraction. A detailed design of the LiDARPheno, based on low-cost and off-the-shelf components and modules, is presented. Moreover, the design of the firmware to control the hardware setup of the system and the user-level python-based script for data acquisition is proposed. The software part of the system utilizes the publicly available libraries and Application Programming Interfaces (APIs), making it easy to implement the system by a non-technical user.

The LiDAR data analysis methods are presented, and algorithms for processing the data and extracting the leaf traits are developed. The processing includes conversion, cleaning/filtering, segmentation and trait extraction from the LiDAR data. Experiments on indoor plants and canola plants were performed for the development and validation of the methods for estimation of the leaf traits. The results of the LiDARPheno based trait extraction are compared with the SICK LMS400 (a commercial 2D LiDAR) to assess the performance of the developed system.

Experimental results show a fair agreement between the developed system and a commercial LiDAR system. Moreover, the results are compared with the acquired ground truth as well as the commercial LiDAR system. The LiDARPheno can provide access to the inexpensive LiDAR-based scanning and open the opportunities for future exploration.

Acknowledgments

I would like to thank my supervisors Prof. Khan A Wahid and Prof. Anh V Dinh. Their continued guidance, supervision and support has been invaluable for my program and this thesis work at the University of Saskatchewan.

I am grateful for the funding support, which made this work possible, from Canada First Research Excellence Fund (CFREF) managed and distributed by the Global Institute for Food Security (GIFS) at University of Saskatchewan.

I would like to extend my sincere gratitude and appreciation to our collaborator Dr. Scott Noble (Mechanical Engineering, University of Saskatchewan) and his group members, David Pastl and Tyrone Keep, for providing me with the commercial LiDAR and its libraries as well as the setup for in-laboratory experimentation. Moreover, their constant support and valuable feedback in this thesis have been of great help in the assessment of the developed system.

I would like to acknowledge Monica Thurlbeck for providing an opportunity to work at the retail service locations at the University of Saskatchewan, which helped me integrate into Canadian culture. I extend my sincere appreciation to Peyman Pourhaj (Dept.of ECE, University of Saskatchewan) for his guidance in some technical aspects of the system design. I thank all my friends in Canada and India for believing in me and being there all the time.

Finally, I cannot describe in words how grateful I am to my parents (Abdulsultan Panjwani and Nasim Panjwani), my siblings (Amin and Saniya), and my fiancée Kinjal Lakhani for their support in the times when I needed it most. All my accomplishments have only been possible due to their unconditional love, care, belief in me and the sacrifices they made for my studies.

Dedication

Dedicated to the two women in my life, my mother (Nasim Panjvani) and my fiancée (Kinjal Lakhani), for their tremendous love, care, support and desire for my continued studies.

Table of Contents

List of Tables

Page Number

List of Figures

Page Number

List of Abbreviations

µm	micrometer
1D	One-Dimensional
2D	Two-Dimensional
3D	Three-Dimensional
AC	Alternate Current
APE	Absolute Percentage Error
API	Application Programming Interface
CA$	Canadian Dollars
cm	centimeters
CSI	Camera Serial Interface
CSV	Comma Separated Value
CT	X-ray Computed Tomography
DC	Direct Current
DPI	Dots per Inch
DSI	Display Serial Interface
fps	frames per second
g	grams
GB	Gigabytes
HDMI	High-Definition Multimedia Interface
HTPP	High Throughput Phenotyping Platform
Hz	Hertz (samples/second)
I/O	Input/output
I2C	Inter-Integrated Circuit
IoT	Internet of Things
IR	Infrared
KB	Kilobytes
LAN	Local Area Network
LiDAR	Light Detection and Ranging
LiDARPheno	A low-cost LiDAR-based scanning system

LiPo	Lithium Polymer
mA	milliampere
MHz	MegaHertz
mm	millimeters
MRI	Magnetic Resonance Imaging
NDVI	Normalized Difference Vegetation Index
NIR	Near-Infrared
nm	nanometers
OS	Operating System
PNG	Portable Network Graphics
PtCloud	Pont Cloud
PWM	Pulse Width Modulation
R^2	Coefficient of Determination
RGB	Red, Green and Blue - Three channels of an image
RMSE	Root Mean Squared Error
ToF	Time of Flight
UAV	Unmanned Arial Vehicle
USB	Universal Serial Bus
V	Volts
VIS	Visible Spectrum Imaging

Chapter 1
Introduction

1.1 Global Food Security Challenges and Potential Solutions

The ever-growing population on earth calls for the need to increase food production by 1.5 times [1], [2]. The population of the earth is expected to reach 9.73 billion by 2050 [2]. If the current practices for farming were to utilize and the agricultural land expansion continues, there will be the more significant impact on the environment with substantial CO_2 emissions by greenhouses and increased nitrogen use [3]. In addition to increasing the food production, global temperature rise, flooding and diseases make the food security a primary concerns across political leaders [4]. There is a requirement for improvements in farming practices and study to increase the crop yield along with high resistance to disease, pests and changing environmental conditions [4].

The concept of Genotype and Phenotype terms first introduced by Wilhelm Johannsen (1909). In general, the genotype is the "genetic constitution of an organism" and phenotype is the "collection of traits possessed by a cell or organism that results from the interaction of the genotype and the environment" [5]. The food quality and food security improvements can be achieved by creating a new crop variety using gene editing technology [4]. While there have been many technological improvements and advances in gene editing/sequencing technologies [6]–[8], the technologies for the plant phenotyping are still developing and are not fully explored, making it a bottleneck for agriculture research [7]. Hence, efforts to make the plant phenotyping high-throughput is a necessity to balance the advances in genotyping with phenotyping.

Traditionally, plant phenotyping has been achieved by manually collecting the phenotypes from the plants to select the best individual variety [9]. Technological advancement in the plant phenotyping has been a topic of interest among interdisciplinary researchers in recent years. The efforts have been put into using and optimizing the available technologies to adapt to the need of plant phenotyping [7]. Ranging from the use of active sensors to measure the biochemical traits to

use of imaging sensors have been explored to find the relation between the genome and the environment [9]. However, most of the developments have been focused on lab experiments with some for in-field experiments, but are unavailable commercially at large scale. The challenge of feeding the increasing population is critical and hence has gained attention from many governments around the world. Research institutes and networks have been established to tackle the issues faced in the plan phenotyping field. For example, Plant Phenotyping and Imaging Research Center (P2IRC) [10] at University of Saskatchewan, International Plant Phenotyping Network (IPPN) [11] in Germany, Australian Plant Phenomics Facility (APPF) [12], North American Plant Phenotyping Network (NPPN) [13], and many others.

Plant imaging using a 2-dimensional (2D) color – visible light spectrum (VIS) – cameras were used by numerous researcher to develop a plant trait characterization algorithms [14], [15]. However, the VIS cameras are prone to the lighting conditions and might perform differently under changing lighting conditions, leaf shadows, overlapping leaves and differentiating leaves from the soil background [16]. Moreover, various other imaging such as thermal imaging, fluorescence imaging, and hyperspectral imaging can provide information related to canopy temperature, biochemical contents and water stress [16].

Tomographic imaging such as Magnetic Resonance Imaging (MRI) and X-ray Computed Tomography (CT) can provide information from the root and shoot architecture and distribution [17], [18]. However, the tomographic imaging is bulky and still remains low-throughput [16]. In addition, 3-dimensional (3D) imaging can provide the detailed view of the plant structure above-ground. Technologies such as Time of Flight (ToF), Light Detection and Ranging (LiDAR), and Stereo Vision cameras have been used to create a detailed map of the vegetation and canopy structures [16]. In contrast to 2D imaging techniques, 3D imaging is slow, expensive and can be bulky for field phenotype acquisition.

The above ground structure of a plant is an essential characteristic to evaluate the plant's ability to resist environmental changes and diseases. Moreover, the above ground organism of the plant is responsible for the process of the photosynthesis – apparently, one of the most critical trait to estimate the yield – and growing the fruit or seeds. Leaf area, leaf expansion, and the ground cover are some of the traits that can be used to estimate the photosynthetic rate [19].

Commercial technologies available for plant phenotyping are few, inaccessible and expensive. Exploring the effect of gene modification and editing at a large scale requires phenotyping technologies to be robust, inexpensive and accessible.

1.2 Research Objectives

The primary objective of this thesis work is to investigate the application of low-cost 3D imaging sensor and to develop an affordable system. The following research objectives were set to meet the goal of developing a cost-effective system:

- To design and develop a scanning system based on low-cost LiDAR sensor that is low-cost, portable and easy-to-build.
- To develop a low-level software program (firmware) to operate the hardware of the system using existing libraries and Application Programming Interfaces (APIs).
- To develop software and algorithms that can process the acquired data including, conversion from raw data to generate a 3D point clouds, cleaning, filtering and correcting the data, segmentation of individual plant structures (i.e., leaves).
- To estimate the traits of the plant using the processed data. In this thesis, Leaf's area, length, and width are estimated using the point cloud data.
- To compare the performance of the developed system with the commercial LiDAR scanner with respect to the estimation of the traits.

1.3 Thesis Organization

The subsequent chapters are organized as follows:

Chapter 2 reviews the literature relating the topic of plant phenotyping and various phenotyping techniques being utilized. In this chapter, different types of phenotypes and recent advances in the estimation of those phenotypes are presented. Moreover, different imaging techniques that are currently being studied and developed are explained.

Chapter 3 provides the detailed design of the low-cost LiDAR scanning system (LiDARPheno). The detailed design requirements, assessment of various low-cost LiDAR sensors, the design of the firmware and software for portability and remote operability, and power consumption and battery life estimation are discussed in this chapter.

Chapter 4 describes the experimental material and data acquisition process. This chapter also describes the commercial LiDAR used to assess the performance of the LiDARPheno system. Various types of plants used for experiments and the acquisition of the ground truth information using manual methods are discussed.

Chapter 5 discusses the processing of the raw data from the LiDAR and introduces the algorithms developed to process the data. The conversion of raw data to coordinate system and cleaning, filtering and segmentation of the individual leaves is described. It also discusses the methods deployed for estimation of the plant leaf area, length, and width.

Chapter 6 presents the results of the experiments performed and the interpretation of the results. Comparison between results obtained with LiDARPheno and commercial LiDAR scanner is presented to assess the performance of the low-cost design.

Finally, *Chapter 7* concludes the findings of this research work and provides direction for improvements to the designed system as well as analysis software.

Chapter 2
Literature Review

This chapter includes the review of plant phenotyping techniques and transition of the plant phenotyping from traditional to modern technological advances in the field. Section 2.1 provides an overview of the term 'plant phenotyping' and the need for the assessment of the physiological characteristics of the plant. Section 2.2 discusses the available sensor technologies and sensors that are being utilized to develop plant phenotyping platforms. Section 2.3 reviews past and recent works in the LiDAR-based plant phenotyping. Section 2.4 provides insights into the phenotyping platforms, and finally, Section 2.5 establishes the need for low-cost phenotyping solutions.

2.1 The Term 'Plant Phenotyping' and its Need

The term 'genotype' and 'phenotype' were first introduced by plant scientist Wilhelm Johannsen about a century ago [9]. As Johannsen stated in [20]:

> *"All 'types' of organisms, distinguishable by direct inspection or only by finer methods of measuring or description, may be characterized as 'phenotypes'."*

The term 'phenotype' is used by a variety of health and life science fields till now. However, there is no standard definition of the term and is used in different ways to define a particular situation [5]. In general, plant phenotyping is an assessment of all the visible, measurable and observable characteristics of a plant. For example, plant height, leaf shape, water contents, nitrogen contents, photosynthetic rate, leaf expansion, ground cover, leaf area, etc.

The technological improvements and new findings in the gene sequencing have brought opportunities to both improve the yield as well as the quality of the crops [4], [6], [9], [14], [15]. However, there is limited research and development towards improving the ordinary methods of the crops' assessment and hence is the bottleneck for the researchers' and plant breeders' capability to perform at the same rate as of genetic modification scientists [14], [15], [18]. Manual measurement and collection of the phenotypes are labor intensive, prone to errors and tiresome for

the breeders. The replacement of the human efforts put into the phenotype collection is required to minimize the errors and to fasten the process of the selective breeding.

The knowledge of how genomic variation interacts with the environment is crucial in understanding the function of different genes, which consequently improves the overall process of producing the new crop. Hence, the phenotyping process plays a vital role in the development of the new crops with higher yield and better resistance to the changing environment. The new crops can help in the major food security challenge which is to feed an ever-growing population by 2050.

Due to the increasing demand for 'good' phenotypic information, which can be helpful in the discovery of the gene-environment interaction, technological advancements in phenotyping has become a crucial field of research. In recent years, there have been many studies on how existing, and new sensors and methods can be deployed at the advantage of the plant phenotyping [7], [15], [16]. Researchers have demonstrated the helpfulness of Visible Spectrum (VIS) imaging from counting the number of leaves to the estimation of biomass [16]. Scientists have developed technologies and processing algorithms by adapting existing sensors for plant phenotyping. Moreover, medical imaging techniques such as Magnetic Resonance Imaging (MRI) and X-ray Computed Tomography (CT) were also utilized for imaging the plant structures [17], [18]. Overall, the imaging technologies might prove to be really helpful in the understanding of the gene-environment interactions.

2.2 Sensors and Imaging Technologies in Plant Phenotyping

The field of digital plant phenotyping may include imaging, measuring and recording environmental parameters, and modeling. There are various types of devices and sensors available for measuring the environmental parameters, such as soil moisture content, temperature, wind speed and direction, humidity, rainfall, sunlight intensity, etc. Also, imaging and reconstruction the plants model can be performed using different imaging and scanning techniques such as VIS or 2D camera, Infrared (IR) camera, Near Infrared (NIR) camera, Hyperspectral camera, fluorescence camera, CT, MRI, Time of Flight (ToF) camera, LiDAR scanners, and laser scanners. All the technologies have some advantages and some disadvantages. The following subsections discuss the different technologies and techniques being studied and utilized in the plant phenotyping.

2.2.1 Single Dimension (1D) Sensors in Plant Phenotyping

1D sensors are capable of measuring some of the plant and environmental traits such as temperature, plant height, field moisture, measuring wind speed and rainfall detection. The optical sensor such as GreenSeeker (NTech Industries Inc., USA) has been used by researchers to monitor the growth and development of the crop [21]. For example, an estimation of the nitrogen uptake by crops has been executed [22], [23]. An Internet of Things (IoT) based system was proposed to monitor the environmental parameters in the field by [24]. The IoT based system utilizes various sensors including soil moisture, rail fall detection, wind speed and wind direction monitoring. Also, it uploads the data on the cloud server, and the data can be utilized to detect fungal in the crop fields.

2.2.2 Visible Spectrum Imaging

Visible spectrum (VIS) imaging has been of great interest to the plant scientists in recent years. The main reason for the popularity of VIS imaging is the availability of the imaging sensors. Most smartphones have cameras included and can be used to take the pictures in the field. The VIS cameras have imaging sensor that captures the light in the visible spectrum of the light (400-750 nm wavelength). The VIS image raw data is stored as 2D data and provides the information in three channels, red (~600 nm), green (~550 nm), and blue (~450 nm) spectrum of the visible light; hence, commonly referred as RGB (red, green, blue) images.

RGB or visible imaging is extensively used by plant scientists due to its ease of use, cost-effectiveness, and maintenance [16]. Moreover, the vast availability of tools and algorithms for RGB images makes the process of data acquisition and analysis easy for plant scientists without the need to learn and develop application-specific software programs. The VIS imaging is mostly used in the controlled environment. However, in the recent years, there has been a large number of attempts to extract the plant traits with the image data taken from the field. Primarily, the RGB imaging is used to count number of leaves [25], [26], estimate shoot biomass [27], [28], leaf morphology [29] and root architecture [30], [31].

Recently many image-based phenotyping algorithms and platforms have been proposed to ease the task of estimating the physiological traits of the plants. For example, Phenotiki [32] is open software and hardware, affordable image-based phenotyping platform that can perform the tasks of analyzing morphology, growth color and leaf count in rosette-shaped plants. The platform

uses off-the-shelf components and can be ordered from many available suppliers. Another example of the high-throughput phenotyping pipeline is HTPheno [33], a plugin to the image analysis software ImageJ, an open source image analysis software. This plugin can analyze the height, width and projected shoot area of the plant.

For past few years, the field of artificial intelligence and machine learning is mostly appreciated by many fields of the science and life science if not left alone. The visible images have been fed into the deep learning networks to train the model for phenotypic traits and then test the network with the data [34]–[36]. The results of the segmentation on images for trait characterization shows a promising future for the plant phenotyping community.

Overall, the visible imaging is a promising technology for the plant phenotyping tasks. However, the visible light imaging suffers from the effect of lighting conditions, the color of the plants and soil, and controlling the overlapping of leaves. The RGB image analysis methods often fail in the presence of minimal brightness differences in the soil and plant, leaf and plant shadows, overlapping leaves, and the influence of the lighting conditions. Due to these uncontrollable conditions, visible light imaging methodologies suffer from the inaccuracy in segmentation, the most crucial step in the image analysis. However, the visible light imaging can provide much insightful information when the lighting and plant conditions are favorable.

2.2.3 Thermal Imaging

Thermal imaging or infrared thermography technology typically operates in the infrared spectrum of the light and detects the radiation by objects in the infrared region of the light spectrum. The typical thermal imaging sensitive spectrum range is 3-5 μm for short wavelengths [16]. The availability of the highly sensitive thermal imaging cameras and its use in the vegetation detection, the thermal imaging is gaining popularity among plant scientists.

The leaf surface temperature measurements can be helpful in understanding the plant water relationship [16]. Thermal imaging has been used for drought phenotyping and understanding the behavior of the stomatal [37]. In [38], authors have used thermal/infrared imaging to study the response of genetic variation in wheat and barley with respect to water deficiency. This study concluded that thermal imaging could prove to be the perfect estimation for water contents in the canopy and is a reliable source for high-throughput measurements. The thermal imaging has been

widely used for crops and trees [16]. Moreover, thermal imaging has also been combined with the spectral imaging to improve the water content estimation [39].

Despite the many benefits of the thermal imaging, they are still expensive and difficult to operate. Moreover, availability of the thermal image processing algorithms limits the use of thermal imaging. It is notable that thermal imaging requires extensive calibration for use in the estimation of water contents. High level of calibration and the requirement of specific knowledge of the environment when the imaging was performed makes the thermal imaging one of the technologies that require technical inclination. Fusion of the information from the thermal imaging and RGB imaging can provide means to separate the soil water contents from that of the plant [16].

2.2.4 Imaging Spectroscopy

The plants tend to absorb most of the light in the visible spectrum (400-700 nm) with the highest reflectance in the green region (~550 nm) of the visible light spectrum. However, the near-infrared (NIR) wavelengths ranging from 700 to 1200 nm have better reflectance from the plant leaves than that of visible light. Moreover, with the increasing wavelengths near 2500 nm, the absorption is higher, resulting in the low reflectance due to water contents in the plant leaves [40]. Plant's spectral reflectance information has been used to develop various vegetation indices by using the difference or ratio of the reflectance data at two or more wavelengths. For example, normalized difference vegetation index (NDVI), which is a good indicator of detection of the vegetation in remote sensing using an aerial vehicle or using handheld detectors. Several indices have been developed using the imaging spectroscopy [16].

The spectral reflectance indices are used to measure the water status, chlorophyll contents, and green biomass in phenotyping the plants. For instance, Schlemmer *et al.* [41] have acquired the reflectance information in the range 350-2500 nm and used the ratios of reflectance at 630 and 680 nm wavelengths and ratio of 600/680 nm to introduce two new indices, namely orange/red chlorophyll absorption ratio (OCAR) and yellow/red chlorophyll absorption ratio (YCAR). The two ratios defined by the authors have shown a strong relation (r^2 = 0.83) to the chlorophyll contents of the plant. Hyperspectral and multispectral cameras are extensively used to estimate the water status in the plants.

The imaging spectroscopy can provide relatively accurate information for plant phenotyping. However, the data produced using the spectroscopy is significant in size. Moreover,

the devices and instruments used for spectroscopy are expensive and limits the acceptance by the breeding programs and plant scientists [16]. Overall, the spectral imaging is a promising technology for the prediction of canopy water contents, green biomass and various indices that can be used to predict vegetation, biomass or photosynthetic rates.

2.2.5 3-Dimensional (3D) Imaging

A 3D imaging can supplement the limitations of the 2D images by adding the 3rd dimension to the scene, i.e., depth. The 3D imaging sensors have been used extensively in the computer gaming industry. The 3D imaging sensor technologies available are 2D photogrammetry [42], light detection and ranging (LiDAR), stereo vision, time-of-flight (ToF) cameras and recently consumer-grade gaming interface Microsoft Kinect [16]. These sensor technologies have been used in the plant phenotyping tasks in recent years.

A 3D imaging can help in the estimation of the traits and architectures of the plants. An approach to constructing a 3D point cloud by using 2D images taken from different angles has been used by researchers. In [43], authors have constructed a 3D model of the plants using 2D images taken from multiple view-angles. The stereo vision cameras are also used in the field of plant phenotyping to construct a 3D model of the plants. For instance, Frasson *et al.* [44] have generated a 3D digital model of the Maize using stereo vision camera. While 3D model reconstruction from the multi-perspective 2D images is possible, the process highly depends on the quality of the 2D images, which suffers from the illumination conditions as explained in the section 2.2.2. In addition, extensive calibration for the 2D cameras is required to estimate the 3D models.

The Time-of-flight (ToF) based cameras can acquire information at the relatively high frame rate (up to 50fps) and are suitable for field data acquisition. However, sunlight affects the performance of the ToF cameras [45]. In [30], authors have constructed a 3D approximation of the plant by combining ToF and RGB data. A successful attempt was made to fuse the stereo image with ToF image by Song *et al.* [46]. Going a step forward, recently, Li and Tang [47] proposed the use of ToF camera to estimate the leaf length, width, area and collar height of the corn plant. A 3D model has been constructed with 23 different views. While ToF cameras are ideal for high-throughput 3D data acquisition, they are influenced by the sunlight, and low resolution limits the adaptation in phenotyping applications.

The LiDAR is best known for the 3D model reconstruction of the canopy due to its accuracy, robustness, and resolution. LiDAR uses a laser light emission and calculates the distance to reflecting object by recording the time of travel from and back to LiDAR. In plant phenotyping, several attempts toward the reconstruction of the canopy have been made. 3D reconstruction of the 3D model allows for the analysis of the complex traits, such as shape, area, and alignment of the leaves. LiDAR-based 3D imaging technology is explained in section 2.3.

2.3 LiDAR-based 3D imaging in Plant Phenotyping

The light detection and ranging (LiDAR), as its name suggests, uses light to measure the distance to the object by calculating the time of travel by the pulse of light. The LiDAR is also used by law enforcement agents to measure the velocity of the car on the roads. LiDAR can estimate the distance very accurately, and two successive measurements can be used to measure the velocity accurately. The fundamental operating principle of the LiDAR is shown in Figure 2-1.

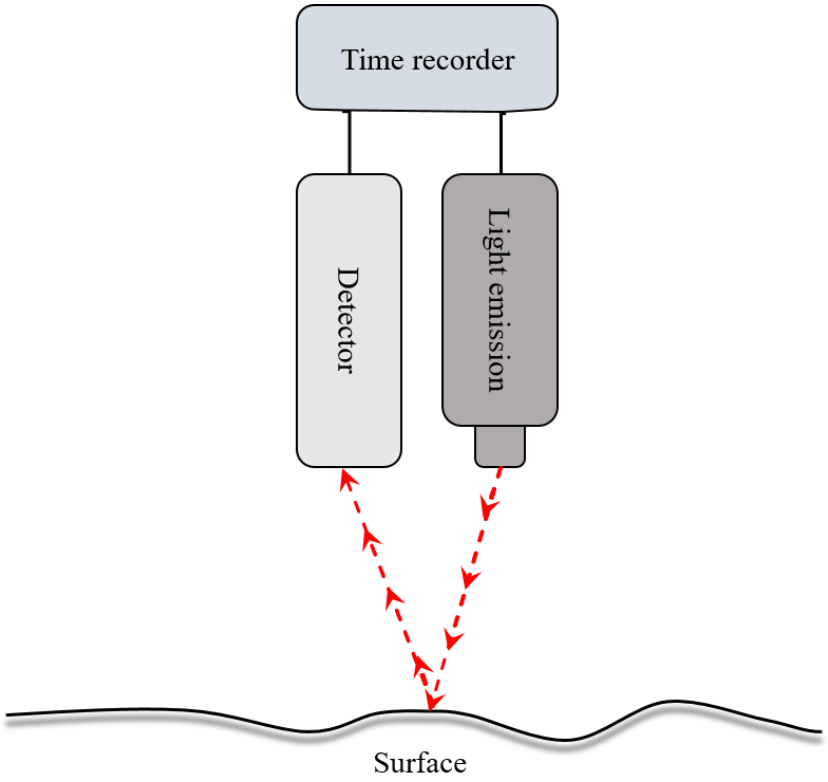

Figure 2-1: The fundamental operating principle of the LiDAR

LiDAR uses the laser emitter to emit light, and a photo/laser detector captures the light reflected by the surface. By considering that the speed of light is constant, the travel time of the light pulse is recorded by a time recorder or timer. The time used for calculation of the distance to the reflecting object is from the emission of the pulse of the light until the reflected pulse is received by the detector. The time is then divided by two and multiplied with the constant speed of light, consequently revealing the distance to reflecting object.

LiDAR became known to general public in the early 1970s when the astronauts used it to map the surface on the moon. Since then, LiDAR has been used in remote sensing applications and generally involves data acquisition with an airplane or helicopter. The LiDAR data is then combined with other information collected during the same flight, such as GPS information to map the acquired data to geolocation [48].

In recent years, LiDAR's accuracy and ability to precisely map the structures drew attention across various fields, especially plant phenotyping community. It is believed that LiDAR can provide an opportunity to look at the plant with more accurate 3D modeling, consequently revealing the critical parameters of the plants such as the shape and structure of the leaves. Moreover, LiDAR uses its own light source, eliminating the illumination limitations of 2D imaging. A 2D LiDAR collects two-dimensional information, generally using a rotating mirror, at a very high speed. The 3D model of the canopy can be constructed while moving the 2D LiDAR along the direction of the scanning plane. While 3D model constructed using LiDAR scans is not as dense as those constructed using 2D images, the scans can provide useful information for extracting the plant morphological traits [49]–[51].

Derry *et al.* [52] have included the 2D LiDAR (LMS400, Sick AG, Waldkirch, Germany) in their field-based phenotyping platform, Phenomobile, for estimating the canopy height in the different height genotypes of the wheat. The higher correlation between the manual measurement of the canopy height and one estimated using LiDAR data was achieved. The study concluded that LiDAR is potentially the best alternative to the image based methods. In a similar study, Tilly *et al.*[53], used the terrestrial laser scanner Riegle VZ-1000 to measure the height of the rice crop. The study concludes that there is a higher correlation between manual measurements and the ones estimated using LiDAR data. In [49], authors have validated the feasibility of 2D terrestrial LiDAR to reconstruct the 3D model of the trees. The authors conclude that 3D modeling of the canopy can reveal new opportunities for assessing the essential structural and geometric traits of the plants. In

[51], the authors use the 2D LiDAR to construct the 3D point cloud by moving the LiDAR along the scan direction. The study concluded with an overall error of 6.84% in height estimation of the cotton plants.

The fusion of the LiDAR imaging with various other imaging techniques can provide a better understanding of the plant. Omasa *et al.*[54], in their study of 3D LiDAR imaging for understanding plant responses, states that there is a potential for better understanding of the plant response to stress condition by combining the approaches of 2D imaging with LiDAR imaging. The structural analysis combined with hyper- or multispectral cameras can provide an opportunity to understand the plant's structure as well as the response to different environmental conditions. In [55], authors have obtained the high correlation between LiDAR estimated leaf area and dry weight of the leaf in the wheat. Moreover, authors prove the usefulness of the LiDAR imaging in the phenotyping of the wheat using portable high-resolution LiDAR.

Recently, in the past two years, the feasibility of LiDAR to construct the 3D model and analyze the 3D to understand structural variety in the plants has drawn attention from many researchers dealing in the plant phenotyping field. In one of the recent studies, Berni *et al.* [56] analyzed the 3D data captured with a 2D LiDAR (LMS400, Sick Inc., Germany). In the study authors integrated the LiDAR on the high-throughput phenotyping platform, Phenomobile, and experiments were performed on fields of the wheat. Phenotypic characteristics included plant height, ground cover, and above-ground biomass. Authors also compared the results obtained using the LiDAR data with the ones obtained using RGB camera and NDVI. The study of wheat ground cover, above-ground biomass and plant height using LiDAR concluded the utility of LiDAR in the field phenotyping application with the non-destructive approach. In another study [57], authors have monitored the leaf movement activity in the indoor plant, linden regel, using terrestrial LiDAR. Moreover, in the study, authors have collected data in the varying lighting conditions including total absence of the light. The study on indoor plant indicates the utility of the terrestrial LiDAR in accurately tacking of the leaf movement parameterization. Following the established methods in [51], the authors performed the in-field experiments for growth analysis for cotton plants in [58]. The analysis of the plant morphological traits such as height, projected canopy area, and plant volume was extracted from the LiDAR data. Moreover, the plot level 3D model was created indicating the high accuracy and feasibility of the LiDAR device in the high-throughput plant phenotyping.

2.4 High-Throughput Plant Phenotyping Platforms

The high-throughput phenotyping platforms (HTPPs) are the platforms that include either a single or multiple sensing technologies with the aim of collecting a vast amount of data from the field that can reveal some beneficial phenotypic information. The platform generally incorporates the high-performance computer or data logger collecting a vast amount of data and storing the data either in local storage or in the remote file servers. The primary objective of utilizing those platform is to overcome the limitation of the manual phenotypic information collection and to generate, organize and store data so that they are accessible and easily accessible for further analysis.

Numerous efforts have been put on developing HTTPs. For example, the Phenomobile Lite® [59] developed by APPF, is a lightweight field-based phenotyping platform that includes an RGB camera, hyperspectral camera, thermal camera and LiDAR sensors. Another example of the field-based platform is HeliPod [59] by the APPF which is equipped with high-resolution RGB and thermal camera. The LemnaTec Corporation provides a fully automated platform for field-based phenotyping as well as solutions for laboratory experiments [60]. PhenoFab® [61] is a greenhouse platform by KeyGene for collecting the digital phenotypes. PhenoSpex PlantEye [62] is the high-resolution 3D LiDAR-based platform for field phenotyping by PhenoSpex. After its introduction to the commercial market, PlantEye has been used to model the plants. In the recent review paper, Rebetzke *et al.* [63] review the high-throughput phenotyping and its effect on enhancing the crop genetic resources.

2.5 Need for Low-Cost Plant Phenotyping Sensors/Platforms

Despite the availability of technologies and platforms for plant phenotyping, there is a need for the low-cost sensors and platforms. The available technologies and platforms are still in the research phase and are not ready for commercial use, and those available commercially are highly expensive, inaccessible and bulky. The devices and technologies are computationally expensive due to sophisticated algorithms for phenotype extraction. For example, 3D photogrammetry using 2D images requires many high-resolution images taken from different angles and high level of calibration is required. Furthermore, the algorithms for processing the images to generate a 3D model are computationally expensive, requiring the use of high-end processors and huge memory.

On the other hand, LiDAR can provide the phenotypic information accurately with reasonably easy processing steps. However, LiDAR sensors are expensive and bulky. The fact that available technologies are expensive, monetarily and/or computationally, limits the exploration by the research community at large. Hence, there is a need to develop the cost-effective solutions for the phenotyping.

This thesis work attempts to investigate the feasibility of low-cost LiDAR sensor and to build a system with inexpensive modules for 3D scanning of plants. The device/system will have ability to use existing libraries and APIs as well as provide a depth information to construct a point cloud for in-lab experiments. The target application of the system is in-lab or in the greenhouse environment and possibly in the challenging field environment for relatively simple trait extraction. The principle targets are rosette-shaped plants such as Canola in their early development phase with application in plant growth monitoring. The scope of this work is limited to controlled environment as the primary objective is to assess the feasibility and utility of the low-cost system for some of the phenotyping tasks.

Chapter 3
Design and Development of LiDARPheno system

This chapter discusses the design and development of 3D scanning system (LiDARPheno) using low-cost **Li**ght **D**etection **A**nd **R**anging (LiDAR) sensor as follows: Section 3.1 sets the requirement of the low-cost LiDAR-based scanning system. Section 3.2 discusses the design of a hardware setup and components used. Section 3.3 explains the firmware design for Arduino Uno and different scanning schemes. Section 3.4 provides the insights into a software program for Raspberry Pi. Section 3.5 discusses power requirement and battery life calculations. Finally, Section 3.6 provides summary of the cost for individual parts of the system.

3.1 Design Requirements

For the design of the low-cost LiDAR scanning system, the following requirements have been set:

- The developed system should be low-cost. It is required and was one of the goals of this research project that a system be inexpensive.
- The LiDARPheno system should be able to capture a depth profile of the scene that is being scanned and provide control over the horizontal and vertical Field-of-View as well as the angular resolution.
- The system should be portable and capable of utilizing the wireless communication with a goal of the remote operation.
- The LiDARPheno should be able to communicate and find the pre-configured Wi-Fi access point at the operating system boot-up.
- The system should have the available hardware resources that can be utilized to interface other sensors and devices, if necessary.
- The developed system should be able to upload data to the user-specified file server, ultimately making it remotely accessible.

3.2 Design of the Hardware for the System

Figure 3-1 shows an underlying architecture of the system. Hardware design includes a selection of a LiDAR sensor, mechanical structure, controlling devices and power module. Various LiDAR sensors and approach to control have been explored to meet the requirement of the hardware design. The following sub-sections discuss the selection of sensor, devices, and approaches utilized in developing LiDARPheno hardware.

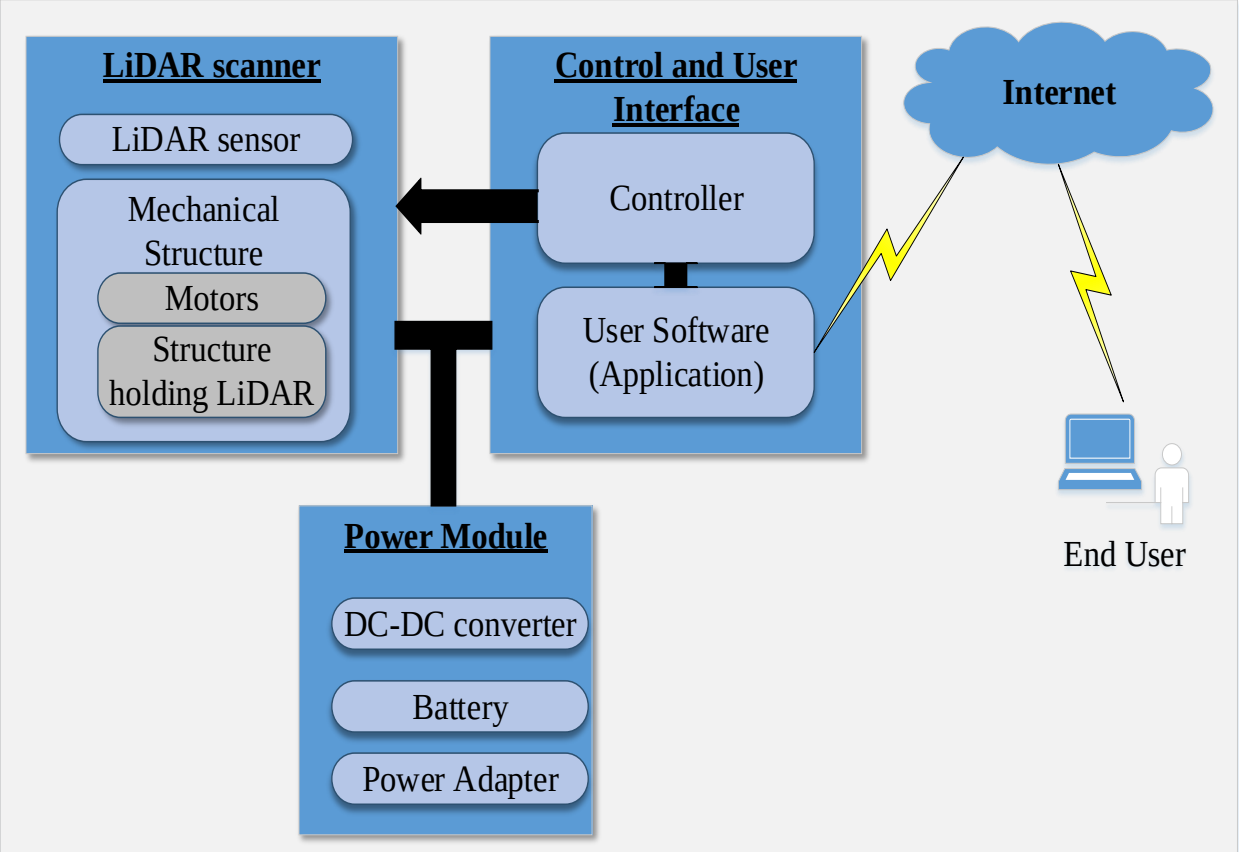

Figure 3-1: Basic architecture of the system

3.2.1 LiDAR Sensor

LiDAR is a distance measurement technique that uses light in the form of pulsed laser to measure range or distance to the reflecting surface. While selecting a LiDAR device, it is necessary to take some of the essential characteristics under consideration as described below:

- *Resolution:* the angular aperture of the transmitted dot or laser point, the characteristic that defines the smallest detectable area.
- *Scan Rate:* It is a property that defines the speed of sample acquisition. For example, 50Hz scan rate means 50 samples/second
- *Laser Wavelength:* Wavelength of the incident laser light is one of the required property to think about as it directly relates to the plant's ability to reflect the light.
- *Range:* Generally measured in meters, range describes the operable range of the sensor. The range is a distance unto which the sensor can measure the distance to the reflecting object.

In this selection process, various low-cost (less than CA $1000) LiDAR sensors have been explored and assessed against different characteristics as mentioned above. Table 3-1 shows the comparison between different low-cost LiDAR sensors.

Table 3-1: Comparison of the low-cost LiDAR sensors

LiDAR Sensor/Device	Range	Field of View	Laser Wavelength	Scan Rate (Point/ second)	Price (as of June 2018)
LiDAR-Lite v3 Laser Rangefinder	0 – 40 meters	N/A	905 nm	500	CA $159.99
RPLIDAR A2 360° Laser Scanner	0.15 – 12 meters	0 - 360°	785 nm	2000-8000	CA $390.00
Sweep V1 360° Laser Scanner	40 meters	0 - 360°	905 nm	1000	CA $450.64
Benewake TF01 LIDAR Rangefinder (10 m)	0. 3 – 10 meters	N/A	850 nm	500	CA $220.19

After assessing various LiDAR sensors, it was decided to select LiDAR-Lite v3 (Garmin Inc., USA) as a potential candidate for the low-cost system. One of the principal reasons for

choosing the LiDAR-Lite v3 was the price, as it would allow building extremely low-cost system. Other reasons for decision included laser light wavelength of 905 nm (plant leaves reflect most of the light at this wavelength), possibility to design customized scanning mechanism, and feasibility of using it in an Unmanned Arial Vehicle (UAV) as it has a range up to 40 meters.

3.2.1.1 LiDAR-Lite v3

LiDAR-Lite v3 works on the principle of Time of Flight (ToF). ToF uses the time between the transmission and reception of pulsed laser light at 905 nm to calculate the distance to the reflecting surface. LiDAR-Lite v3 can measure distances with an accuracy of ±2.5 cm. This low-cost LiDAR sensor is a low power device with operating voltage of 5V DC and current consumption of about 130 mA while in continuous operation (105 mA when idle) [64]. Figure 3-2 presents a picture showing LiDAR-Lite v3.

Figure 3-2: LiDAR-Lite v3 by Garmin Inc. (picture source: https://www.sparkfun.com)

LiDAR-Lite v3 can operate in -20 to 60°C temperature range and weighs 22 grams. It has a maximum repetition rate of 500 samples/second or 500Hz. The sensor provides two interfacing options: 1) I2C (Inter-Integrated Circuit) and 2) PWM (Pulse Width Modulation). Either can be used to interface the sensor with a controller. However, I2C provides a better option and configurable device address, which helps to interface multiple devices to one I2C bus of the controller.

Moreover, the manufacturer provides an open source library for interfacing the sensor with Arduino (an open source, open hardware platform) controllers. Full technical details and specifications of the LiDAR-Lite v3 are available in [64].

3.2.2 Rotating Mechanism for the Scanner

As LiDAR-Lite v3 is not a scanner, the mechanism needs to be designed to use this sensor for building a 3D scanner. Two small hobby servo motors have been utilized to build a scanning setup, which fulfills the requirement of portability. Figure 3-3 shows the mechanical setup of the scanner using two multipurpose, two long "C" brackets and two servo motors.

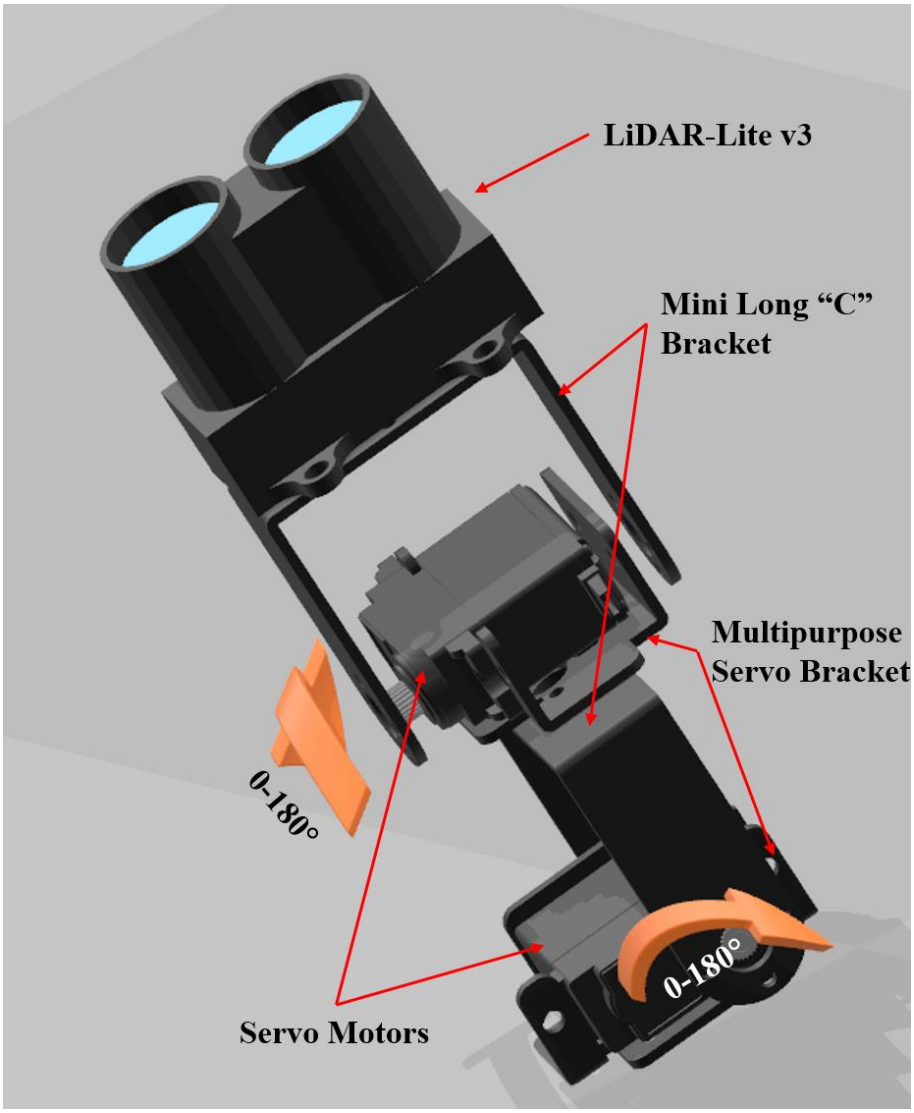

Figure 3-3: Mechanical design of the scanning setup[1]

[1] (Sources for individual 3D models of the components: www.grabcad.com, www.sketchup.com, and www.lynxmotion.com)

The scanning setup consists of two mini long “C” brackets (ASB-303, lynxmotion – RobotShop Inc., Canada), two mini multi-purpose (ASB-301, lynxmotion – RobotShop Inc., Canada) and two micro servo motors (HS-85BB, Hitec, South Korea). First servo motor at the base level controls the vertical motion of the LiDAR, and another motor in the middle of the setup controls the horizontal motion of the system. Servo motor HS-85BB operates at 4.8V-6.0V DC with current consumption around 280 mA (8 mA while idle) [65]. Servo motor, brackets and LiDAR sensor were assembled using manufacturer supplied screws, bolts, and nuts.

3.2.3 Microcontroller and its Specifications

An open-source electronics hardware platform, Arduino [66], has was chosen to control the assembly and connect the LiDAR device. Specifically, Arduino Uno Rev3 (Arduino SRL, Italy) was utilized due to its operating speed, availability of 14 digital input/output pins (including 6 PWM outputs) and six analog inputs, and provision of various communication protocols consisting of UART, I2C, and PWM. Apart from the proper technical specification, Arduino Uno is an inexpensive platform for prototype development and has a vast number of tutorials available on their website. Availability of some tutorials makes it an easy-to-use platform. Moreover, the manufacturer of the LiDAR sensor provides an open-source library [67] to interface LiDAR-Lite v3 with Arduino, which matches with one of the goals for this project – minimum code development.

Figure 3-4: A picture of Arduino Uno Rev3 (picture source: https://www.arduino.cc)

Figure 3-4 shows a picture of an Arduino Uno rev3 and Table 3-2 provides detailed technical specifications of the Arduino Uno rev3 (taken from https://store.arduino.cc/arduino-uno-rev3)

Table 3-2: Specification of the Arduino Uno Rev3

Detailed Specification of Arduino Uno Rev3 platform	
Microcontroller	: ATmega328P
Operating Voltage	: 5V
Input Voltage (recommended)	: 7-12V
Input Voltage (limit)	: 6-20V
Digital I/O Pins	: 14 (includes 6 PWM output pins)
PWM Digital I/O Pins	: 6
Analog Input Pins	: 6
DC Current per I/O Pin	: 20 mA
DC Current for 3.3V Pin	: 50 mA
Flash Memory	: 32 KB
SRAM	: 2 KB
EEPROM	: 1 KB
Clock Speed	: 16 MHz
LED_BUILTIN	: 13
Length	: 68.6 mm
Width	: 53.4 mm
Weight	: 25 g

At first, Arduino Uno was used for testing and evaluating LiDAR-Lite v3 and to understand the operation of the LiDAR sensor. Arduino Uno was connected to LiDAR using I2C communication interface. After some initial knowledge acquisition, the controller platform was interfaced with two servo motors to build and operate the scanner. Initial testing and learning were performed while Arduino was connected to the computer (Lenovo ThinkCentre, Intel Core i7 @

3.4 GHz with 64-bit windows operating system, 16 GB RAM) using USB serial communication interface. To meet the requirement of portability and remote connectivity, an open-source mini-computer, Raspberry Pi 3 Model B, was introduced in the design for user software requirement. The following sub-section discusses raspberry pi and its specifications.

3.2.4 Raspberry Pi, a Camera Module, and their Specifications

Raspberry Pi is a credit-card-sized portable and affordable computer and has been accepted by many electronics hobbyist and developers. It has almost all the functionality of a regular computer. In this study, raspberry pi provides connectivity to the internet and remote operability. It operates on the light-weight distribution of Linux operating system (raspbian OS). Figure 3-5 shows a photograph of raspberry pi 3 model B.

In addition to being an inexpensive computer system, raspberry pi provides 40 general-purpose I/O pins, 4 USB 2.0 ports, HDMI video output, wireless LAN, Bluetooth, Ethernet connectivity, CSI camera interface, and DSI interface for connecting a touchscreen display. Detailed specification for the raspberry pi 3 model B is available at [68].

Figure 3-5: A picture showing raspberry pi 3 model B (source: www.raspberrypi.org)

The primary reason for using the raspberry pi and Arduino together, even though raspberry pi is capable of doing the job, is to utilize the already developed and publicly available libraries. For instance, manufacturers of the LiDAR device provides the library to interface it with Arduino and APIs can be easily installed on the raspberry pi to get the functionality of uploading data. Moreover, the raspberry pi can be utilized as the single point processing unit, which can process

data as it is acquired and finally upload the results to the desired file server. On top of that, if necessary an independent scanning system with Arduino alone could be attached to central raspberry pi to make a network of the systems. This arrangement provides low code development time, plug-and-play operation, simple processing algorithms and cost-effective arrangement.

3.2.4.1 A Raspberry Pi Camera Module

Figure 3-6: An image showing pi camera module rev1.3 (source: www.amazon.ca)

A raspberry pi camera module rev1.3 was included in the design to take a still 2D image of the scene. A 2D image provides the color details of the scene and can be used to combine with 3D information if required. The camera module has FoV of about 54° and can acquire 2592x1944 pixels still images. It uses OmniVision OV5647 camera sensor. Detailed technical specifications are available at [69]. Figure 3-6 displays an image of the camera module.

3.2.5 Power Module

Power module consists of the DC-to-DC voltage converter, a battery, and a power adapter. These three components/devices are necessary to provide portability of the LiDARPheno. With the addition of the battery to this design, the system could be placed in the anywhere to acquire data without the hassle of the wires.

For this project, a step-down DC-DC power converter by DFRobot is used [70]. This DC-DC converter has 5V or variable voltage selection switch. The input voltage can range from 3.6V to 25V and can provide up to 5A power at the 5V output. Moreover, it provides three different

interfaces for output and total of 5 output ports, making it the best device to include in the design as variability of the components in the system. Figure 3-7 (A) shows the DC-DC converter.

A battery is an essential component of any mobile/portable system. Lithium-Polymer (Li-Po) battery was included in the LiDARPheno design. A 7.4V 2000mAh LiPo battery by Robotshop Inc. is a better option as it provides three different connectors and has a capacity of 2Ah [71]. Figure 3-7 (B) represents a picture of this LiPo battery.

A manufacturer recommended power adapter, which can charge the LiPo battery and provide power supply to the system, was used with this design and is shown in Figure 3-7 (C).

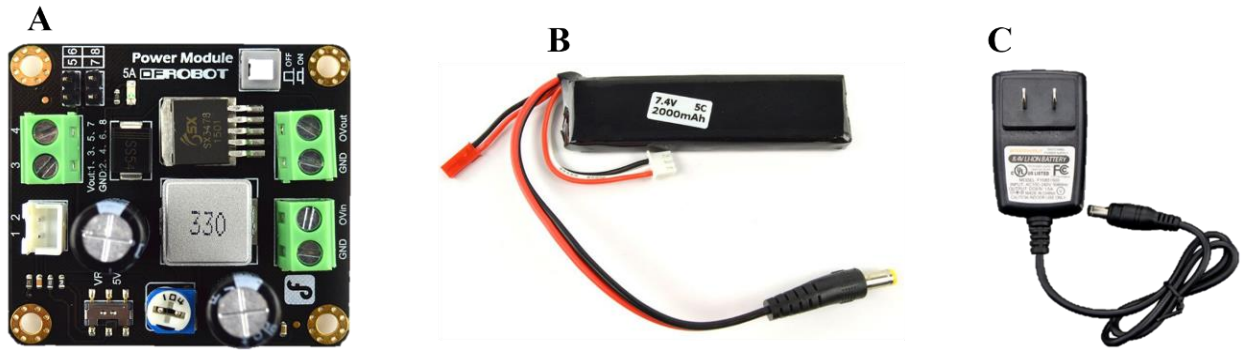

Figure 3-7: **(A)** DC-DC power converter, **(B)** LiPo 7.4V battery, and **(C)** power adapter.

In addition to the components mentioned above in the power module of the system, a power MOSFET was included to restrict the power to servo motors while they are not operational. Design includes power MOSFET IRL 620 by Vishay Siliconix, USA, which is a fast switching and cost-effective device. A control output pin on raspberry pi operates the MOSFET, which provides the power saving by reducing the current requirement while the system is not operational.

3.2.6 Full Design of the Hardware and Wiring Diagram

All the components and rotating mechanism were integrated to make a final full design of the LiDARPheno system. These components and setup were then placed into a housing box to make the system portable and easy to carry. Figure 3-8 shows the prototype of the system.

The prototype of the LiDARPheno system consists of all the modules, devices and setup described earlier in this chapter. A red colored housing box holds all the wires, raspberry pi, power module and Arduino Uno inside of it. Moreover, the box was carved so that the raspberry pi's USB

and Ethernet ports are accessible. A camera module is aligned and fixed so that the camera can capture the still 2D color images of the scene being scanned. The power supply wires are left open so that either power adapter (for in-lab use) or a LiPo battery (for remote use) can be connected to power the system.

The system on the back side of it has two holes on each side, which are used to hold the system. The prototype system can be attached to an aluminum bar to hold it on the tripod or attach it wherever required.

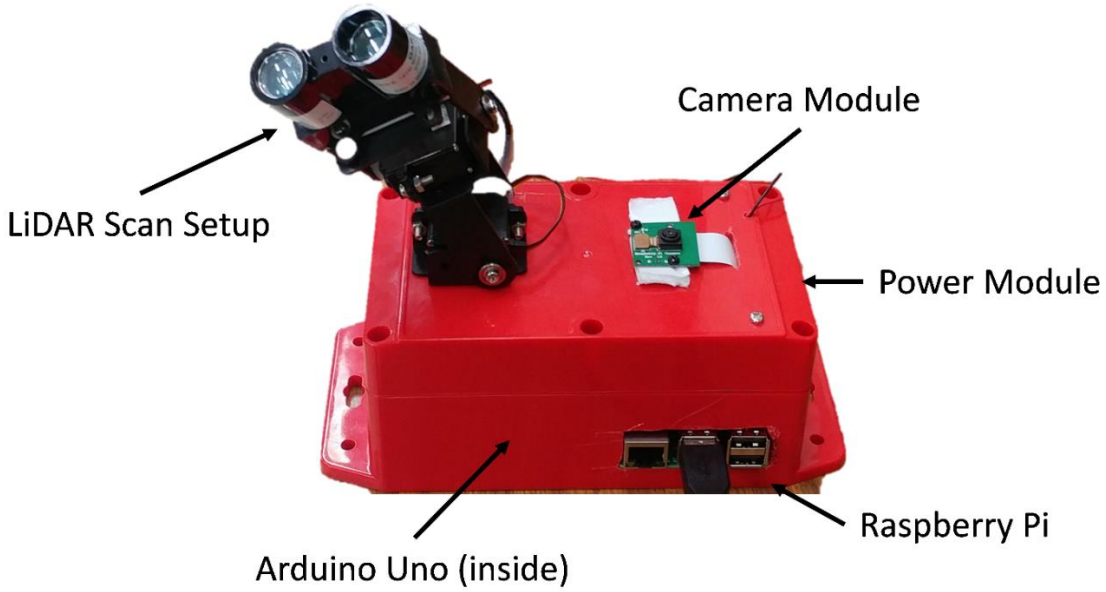

Figure 3-8: A prototype of the LiDARPheno

The wiring diagram of the LiDARPheno system prototype is presented in Figure 3-9. The LiDAR sensor (LiDAR-Lite v3) has six pins, out of which two are for power supply (red and black), green and blue colored wires are for communication using I2C communication interface, yellow is for mode control or PWM communication interface and orange is for power enable pin. The power supply pins were connected through the power module, and I2C (SCL and SDA) pins were connected to Arduino Uno's I2C interface pins (SCL and SDA). Mode control and power enable pins (PWM interface) are left non-connected.

Servo motors, in general, have three pins (two for power supply and one for control using PWM). Power supply pins of both the servo motors (horizontal scan control and vertical scan

control) are connected to the power MOSFET to restrict the power supply while the system is not operational. This arrangement reduces power usage while in a remote location. On the other hand, control pins of both the servo motors are connected to Arduino's digital PWM pins (pin #9 and #11) to control the movement of the servo motors.

Arduino Uno and Raspberry Pi receive power supply from the power module (constant 5V DC). Both the controllers/devices communicate using Universal Serial Bus (USB) interface. Moreover, the MOSFET that controls the power to servo motors is connected to a raspberry pi's general purpose I/O (GPIO) pin and controls when to provide power to servo motors.

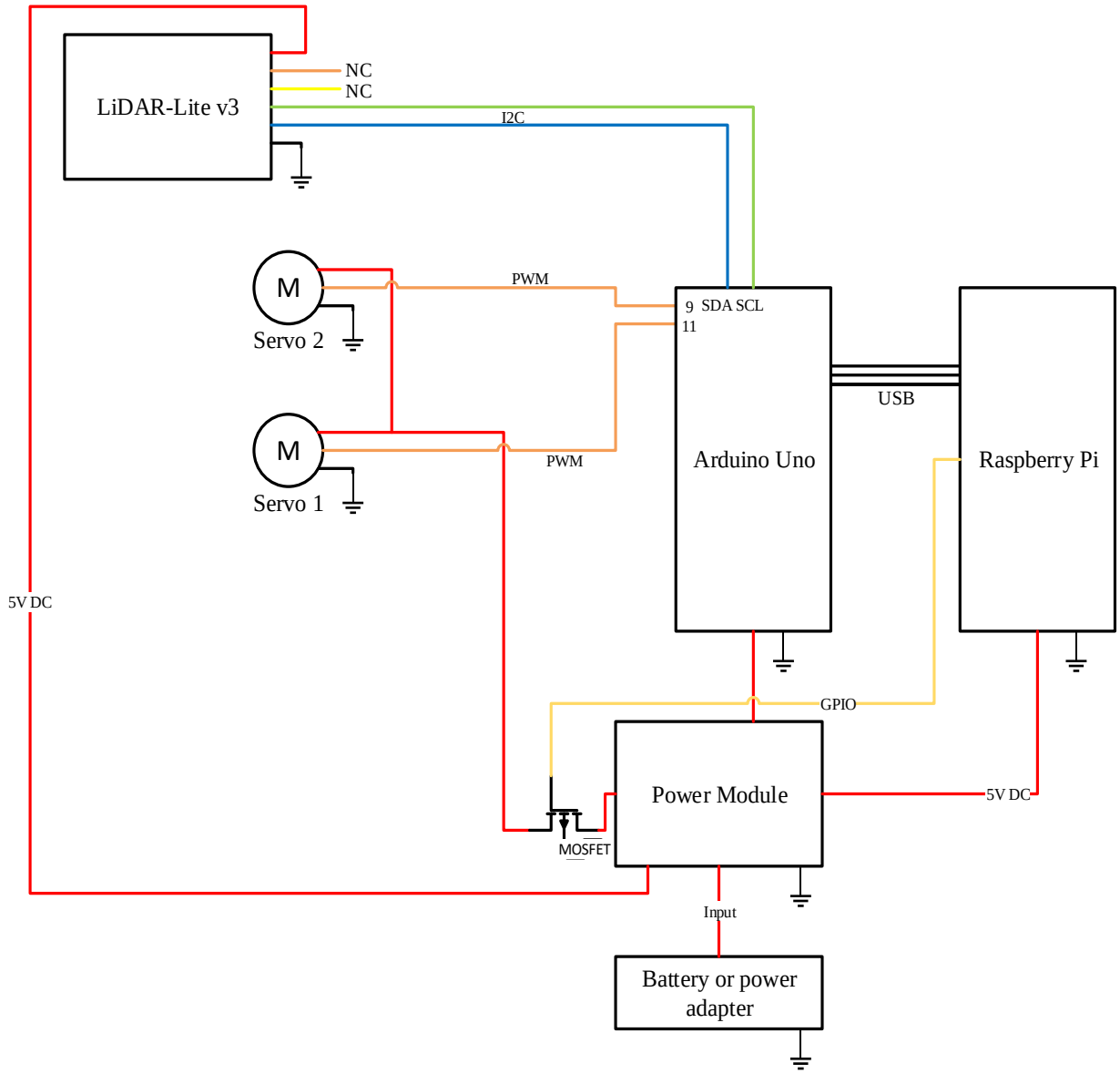

Figure 3-9: Wiring diagram of the LIDARPheno hardware system

3.3 Firmware for Arduino Uno

The firmware of the LiDARPheno system provides an operating instruction for the system. As mentioned earlier in the design section, the Arduino platform controls the operation of the two servo motors as well as data acquisition from the LiDAR sensor. Hence, the program for Arduino (firmware) should be able to control the scanning operation and be the point of contact for communication between the raspberry pi and the scanning system. Figure 3-10 shows a flowchart of the program for Arduino.

Arduino software is a forever running program, i.e., a loop that keeps running forever or until rebooted. As it is visible from the Figure 3-10, at the boot-up/start of Arduino, the program initializes the required libraries. In this firmware, libraries include Servo [72], Serial [72] and LIDARLite [67] for Arduino Uno. After the library initialization, some of the macros are defined that are required for the operation of the LiDARPheno prototype. In this program, the following macros are defined:

- *centerPos:* the center position of the servo motors, typically 1500 µs.
- *cornerPos:* corner position for the system, set to 1900 µs. By setting a servo to this value, the servo will move to about 130° making it parallel to the surface of the housing box. It is used so that the LiDAR mechanism is not in the FoV of the pi camera module while capturing the 2D image.
- *angularStep:* This defines the angular resolution of the scan in microseconds
- *horStart:* this macro defines the angle at which scan starts for the horizontal direction
- *horEnd:* angle at which the horizontal scanning stops
- *verStart:* vertical angle at which the scanning starts
- *verEnd:* vertical angle at which the scanning stops

After the macros are defined, the LiDAR and Servo instances are created. At the same time, some of the variables that are required for setting the servo positions and reading distance information are defined. This results in the creation of *myLidarLite*, *myServoVer*, *myServoHor*, *posH*, *horDirection*, *doScan*, and *posV*.

In the method *setup()* servo objects are initialized by *attach()* method of *Servo* class to connect the servo motors to PWM pin number 9 and 11 of the Arduino Uno and LiDAR object is

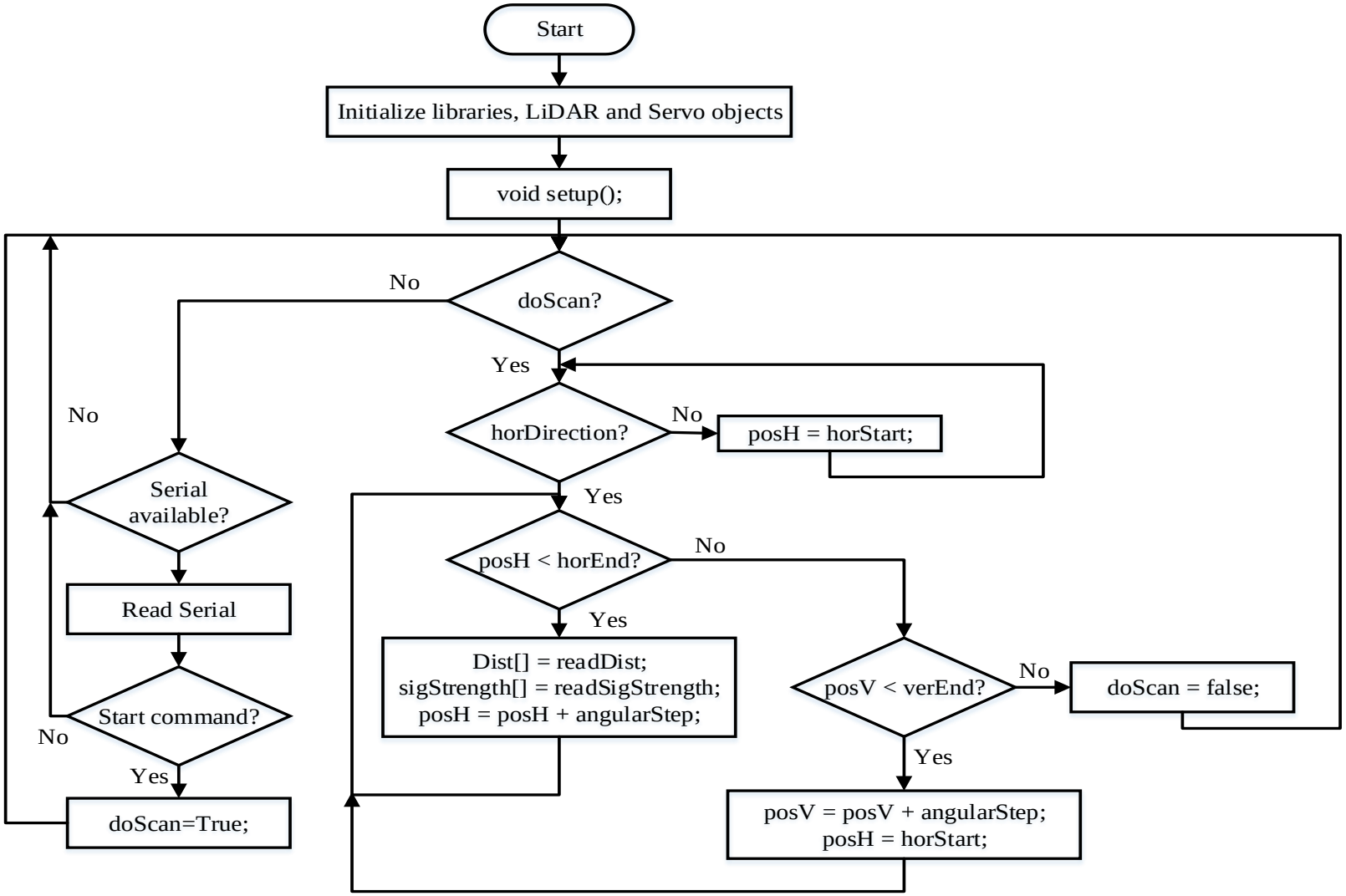

Figure 3-10: Flowchart of the program for Arduino in the prototype for LiDARPheno

initialized using the *begin()* method of the *LIDARLite* class. After the initialization, the servo motor is set to *cornerPos* using the method *writeMicroseconds()* of the *Servo* class.

The Arduino program then enters into an infinite loop which keeps running until interrupted by resetting the Arduino. The scanning and data acquisition functionalities are written inside the *loop()* function of the Arduino program.

First of all the Boolean variable *doScan* is verified, if the variable is set to *false*, then the program checks for the availability of the serial interface and if there is any data on the serial buffer. If there are data, program checks if the data that were received is a scan initialization command. If the scan command is received, the variable *doScan* is set to *true* and returns to the condition where it checks for the *doScan* variable.

On the other hand, if the Boolean variable *doScan* is set to *true*, the program checks the direction of the horizontal servo motor, i.e., left-to-right or right-to-left, and adjusts the horizontal servo motor to *horStart*. After setting the position of the horizontal motor, the program enters into a *for()* loop, where the distance and signal strength data is acquired while increasing the position of the horizontal servo motor by step angle after each point acquisition. Once the horizontal motor position reaches the defined stopping angle, the program increases the position of the vertical scanning motor with a stepping angle and starts the horizontal scan. The process of the horizontal line acquisition repeats until the vertical servo motor reaches the *verEnd* position. During this operation, after each horizontal line scan, the program sends data to the raspberry pi using serial communication.

After the scan finishes, the Arduino waits for the command to start the scanning as described earlier. It is worth to note that the use of each *writeMicroseconds()* method needs 15miliseconds before servo motor can respond the set the specified position. The time calculation for different FoV and step angle are discussed below.

3.3.1 Scan Time: the Time Required for a Single Scan

The calculation of the scanning time for different FoV and step angle is calculated using the following equation:

$$\text{ScanningTime} = \text{Time}_{\text{point}} * \frac{\text{Vertical FoV}}{\text{Step Angle}} * \left(\frac{\text{Horizontal FoV}}{\text{Step Angle}} + 1\right) \quad (3\text{-}1)$$

where $Time_{point}$ is a time required to acquire one point, *Step Angle* is an angular resolution in degrees, *Vertical and Horizontal FoVs* are the Field-of-View for each direction.

The time required to scan a particular scene at a defined FoV and required angular resolution varies because of the use of servo motors in the design. The time to acquire one point is approximately 18 milliseconds, which includes 15 milliseconds for a servo to detect a change in the PWM wave and 3 milliseconds to acquire the data from the LiDAR sensor. Figure 3-11 shows the comparison between different FoV and angular resolution in terms of approximate time required to scan.

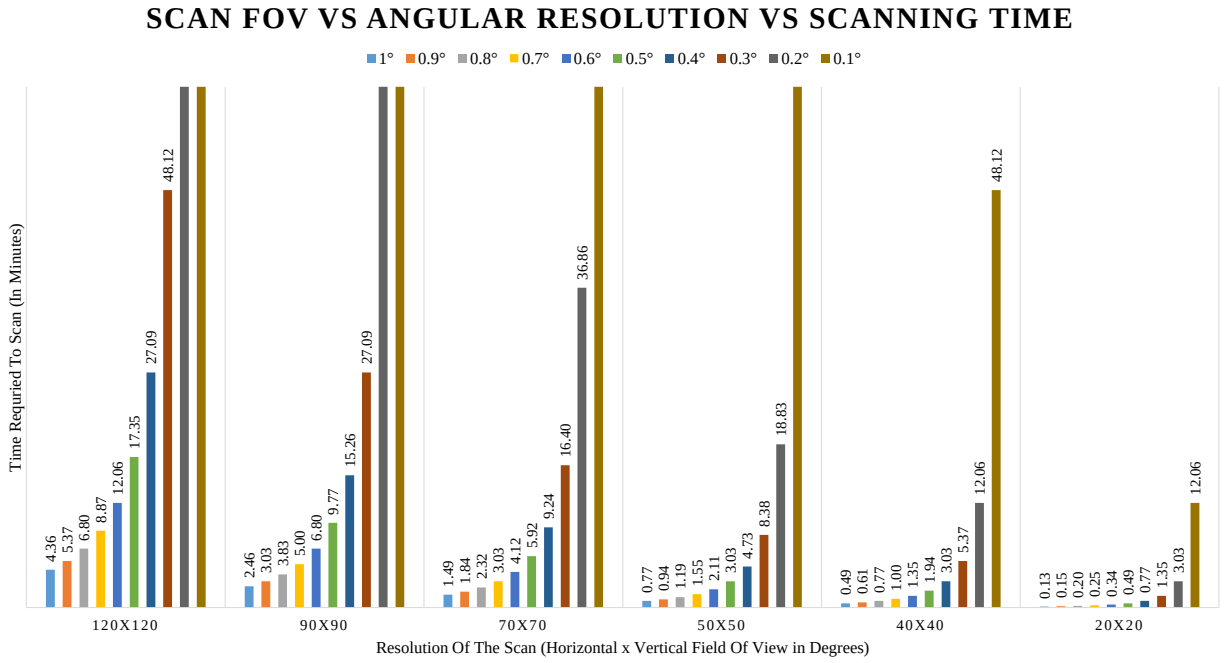

Figure 3-11: Comparison of scanning time for different FoV and angular resolution.

The bar graph in Figure 3-11 indicates that the angular resolution or stepping angle of the scanner mostly affects the time required to scan at different Field of View. Also, it is worth to note that the stepping angle determines the distance between two points, i.e., smaller the stepping angle, smaller the distance between two points. In a way, it can also be thought of as the smallest detectable area. In this study, different FoV experimented, and it was concluded that, if the LiDARPheno is kept about 100 cm from the scan subject and scanned with the FoV of 40°x40°, it can scan the area of approximately 68cm x 68cm. Also, the angular resolution of 0.2° provides the distance resolution (distance between two points) of about 4 mm and the scanning time required to perform the scan with this FoV, and angular resolution is about 12 minutes.

3.4 A Software Program for Raspberry Pi and Data Formats for LiDAR Raw Data

The software for raspberry pi offers and user interface, where the user can operate the scanner and provide the instruction on how the scan should be performed. It should also provide the user with the flexibility of defining where the data should be stored and in which format. For this study, however, the pre-defined or hard-coded parameters are used. However, it is feasible and easy to implement the user-defined parameter selection in raspberry pi as well as Arduino program. Figure 3-12 shows the flowchart of the software script written using Python [73] programming language.

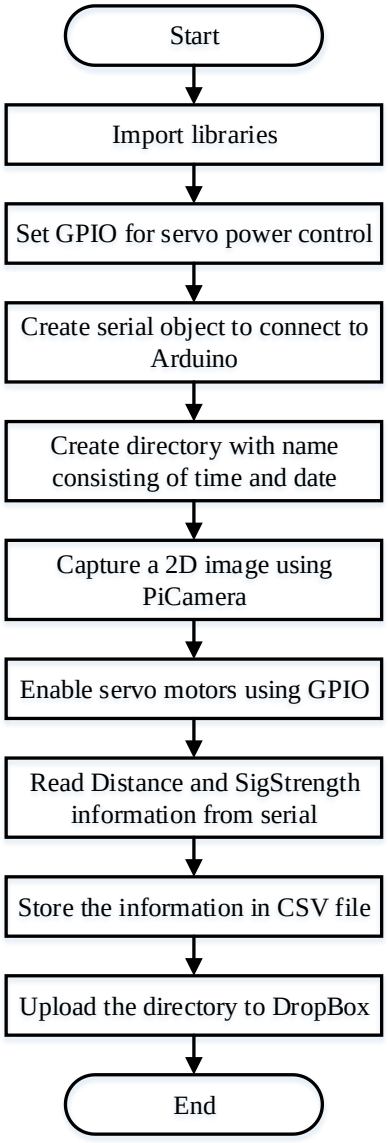

Figure 3-12: Flowchart of the software program in the raspberry pi

The raspberry pi software script written using Python programming language provides the operation of storing and transmitting the data to the file server. In this project, the DropBox cloud storage service is used to store the data. Raspberry pi was configured to connect to the internet at the operating system boot-up. Once connected, the raspberry pi can be remotely connected to the RealVNC viewer, and the user can start the software program mentioned above.

The program can be executed using the command line or by using the mouse pointer. To use the command line user can use the command *"python filename.py"*, where filename is the name of the script. The script utilizes the following python libraries:

- *serial:* The serial library provides access to functions that can be used to operate serially connected devices.
- *numpy:* NumPy library is scientific computation library and is similar to matrices in MATLAB.
- *RPi.GPIO:* The GPIO library has functions to control the General Purpose Input/Output of the raspberry pi.
- *Picamera:* This library provides functionality for operating the camera attached using the CSI interface.
- *Datetime:* Date and time library provides functions to access the current time and date and to represent it in different formats.
- *OS:* the operating system (OS) library can be used to access the operating system commands.

The execution of the program starts with importing the above-mentioned libraries. Then the GPIO pin is configured to control the power to servo motors as mentioned in the wiring diagram of the system. Then the program creates a serial object to connect to Arduino Uno over USB serial port (baud rate of 115200 was used). After the serial object creation, a directory is created to using the naming convention so that the scan time and date can be easily identified. At the same time, the file names have a naming convention that follows the same format. Following are the directory and file names created:

- Directory: '*LidarPheno_Data_%Y_%m_%d_%H_%M_%S*'
- Distance Info: '*depthVal_Data_%Y_%m_%d_%H_%M_%S.csv*'
- RGB image data: '*rgb_Data_%Y_%m_%d_%H_%M_%S.png*'

- Signal Strength data: '*sigVal_Data_%Y_%m_%d_%H_%M_%S.csv*'

where %Y, %m, %d, %H, %M, %S are Year, Month, Date, Hour, Minute, and Seconds, respectively.

The still 2D image of the scene is captured using the PiCamera library. When a GPIO pin is set to allow power to the servo motors and a command to start the scan is sent over the serial communication to Arduino. While the scan is in progress, the program continuously monitors for the data on serial bus and stores the received data to a NumPy array. When the scan finishes, the raspberry pi stores all the data received to a Comma Separated Value (CSV) file with a comma delimiter and at the same time power to servo motors is disconnected by setting GPIO to a LOW level.

The program utilizes the *dropbox_uploader* bash script by Andrea Fabrizi and is publically available at [74]. The setting-up of the script on the raspberry pi is easy and requires the user to create an Application Programming Interface (API) on Dropbox developers DBX platform. The API key provides access to the user-specified app folder on Dropbox. The API key is supplied to the *dropbox_uploader* bash script, and then simple commands can be used to upload, delete and list the contents of the application folder on the Dropbox server. This script match with one requirement of the project, i.e., lowest code development, and is easy to use by a non-technical person. The use of Dropbox makes it easy to upload the scan data files and access from the remote terminal.

The file format for storing the raw LiDAR data is CSV. The CSV file format has been used for a long time now and is particularly easy to import in most of the programming languages. The typical file size of the CSV file for the scan is dependent on the FoV, angular resolution and distance to object. For example, a single scan of 40°x40° at an angular resolution of 0.2° and distance about 1 meter has a file size of approximately 150 KiloBytes (KB).

3.5 Power Consumption Analysis for LiDARPheno

The power consumption analysis provide an estimate of the battery life. Table 3-3 provides details of the power consumption by each device used in the LiDARPheno design. From the measurement of current consumption of the devices, the most power is used by raspberry pi while the lowest consumption is by servo motors, as they are only operational when the power is allowed to them.

Table 3-3: Power consumption analysis of individual devices of the LiDARPheno

Device	Power consumption
PiCamera	120 mA
LiDAR	105 mA
Arduino	65 mA
Rpi	150 mA
Servos	60 mA

Based on the current consumption data, the running time of the battery can be estimated. LiDARPheno uses LiPo battery with 7.4V and 2Ah capacity, which means the battery can last one hour if the constant current of 2 amperes is drowned. Based on the knowledge of battery capacity and average power consumption of the system while operational, total time for which the battery can supply enough power is estimated. The LiDARPheno system consumes an average current of 0.4A while operational and about 0.3A while idle. Using the information on current consumption the battery can last up to 5 hours while operated continuously. Moreover, one scan at 40°x40° FoV and 0.2° angular resolution take about 14 minutes including the data transfer to the Dropbox. If operated continuously, about a maximum of 20 scans can be obtained with the one full charge of the battery.

3.6 Summary of the Hardware Cost

Summary of the hardware cost for building the LiDARPheno system is given in Table 3-4. Most parts are available in Canada from various suppliers including Amazon Canada and RobotShop Canada. The total hardware cost for building the LiDARPheno system is CAD $409.68 as shown in the table. The enclosure is used for housing all the components of the system. Moreover, the enclosure is a made from the hard plastic and can be easily carved to make the required modifications. The raspberry pi, Arduino and power module including all the wiring needs are enclosed in the enclosure box. This red color box is shown in Figure 3-8.

Table 3-4: Summary of the hardware cost for the LiDARPheno system

Component/Module	Quantity	Total Cost
LiDAR-Lite v3 Laser Rangefinder	1 @ $159.99	$159.99
Raspberry Pi 3 Model B	1 @ $54.99	$54.99
Arduino Uno Rev3	1 @ $35.99	$35.99
Servo HS-85BB	2 @ $26.19	$52.38
Multi-Purpose Micro Servo Bracket Pack of Two	1 @ $15.32	$15.32
Long "C" Micro Servo Bracket Pack of Two	1 @ $4.09	$4.09
Step-down DC-DC converter	1 @ $11.89	$11.89
7.4 V LiPo Battery	1 @ $19.72	$19.72
LiPo battery charger	1 @ $21.54	$21.54
Enclosure	1 @ $11.78	$11.78
Total:		**$409.68**

Chapter 4
Experimental Setup and Data Acquisition

This chapter discusses the laboratory experiments, setup and data acquisition process. Section 4.1 describes the materials (plants and devices) used in the experiments. Section 4.2 describes the setup for data acquisition. Section 4.3 provides information on data acquisition using a commercial LiDAR, LiDARPheno system, and ground truth acquisition. Finally, Section 4.4 explains the data formats used to store the data acquired.

4.1 Materials Used for the Experiments

4.1.1 Plant Material

The laboratory experiments were performed on different plants. In the first experiment, five different indoor plants from three different families were used. In the second experiment, three plants of canola were used as scan subjects.

In the first experiment, plant varieties include Orchid, Aglaonema and an arbitrary wild plant, which are readily available from gardening stores. Total of five plants have been brought to a laboratory and was given adequate water every two days. There were three different plants of Aglaonema with varying sizes and leaf numbers. Figure 4-1 shows a digital image of all five of them. All three different species of plants have varying leaf shape and sizes. The images shown in the figure are taken from the top of the plants using the raspberry pi camera module.

For use in the second experiments, canola plants were used. The canola seeds were put into the regular drinking water in a transparent bag and hanged on the window for them to get the sunlight on March 22nd, 2018. After two days, the canola seeds started growing roots, and these seeds with emerged roots were transferred to a pot on March 24th, 2018. Approximately a week after transferring to the pot, canola started emerging. Pictures of the canolas growing are shown in Figure 4-2. The experiment was performed on the canola plants on June 3rd, 2018 and June 17th, 2018. Canola has more compound leaves and is hard to phenotype due to surface curvature and

non-uniform structure of leaves. The indoor plants are used for the development and canola plants for validation of the post-processing algorithms and software.

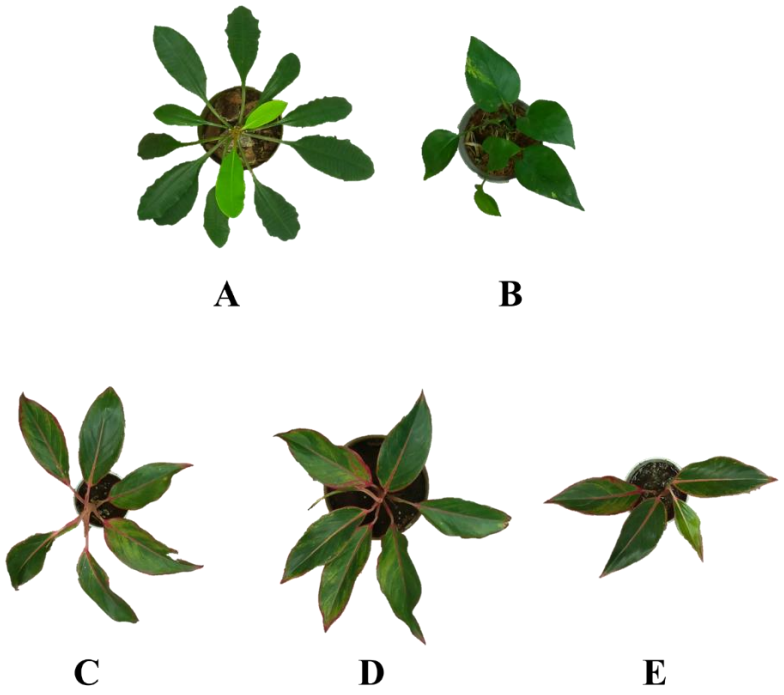

Figure 4-1: Digital images of the indoor plants used for the experiment in the laboratory: (**A**) an arbitrary wild plant, (**B**) orchid and (**C-E**) Aglaonema plant

4.1.2 High-Resolution Commercial 2D LiDAR

A commercial 2-dimensional (2D) LiDAR was used to capture the 3D information from the plants. The data acquired with the 2D LiDAR were used to assess the performance of the LiDARPheno system. The LiDAR LMS400-2000 (Sick Inc., USA) is a 2D LiDAR that can capture the distance and reflectance information and uses the red laser-light with a wavelength of 650-670 nm. Figure 4-3 shows the image of an LMS400-2000 LiDAR. Moreover, many researchers have proved the utility of SICK LMS400 LiDAR in plant phenotyping tasks [51], [52], [56], [58], [75]. Hence, the proven utility of this particular LiDAR device and availability of this expensive LiDAR from one of our collaborators Scott Noble (Mechanical Engineering, University of Saskatchewan) makes this device an ideal candidate to assess and compare the performance of the developed system. From now on the LiDAR device is addressed as LMS400.

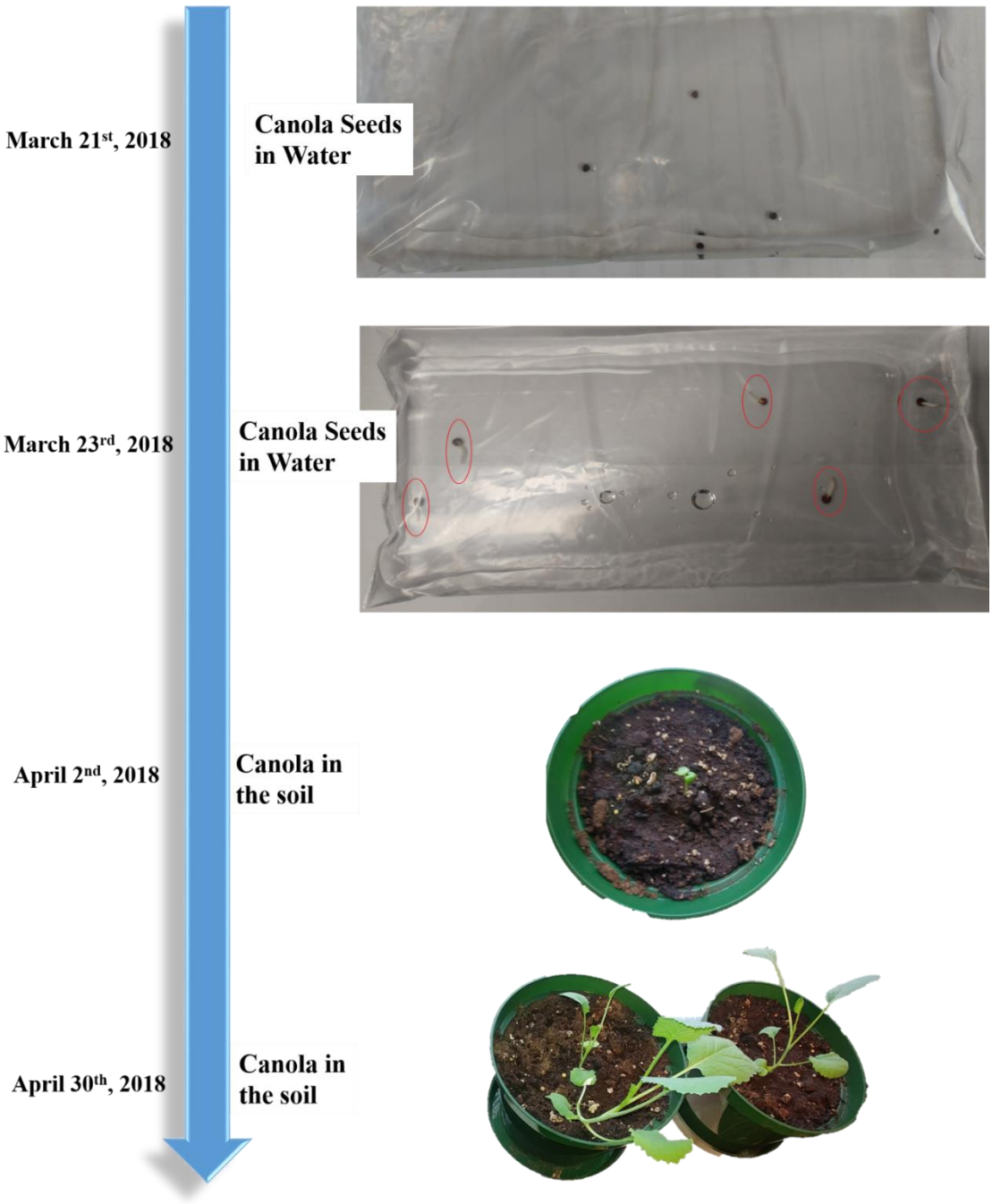

Figure 4-2: Growing canola in the laboratory

LMS400 is used for commercial applications and is utilized in the production lines. Furthermore, the library for accessing the data acquisition has already been developed by our collaborator Scott Noble (Mechanical Engineering, University of Saskatchewan). The availability

of the program for data acquisition and the LMS400's popularity among researchers will make the use of this device easy to operate. LMS400 utilizes a rotating mirror to capture distance and reflectance information at speed up to 320 Hz, i.e., 320 lines per second.

Figure 4-3: Sick LMS400-2000 (source: https://www.nexinstrument.com/LMS400-2000)

4.1.3 Document Scanner

The document scanner LiDE 220 (flatbed document scanner) by Canon (USA) was used to scan individual leaves of the plants for the ground truth data acquisition. The individual leaf scan provides a color picture with the resolution at which the scanning is performed. Flatbed document scanner can be used to accurately estimate the area of the pixel by using the information of dots per inch (DPI), which is a number of pixels in one-inch physical dimension. A picture showing the document scanner is presented in Figure 4-4.

Figure 4-4: Canon LiDE 220 (Canon, USA)

4.2 Experimental Setup

The data acquisition setup consists of two parts, setup for LiDARPheno and setup for LMS400.

4.2.1 Experimental Setup for LMS400

The data acquisition or experimental setup for the laboratory experiments using SICK LMS400-2000 LiDAR is shown in Figure 4-5.

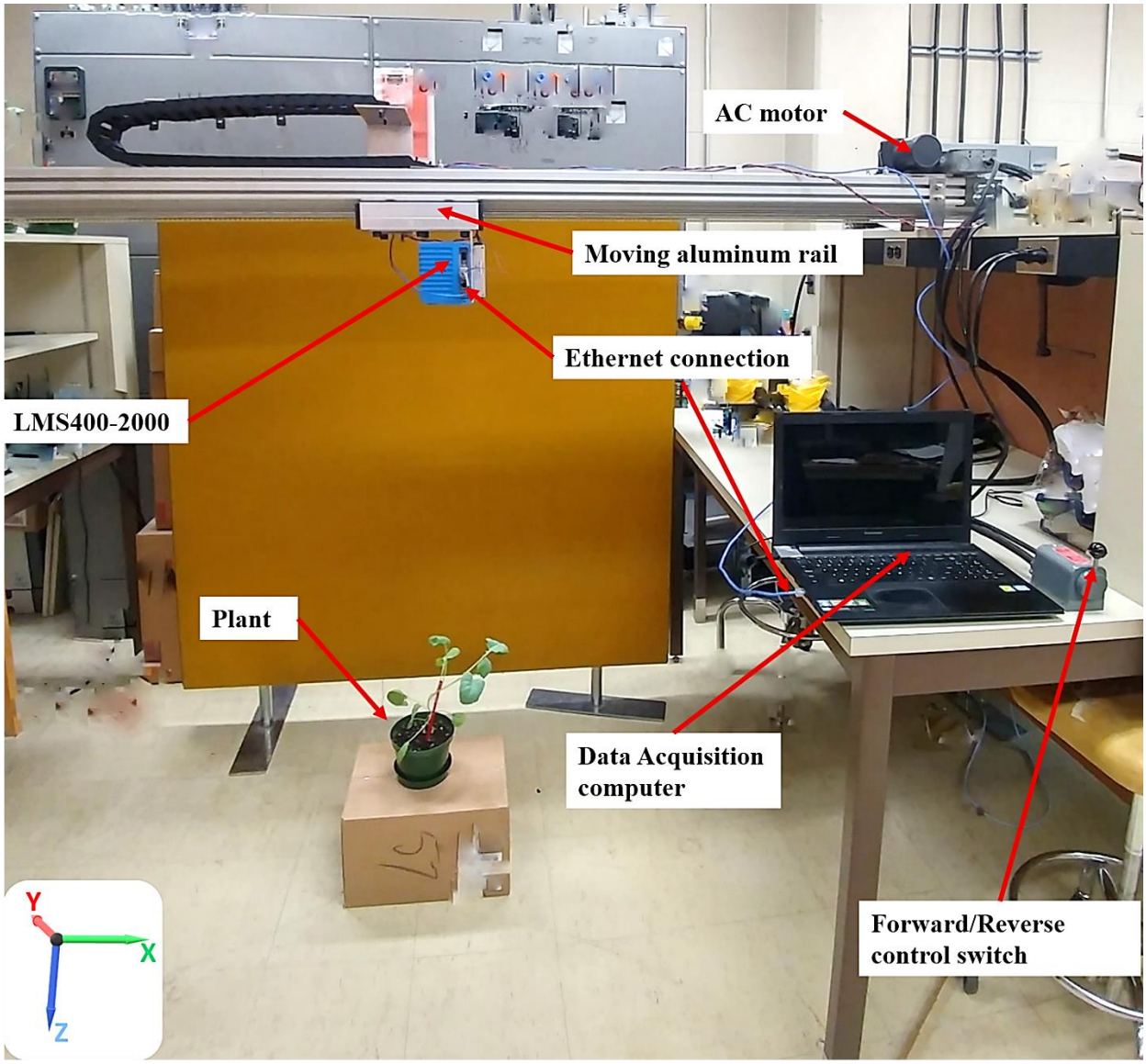

Figure 4-5: Data acquisition setup for LMS400

The conveyer belt based mechanical setup consists of:

1) An aluminum railing which can support the weight of LiDAR system combined with a conveyer belt and an alternate current (AC) motor with forward and reverse switched control has been built by our collaborator Scott Noble (Mechanical Engineering, University of Saskatchewan) group for in-lab experiments. It provides control over forward and reverses the motion of the attached device for scanning and data acquisition purpose. The setup moves at the constant speed of 18.0724 cm s-1.
2) The mount for LiDAR is made from aluminum sheet capable of holding LMS400-2000 and providing access to power and Ethernet cable. This makes LiDAR data accessible from a computer that can be placed far away.
3) A data acquisition computer that can run a python script for acquiring the data from the LMS400 via Ethernet.

LMS400 has been attached to this setup when data acquisition was performed. At a scanning frequency of 360 Hz (line scans per second), each line scan is approximately 0.5mm apart. A data acquisition computer controls the operation of user-access control and operation of the LMS400.

4.2.2 Experimental Setup for LiDARPheno

LiDARPheno is designed to avoid the need for any external moving part. Unlike LMS400, where the external moving mechanism is required to acquire data along the scan direction, the LiDARPheno has two servo motors to control the horizontal and vertical scanning operations. Hence, the LiDARPheno can be attached to any tripod or railing. In the laboratory experiments, the LiDARPheno was attached to the same aluminum railing used for LMS400, except the railing will not move. For simplicity, the LiDARPheno is attached with the aluminum railing with Velcro (hook and loop fastener). Moreover, the use of the aluminum railing, which is used for the LMS400, for LiDARPheno provides the same height from the plant as LMS400. The benefit of having the same height as that of LMS400 will provide a better opportunity to compare the results of the two different systems and assess the performance of the developed LiDARPheno system. Figure 4-6 shows the setup for data acquisition with LiDARPheno.

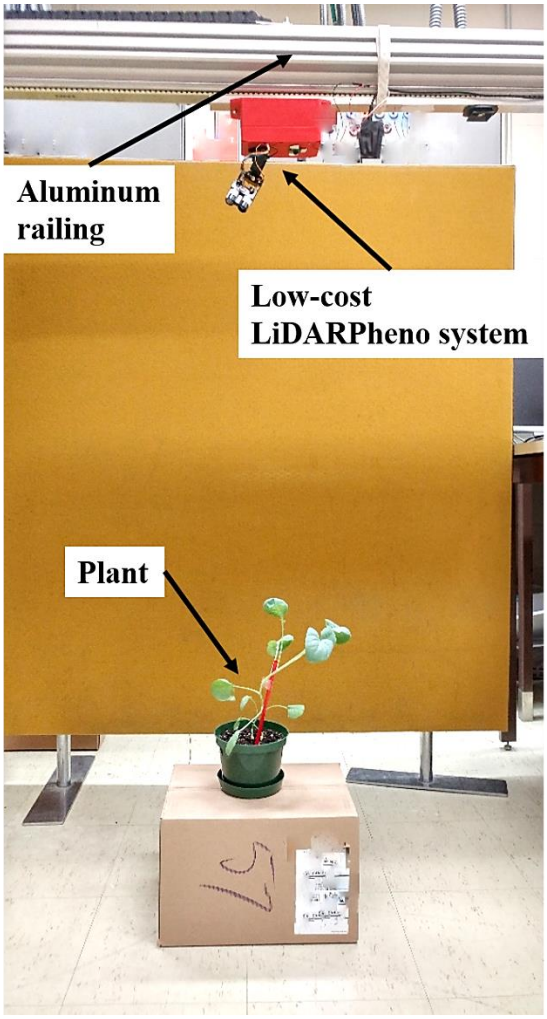

Figure 4-6: Data acquisition setup for LiDARPheno system

4.3 Data Acquisition

Data acquisition process for both the experiments using both LiDARPheno and LMS400 are described in the following sub-sections. Moreover, calculation of ground truth leaf area measurement, leaf length measurement, and leaf width measurement for reference is discussed.

4.3.1 Data Acquisition using LMS400

The data acquisition using LMS400 LiDAR device was performed using the Python 2.7 program. As described in the experimental setup, the LMS400 LiDAR device communicates using

the Ethernet connection. Accessing the data from LMS400 is based on the message passing between acquisition computer and LiDAR using the Ethernet communication.

Python is easy to use and learn open source programming language, providing access to many functionalities including file storage, scientific computation libraries, hardware control and parallel processing. The python library for controlling and accessing the data from LMS400 is written by David Pastl (Mechanical Engineering, University of Saskatchewan) as part of the instrument integration project of theme 1.2 of the P^2IRC project. In this work, the developed library for LMS400 is used as the base program to write a python script to control the LiDAR operation as well as access the reflectance and distance information from the LMS400.

The distance information from LMS400 contains the polar distance to the reflecting surface. Reflectance information is a digital number ranging from 0 to 255 and indicates the percentage reflectance of the surface is illuminated with the laser light. The reflectance data is essential information regarding the surface because each object has a different response to a particular wavelength of the light. The reflectance percentage can help in distinguishing the plant and non-plant objects, ultimately making the background removal task easier. As recently published in a research article by Berni *et al.* [56], the plants typically absorb the most light in the red spectrum, the separation of the plant from the soil can be done just by introducing a threshold in the red reflectance data.

The data were acquired with a Lenovo G500 (Intel Core i5 @2.6 GHz, 8 GB RAM) via Ethernet communication to the LMS400 LiDAR. The python script initializes the LMS400 and logs into the LiDAR system at the user-level access. Then file names with the current time and date are created. The forward/reverse switch is used to move the LMS400 along the scan direction. As the speed of the motor that moves the LMS400 is constant, the distance between two successive line scans calculates to approximately 0.5 mm. This distance separation between two successive lines scans, the angles of a single line scan and angular resolution are the prior knowledge for the post-processing of the data acquired with LMS400. The files are stored in the local storage of the acquisition computer. Each of the plants was scanned using the above-mentioned data acquisition process.

4.3.2 Data Acquisition using LiDARPheno

Unlike LMS400, data acquisition process for the LiDARPheno low-cost system is straight-forward. The LiDARPheno itself is a whole scanning setup and does not require the external setup for data acquisition. The low-cost LiDAR-based design is genuinely wireless and can be remotely operated due to the advantage of wireless connectivity already integrated with Raspberry Pi mini-computer. The system connects to available Wi-Fi and user can control it via a remotely located computer system. Once the user command is received, the system starts scanning the scene. The data being captured are LiDAR distance data, reflectance information and a digital image of the scene. Once acquired, it automatically sends all the data to predefined Dropbox (Dropbox, Inc., https://www.dropbox.com/) directory. Distance and reflectance information is stored in a CSV file whose name is according to the time and date of the scan. The acquired digital image is also uploaded along with CSV files so that data from a distance can be compared to the digital image. Figure 4-7 shows the data flow diagram of the data acquisition using a low-cost design.

A user initiates a command via the remote terminal (a computer or a smartphone) to scan the scene, raspberry pi creates files for storing data and forwards the command to Arduino via Universal Serial Bus (USB) communication and then Arduino communicates to LiDAR scanning using I^2C communication protocol and controls the servo motors using Pulse Width Modulated (PWM) signals. After a scan of the scene is finished, raspberry pi uploads all the data to a remote file storage server. In this work, DropBox is used as file storage server.

Alternate mode of communication can be used if the Wi-Fi connectivity is not available. For example, the acquired data can be stored in the local storage and later transferred to the local file server using ad-hoc network between raspberry pi and remote system.

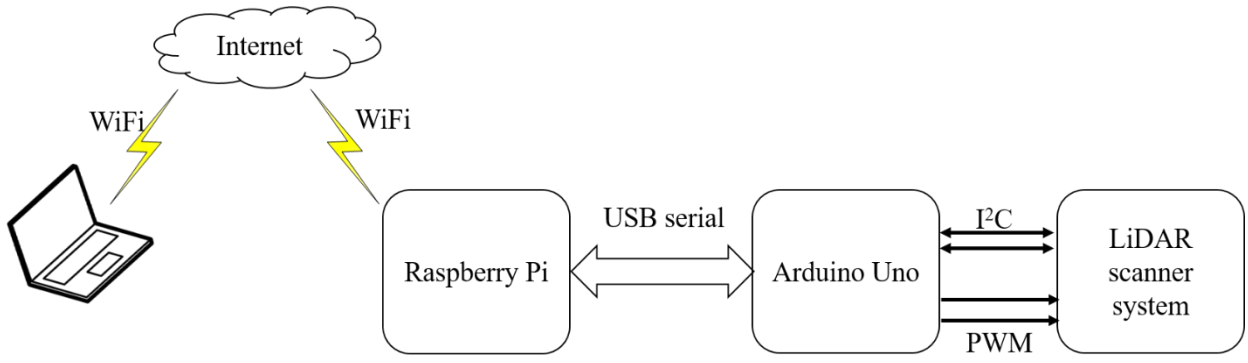

Figure 4-7: The data flow diagram of the acquisition using LiDARPheno

4.3.3 Ground Truth Data Acquisition

For this study, the aim is to estimate the leaf geometric parameters such as length, width, and area of individual leaves of the plants. Hence, the ground truth data or manual measurement of the traits is recorded. The ground truth data is necessary to evaluate and validate the reliability of the estimated traits using LiDAR data. In the later stage of this thesis, the estimates of the plant leaf traits are compared with the manually acquired ground truth information to calculate the error rate.

Leaf length and width are manually measured using the measuring tape, and leaf area is estimated by scanning and processing each leave of the plant using the flatbed document scanner (Canon LiDE 220). The document scanner flattens the leaf while scanning it, which ensures the whole leaf area has been exposed to the scanner. As the whole area of the leaf is exposed to the scanner, the measurement of the leaf area can be done using the simple image processing technique. The ground truth data acquisition process, each leaf is scanned at the resolution of 300 dots per inch (DPI). If calculated for 300 DPI, area of each pixel accounts to ~7168.44 μm^2. The calculation for the area of one pixel can be done by simply diving the equivalent of 1 $inch^2$ in cm, which is ~6.4516 cm^2, by a number of pixels in the area, which is 90,000. By doing this calculation area of one pixel is obtained and the obtained image can be considered as a large graph paper with each grid of 7168.44 μm^2. The process of acquiring the ground truth leaf area is shown in Figure 4-8.

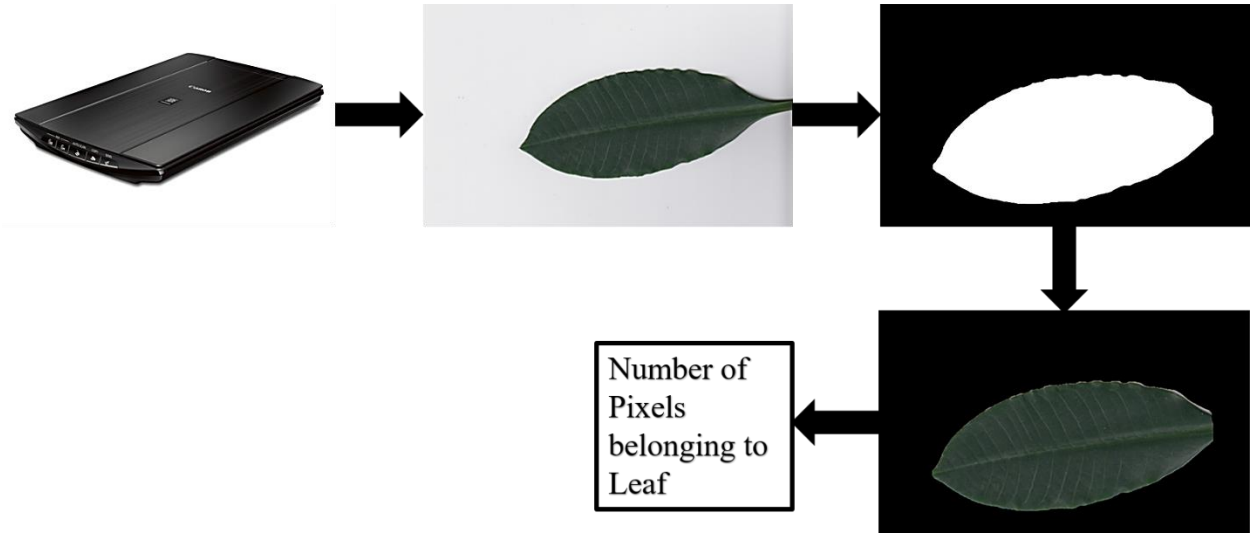

Figure 4-8: The process of acquiring ground truth leaf area information

After acquiring the scan of the leaf, the image is segmented using a color threshold to get the number of pixels belonging to the leaf. The area of the leaf is obtained by multiplying the number of pixels to the area of one pixel (7168.44 μm^2) as obtained by the calculation on the scan resolution. All the ground truth data, with a leaf number assigned to each leaf while looking from the top, were stored into a comma separated value (CSV) file.

This method of obtaining the ground truth information for leaf area was validated by using a centimeter graph paper. One of the grids of the centimeter graph paper was colored green and then scanned using the document scanner at the resolution of the 300 DPI. Then the process of segmentation was performed as mentioned above and the accuracy for estimating the green colored box in a graph paper was 99.98%. With this validation experiment performed, the ground truth leaf area can be considered highly accurate measurement. The utility of the flatbed document scanner voids the need to buy a commercial leaf area measurement device and meets the primary goal of the thesis – low-cost development.

4.4 Data Formats

The format for storing the data acquired using LMS400, LiDARPheno, and ground truth information is dependent on the type of data. The LMS400 has two different data and are stored in separate files. One is reflectance data, and another is distance information. The comma-separated value (CSV) file format has been used for both the reflectance and distance information. Each line scan has a fixed number of points that are acquired, and each line is one row in the CSV files. A number of columns in the CSV file are equivalent to the number of points in the single line scan. Moreover, the naming of the files is kept such that each filename contains the information regarding the type of data it contains, i.e., reflectance or distance, and time and data when the data was acquired. The naming convention for files helps in identifying the data files from a large number of files.

The LiDARPheno uploads all the information to the dropbox containing the date, time and directory with the information. Three different types of the information are acquired by the LiDARPheno, signal strength, distance information, and an RGB image of the scene. Signal strength values and distance information is stored in the CSV files in the same manner as that of the LMS400. However, the number of points or values that these files contain differ from that of

the LMS400 data. An RGB image of the scene is stored with high resolution in a portable network graphics (PNG) file format.

The ground truth data, as mentioned in the ground truth acquisition section, are stored in the CSV file and contains the length, width, and area for the individual leaf. Moreover, the scan images are stored in uncompressed TIFF file format. Furthermore, an image containing the leaf number assigned while collecting the ground truth information is also stored as PNG file for reference to the numbered leaves.

Chapter 5
Data Analysis/Post-Processing

This chapter seeks to provide an understanding of the post-processing and analysis of the acquired LiDAR data. Section 5.1 discusses the data import and conversion from raw data to the 3D point cloud. Section 5.2 provides the procedure to convert the raw data to the Cartesian coordinate system to generate 3D point cloud data. Section 5.3 discusses the background removal process. Section 5.4 describes the data cleaning and algorithm developed for filtering the point cloud data. Section 5.5 explores the segmentation in 3D point cloud data. Finally, Section 5.6 explains the techniques for extracting the leaf traits.

5.1 LiDAR Raw Data

The LiDAR raw data is stored in the CSV file and can be imported in most computer programming languages. The raw data is polar distances from the sensor to the reflecting surface and needs to be converted to the Cartesian coordinate system to get the additional dimensions of the point cloud (i.e., X and Y coordinates). Figure 5-1 shows the raw polar distances represented by scaled color.

The CSV files containing raw distance information from the LMS400 and LiDARPheno were imported to the MATLAB R2017a® (MathWorks, USA) workspace using the CSV file manipulation functions. The *imagesc()* function of the image processing toolbox provides functionality to represent any numerical data with scaled colors. Another raw information from the LiDAR-based systems is reflectance data. In LMS400 reflectance data is a digital number from 0 to 255, whereas for LiDARPheno the data ranges from 0 to 255 representing the strength of the returned signal and can be directly related to the reflectivity of the target surface. The scaled color image of the reflectance and signal strength information is shown in Figure 5-2.

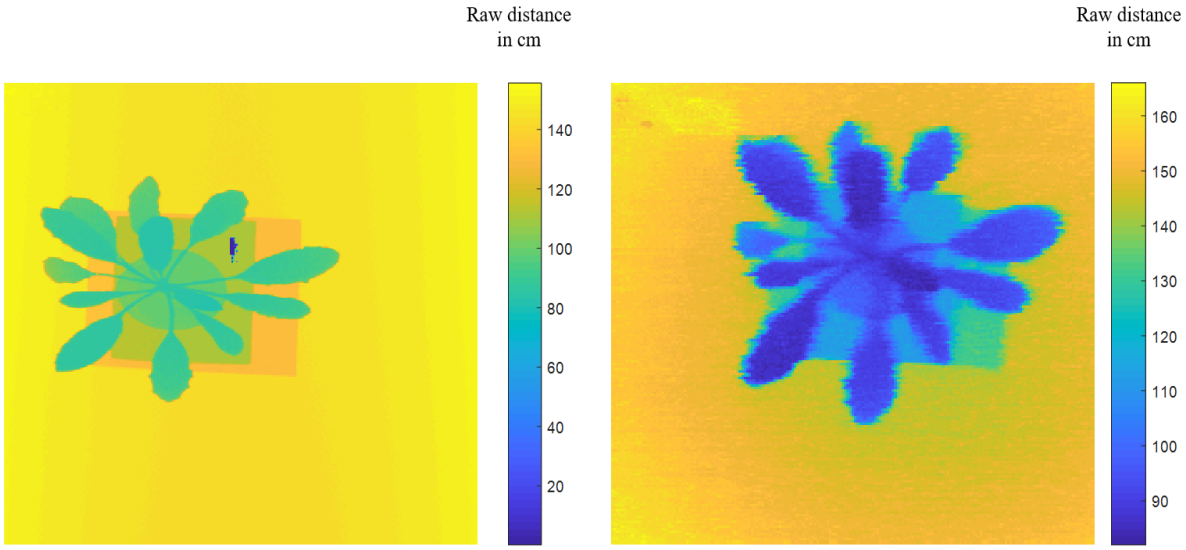

Figure 5-1: Raw distance data acquired from an arbitrary wild plant

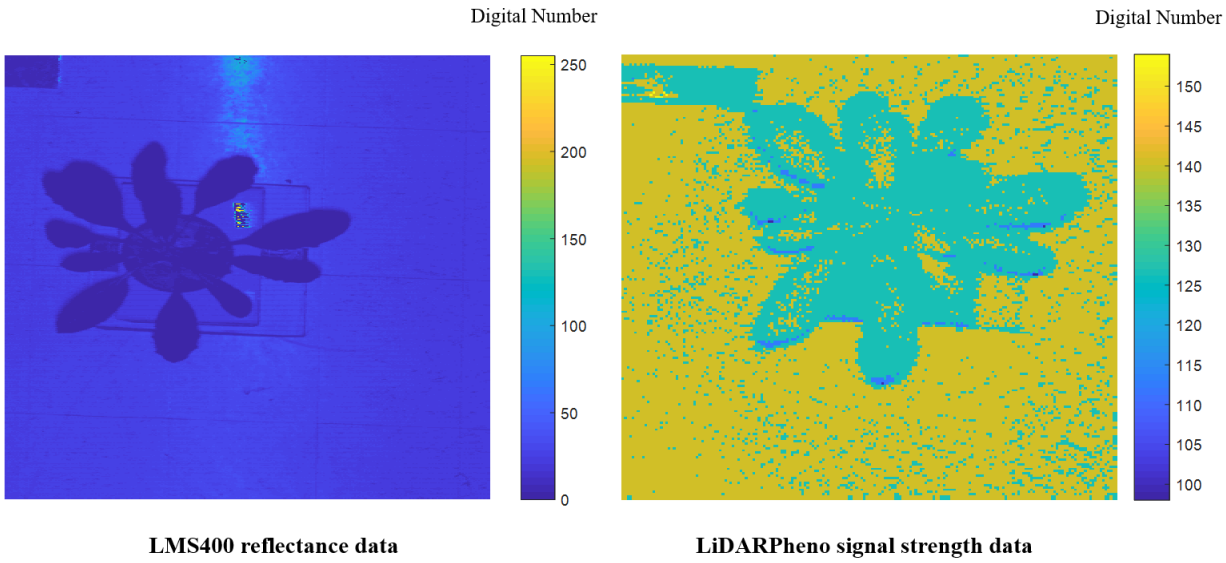

Figure 5-2: Reflectance and signal strength information for an arbitrary wild plant

5.2 Conversion to Cartesian coordinate system

As the LiDARPheno system is standalone system and horizontal and vertical angles are known from the user-specified FoV, range data acquired with LiDARPheno system are converted to Cartesian coordinates using following equations (5-1), (5-2), and (5-3) below:

$$X = rho * cos(\phi) \tag{5-1}$$

$$Y = rho * sin(\phi) * cos(\theta) \tag{5-2}$$

$$Z = rho * sin(\phi) * sin(\theta) \tag{5-3}$$

where:

- "rho" is the polar distance between reflecting surface and a sensor
- ϕ is Azimuth (vertical) angle of scan for particular point
- θ is Elevation (horizontal) angle of scan for a particular point

On the other hand, LMS400-2000 has only one rotating mechanism that is horizontal movement angles and hence does not require the full conversion. In our experiments, we assumed X to be the values of the moving part, i.e., the start of scan is 0 cm, and each line scan is 0.5 millimeters (mm) apart. Hence, only Y and Z values need to be converted from a polar distance. This conversion is performed using equation (5-4) and (5-5).

$$Y = rho * cos(\theta) \tag{5-4}$$

$$Z = rho * sin(\theta) \tag{5-5}$$

After conversion to the Cartesian coordinate system, X, Y, and Z represent corresponding coordinates in the real-world system in centimeters (cm). These coordinates can be plotted using a 3D scatter plot to visualize a point cloud of the scene. Figure 5-3 shows a sample 3D point cloud obtained with LMS400 and LiDARPheno for one of the scanned indoor plants represented by scaled color according to Z distances.

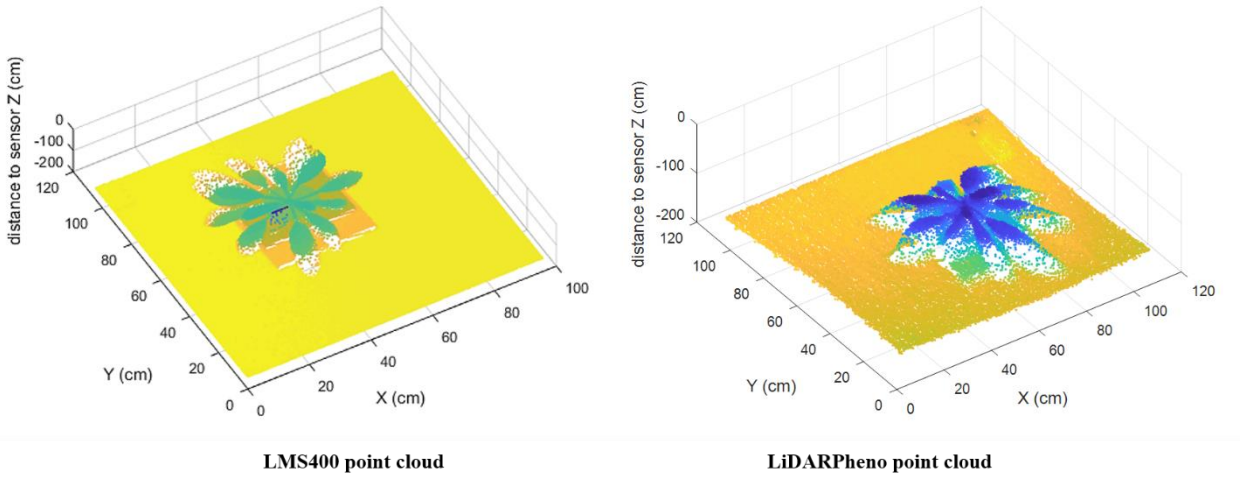

Figure 5-3: Point cloud representation after conversion to Cartesian coordinates

5.3 Background Removal

The LiDAR data contains the information that might not be necessary for the use in the plant trait extraction. For example, the point clouds shown in Figure 5-3 contains the data belonging to the floor, which is not useful in the task of leaf traits extraction. Hence, the data that doesn't belong to the plant is considered the background and needs to be removed so that the information can be reduced, and processing algorithms don't have to process the background data. This process of background removal makes the processing of point cloud computationally light-weight.

For the background removal task, two thresholds were introduced. One is distance threshold which is applied to the Z (distance) information and another is reflectance threshold, which is applied to the reflectance (for LMS400) and signal strength (for LiDARPheno) data. The thresholds remove the background or non-plant objects from the point cloud data. Figure 5-4:

Histograms of the percentage reflectance and signal strength of the wild plant.Figure 5-4shows the histograms of the reflectance data and signal strength data obtained using LMS400 and LiDARPheno, respectively.

Red reflectance data of the LMS400 can be used to differentiate between the materials of the objects. A typical plant absorbs the light in the 650-670 nm wavelength region and has relatively low-reflectance. It can be seen from the histogram of the LMS400 reflectance data from

an arbitrary wild plant that there are mainly two peaks, one is below 10%, and another is above 10%. This reflectance can be applied to the point cloud to reduce the background points. However, for LiDARPheno, the signal strength values are difficult to use for differentiating the plant from a non-plant object in the scan.

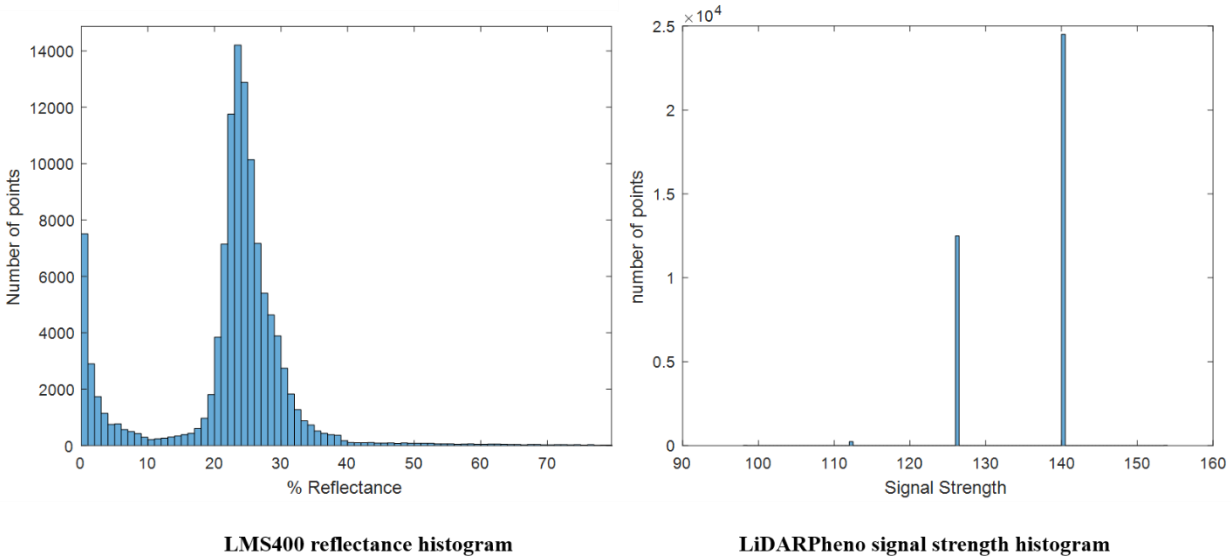

Figure 5-4: Histograms of the percentage reflectance and signal strength of the wild plant.

Another threshold is applied to the distance or depth values of the point cloud. The same technique of plotting the histogram is applied for the distance threshold. Figure 5-5 shows the histograms of the Z distances in both the LMS400 and LiDARPheno data. It is visible from both the histograms that there are peaks for the background object as well as the plant surface. The threshold can be determined from the peaks, making it possible to remove the background without the computationally large operations as in the image based background removal.

The histograms for both LiDARPheno and LMS400 acquired distance clearly represents a peak at the highest distance. This highest distance corresponds to the ground or floor data. In the background removal process, these peaks were used to determine the distance and/or reflectance thresholds. For example, an arbitrary wild plant's reflectance and distance thresholds are 10% reflectance, more than that is discarded, and distance threshold is 140, points with distance more than 140 cm are discarded. By this process of applying a threshold, the point that does not belong

to plant surface is removed from the point cloud and are not processed in further steps. Figure 5-6 shows the point clouds after the thresholds are applied.

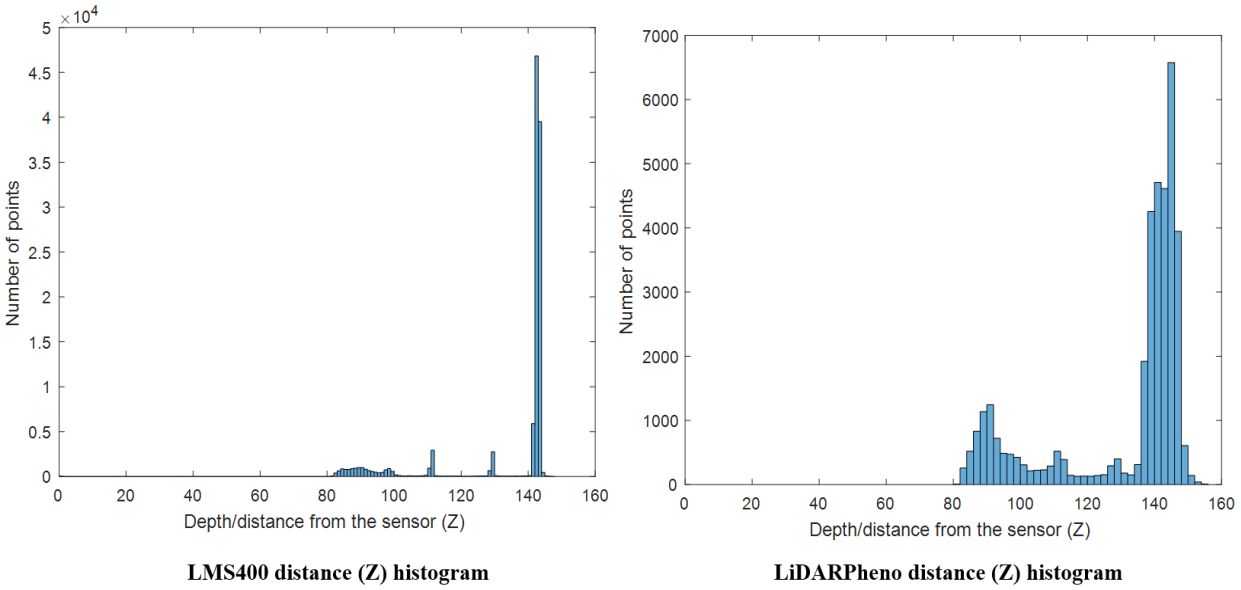

Figure 5-5: Histogram of the distance to the sensor

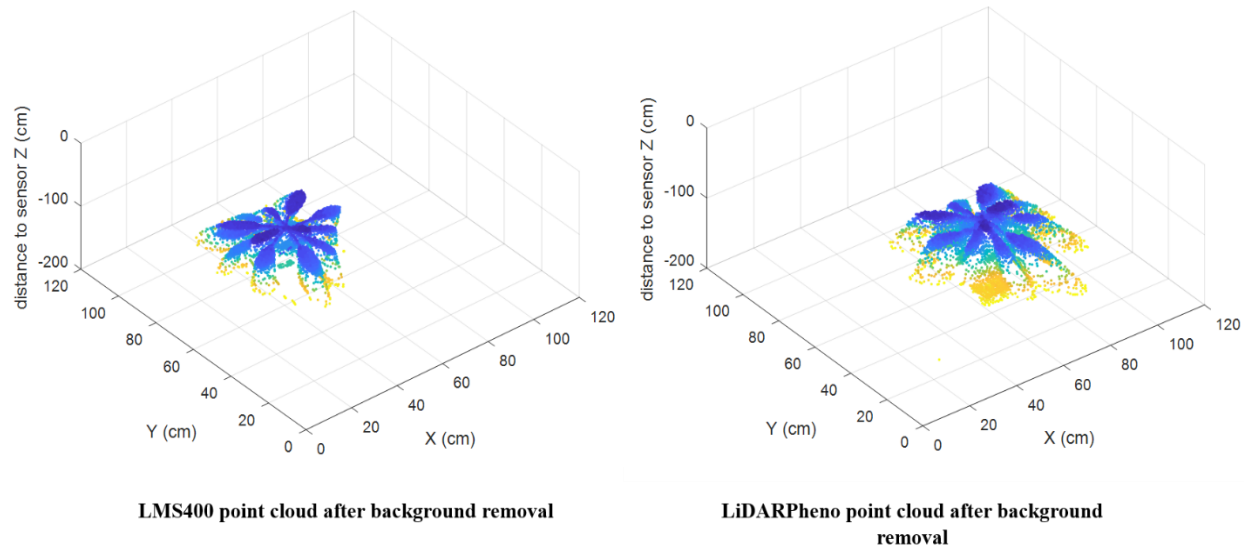

Figure 5-6: Point cloud representation after applying the distance and reflectance threshold

5.4 Filtering and Cleaning the Point Cloud Data

LiDAR range data tends to be noisy and have outliers because of the scattering of the light near the edges, reflectance property of an object, inclination angle of an object surface, and some environmental parameters (such as light intensity). Hence, often, it is required that the acquired point cloud be processed and filtered through a filtering algorithm. In our experiments, we have processed the point cloud data using various filtering algorithms including bilateral filter [76], but due to the nature of the plant leaf surface, they fail to perform satisfactorily. Consequently, a neighborhood-based filtering algorithm was developed for processing the point clouds. The algorithm developed for the point cloud filtering is presented in Algorithm 1. As there is no standard optimized algorithms (that the author know of) are available for specific trait extraction for LMS400 sensor, the ones presented in this thesis are used for processing and comparing the performance of the LiDARPheno acquired data.

Neighborhood-based filtering has been used widely in the field of image processing. The main idea behind this filtering algorithms is to find the neighbor points based on the user-defined window side. For each point in the point cloud, the algorithm finds its neighborhood based on the user-defined 3D window and number of points within that 3D box (voxel). If neighbor points within that window are more than the user-defined threshold, then the point is refined based on the average height of the neighboring points otherwise that point is discarded. Hence, it provides the functionality of both, point cloud filtering and outlier removal, in a straightforward algorithm. In the experiments, two iterations of this algorithm were used to refine the obtained point cloud. Parameters (3D voxel size and number of neighbors) can change for different leaf structures and sizes. The result of data point cleaning and filtering is shown in Figure 5-7.

5.4.1 Choosing parameters for Point Cloud Filtering algorithm

The parameters *voxelSize* and *numOfNeighbours* are dependent on each other. For example, the scan obtained at with the sensor at height of 80 centimeters and angular resolution of 0.2° will result in distance of ~3mm between two acquired points. Considering this theory, for a particular point in the point cloud, a box (voxel) of 2x2 cm around the point should have about 40 points in it when the point is located on the center of the leaf. The point that is on the edge of the plant's leaf might have around 20 points and the one on the tip of the leaf will have at least 5 or 6 neighboring points in the voxel of size 2 x 2 cm. The parameters for the filtering algorithm have

been chosen with this theory. Also, it is worth to note that angular resolution for LiDARPheno and LMS400 are different. Hence, the parameters change accordingly as well for LiDARPheno and LMS400.

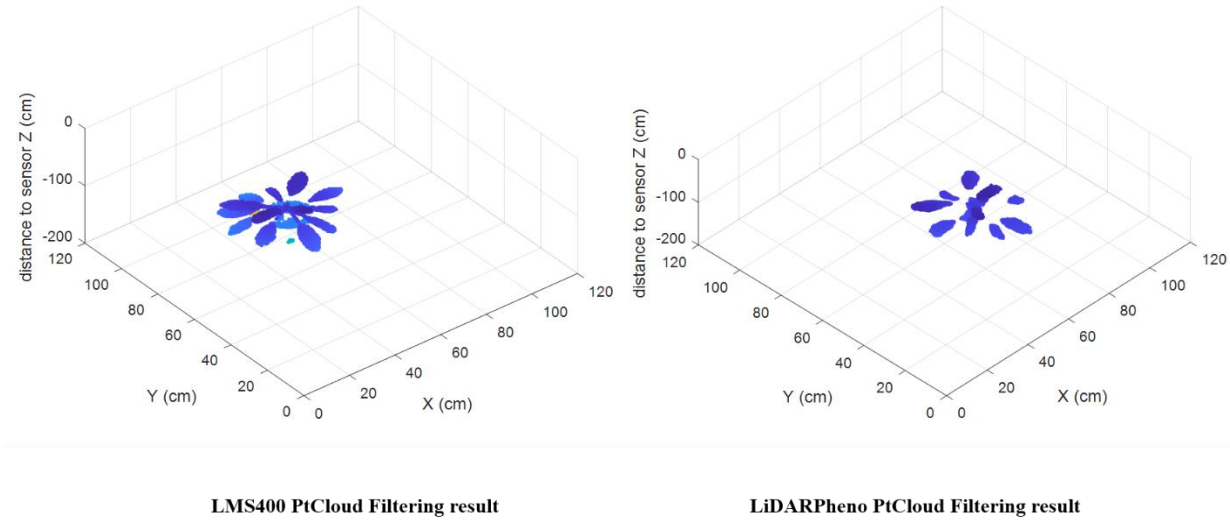

Figure 5-7: Point clouds after cleaning and filtering the noisy data points

Algorithm 1: Point Cloud Filtering

input: ptCloud, voxelSize, numOfNeighbours

output: filteredPtCloud

for each *point* $\in$ *ptCloud* **do:**

find euclidian distance to all points of *ptCloud*;

find neighbors belonging to the voxel of size *voxelSize*;

if neighbours >= *numOfNeighbours*

point = mean(neighbours);

else

point = 0;

end

end

5.5 Point Cloud Segmentation

Segmentation is the process of identifying each individual object from the image/point cloud. Generally, segmentation algorithms look at the features of the image or point cloud and use the pixels to group them into a region. This group of pixels in single or multiple regions indicates the individual object in the captured scene. In image-based segmentation methods, the intensity of a pixel is the sole support for the process. In contrast to images-based, point cloud segmentation provides a physical location of the point, and the 3 coordinates (X, Y, and Z) plays a vital role in the identification of the objects. However, the noise present in the point clouds may affect the performance of the algorithms. Hence, a proper point cloud filtering is required for the segmentation task.

In this work, a modified region-growing algorithm for segmentation of each leaf is used. Region-growing is a neighborhood-based algorithm that determines whether neighbors belong to a region or not. Conventional region growing segmentation algorithm (for image processing) requires a seed (pixel) to be selected beforehand and then the algorithm segments the image in different regions. In the modified algorithm, it not only selects seeds itself, but it also works with 3D point clouds. However, this modified region-growing algorithm segments the data at a slow rate and hence the improvement was added for it to work with so-called OcTree data structure, which improves the processing time by a massive amount because of the fact that instead of processing all the data points in the point cloud, it processes a block of points. This process of individual leaf segmentation results in each leaf identified and provides a set of points belonging to a particular leaf. Algorithm 2 below presents the working of the developed region-growing based segmentation algorithm.

In the segmentation algorithm, the octree structure of the point cloud is passed as an input along with maximum distance for the points to be considered in the region, a number of voxels necessary for a voxel to be in the region and threshold to merge the labels that belong to the same region. The segmentation algorithm checks each voxel in the octree of the point cloud and finds the neighbor within the maximum distance threshold. These neighbors are assigned a label that they belong to a particular region. After the main segmentation task is performed, there will be points which have been assigned different labels even though they belong to a single region.

Hence, the merging of that region is necessary. The merging is performed using the merge threshold. The threshold defines the maximum distance, in which if there are two different labels,

Algorithm 2: Point Cloud Segmentation

input: ocTree, maxDist, numOfNeighbours, mergThresh

output: labels, ptCloud

for each *voxel* $\in$ *ocTree* **do:**
    if *voxel* $\in$ *labels*
        do *nothing***;**
    else
        find euclidian distance to all *voxels* of *ocTree*;
        find neighbor voxels within *maxDist*;
        if neighbours >= *numOfNeighbours*
            assign a *label* to points belonging to that *voxel;*
        else
            voxel belongs to *non-region;*
        end
    end
end

for each *label* $\in$ *labels* **do:**
    find euclidian distance to all *other labels*;
    if any *label* within *mergThresh*
        merge labels;
    else
        do *nothing;*
    end
end

that two labels will be merged into a single label. Similar to point cloud denoising algorithm, the parameters for the segmentation have been chosen.

A result of segmentation on both the point clouds acquire with LMS400 and LiDARPheno are shown in Figure 5-8.

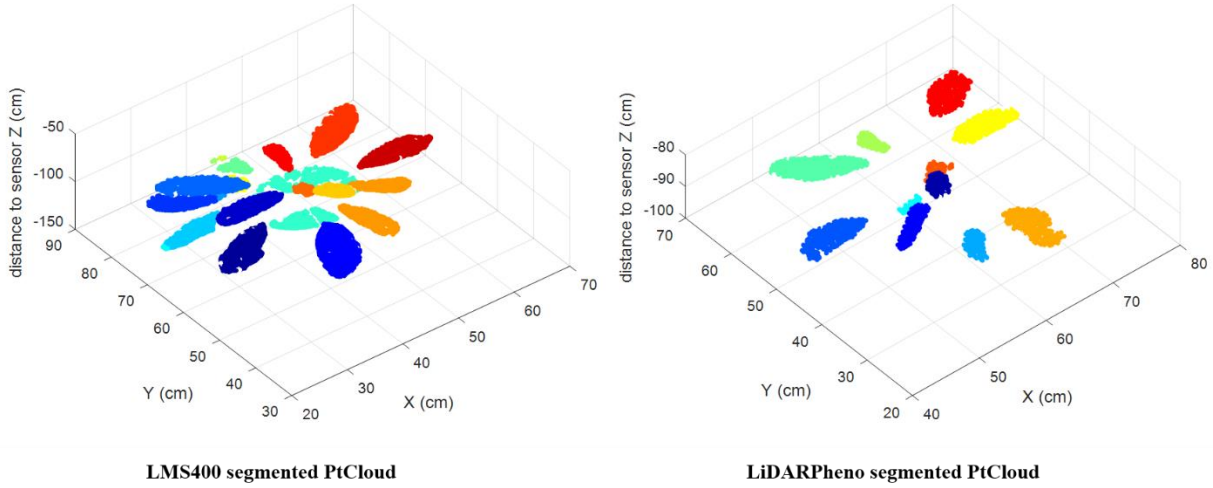

Figure 5-8: Result of segmentation on the point cloud data

5.6 Leaf Trait Extraction

Segmentation process identifies each leaf and assigns different color labels to each region identified which can be seen from Figure 5-8. These individual segments are treated as individual leaf and fed to the trait extraction module, where different traits (length, width, and area) are estimated using the point cloud data. In this work, the focus was on the extraction of leaf length, leaf width and leaf surface area. Methods of extracting each trait are explained in the following subsections.

5.6.1 Leaf Length

Extraction of leaf length from each of the segment was tricky part as each leaf might have a different orientation, size, and structure. Curve fitting on X and Y coordinates of the segmented points are used for the leaf length extraction.

First, the orientation of leaf is estimated using the minimum and maximum values of the X and Y coordinates of the segment. The absolute difference between the minimum and maximum

values provides the distance between these two. If the leaf is oriented along X-axis, the distance value between minimum and maximum along the X-axis will be the highest and vice versa. Then a polynomial of degree 2 is applied to fit X and Y coordinates which results in an equation (5-6).

$$Y = a * X^2 + b * X + c \tag{5-6}$$

where:

- X is a vector of X coordinates in the segment containing 3D data points
- Y is a vector of Y coordinates that can be estimated using the equation
- a, b, and c are constants that are obtained using polynomial fit to X and Y coordinates of the point cloud data

If the leaf is oriented along X-axis, 50 equally spaced samples are taken between the minimum and maximum value of X coordinates in that segment, and corresponding Y coordinates are estimated and vice-versa. With these obtained X and Y coordinates, nearby points from the original segment are obtained to get a straight line between the minimum and the maximum value of the X or Y coordinate. After that Euclidean distance between each point of the obtained line is calculated using equation (5-7).

$$euclidean\_distance(a, b) = \sqrt{(a_x - b_x)^2 + \left(a_y - b_y\right)^2 + (a_z - b_z)^2} \tag{5-7}$$

where:

- "a" and "b" are two points in a 3D space
- a_x, a_y, a_z and b_x, b_y, b_z are corresponding x, y, and z coordinates of point "a" and "b", respectively.

All these Euclidean distances are added together, which results in the length of the leaf. This process of obtaining leaf length is repeated for all the segments (leaves). Figure 5-9 presents the point cloud of a single leaf, segmented using a segmentation algorithm. This one segment is used to measure the leaf length using the above-mentioned method of curve fitting on the X and Y coordinated of the segment of the point cloud. The red color dots in the 3D scatter plot shows the curve fitting points, and blue color points are the actual point cloud data points. The similar technique is used for width measurement.

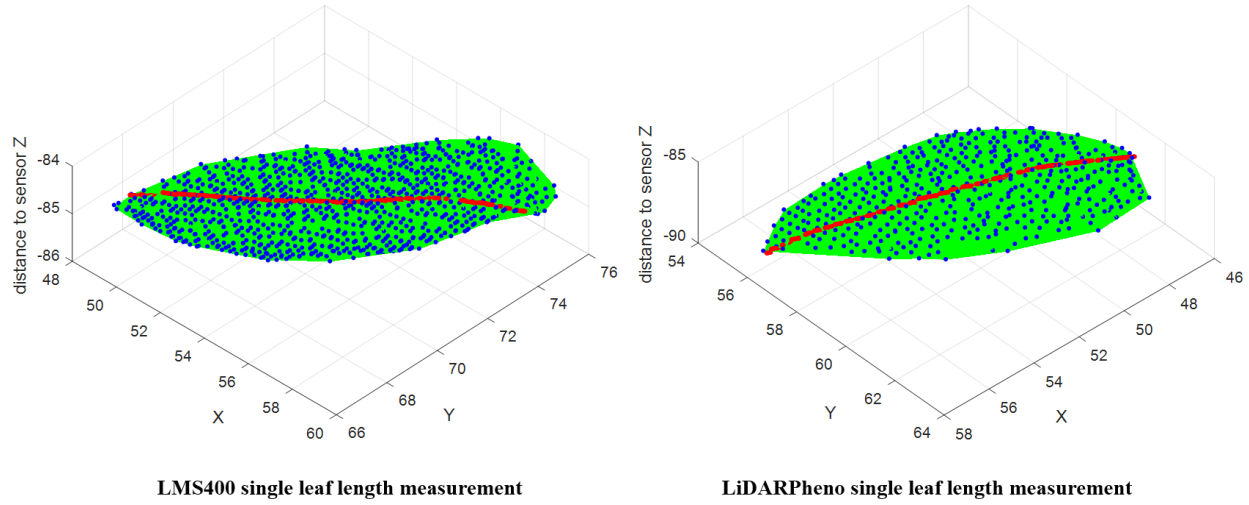

Figure 5-9: Measurement of leaf length using a curve fitting method

5.6.2 Leaf Width

Similar to the process of the leaf length estimation, each segment is processed through curve fitting and estimation of line. However, the only difference in width estimation is that if the leaf is aligned to X-axis, leaf width is estimated along the Y-axis and vice-versa. The main idea here is to use the processing of leaf length estimation and drawing a parallel line with the leaf length estimation line. Consequently, estimation of leaf length makes leaf width estimation relatively less complicated as it used the same technique as the length estimation.

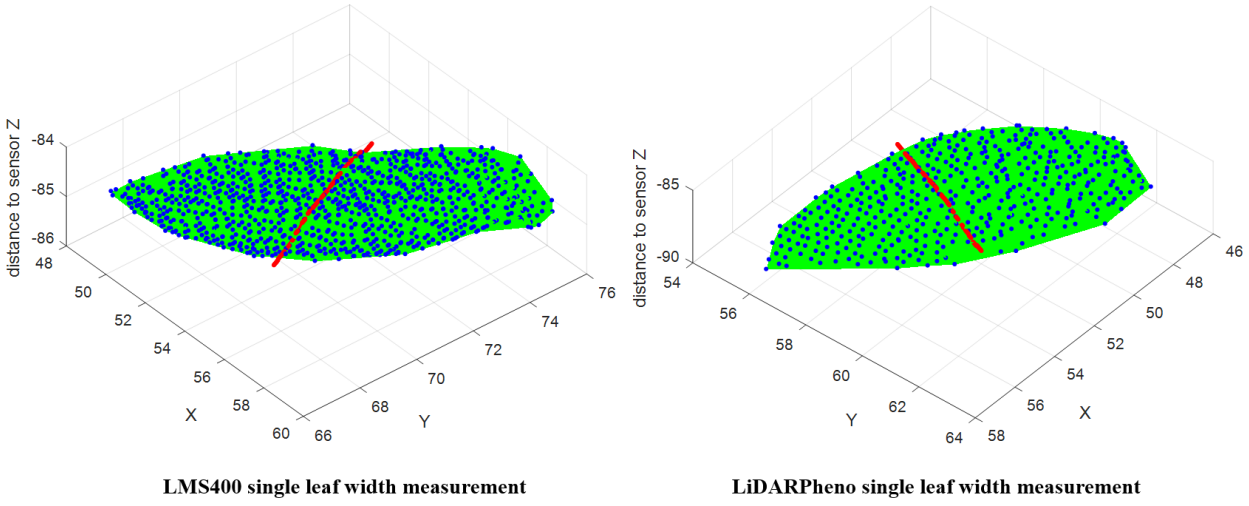

Figure 5-10: Measurement of leaf width using a curve fitting method

Similar to Figure 5-9, Figure 5-10 represents a single leaf, segmented using the segmentation algorithm. The red colored points represent the sampling points used for leaf width measurement and blue points are the actual point cloud points. Values on the graph are in centimeters (cm).

5.6.3 Leaf Area

Leaf surface area estimation is a different process than the estimation of leaf length and leaf width. Data points for each leaf are available, which can be used to estimate the leaf surface area. We have used a widely accepted Delaunay triangulation [77] method for generating triangles or surface from 3D point cloud data. Figure 5-11 shows the triangulation of one of the segmented leaf of an arbitrary wild plant scan using LMS400 and LiDARPheno. All the axis values are in centimeters (cm).

We use MATLAB function *delaunayTriangulation()* for generating triangles from the 3D data points[2]. Then the area of each triangle is calculated and added to get the area of the surface. For any three points A(x, y, z), B(x, y, z), and C(x, y, z) in a 3D space, surface area of that 3D triangle can be calculated using equation[3] (5-8).

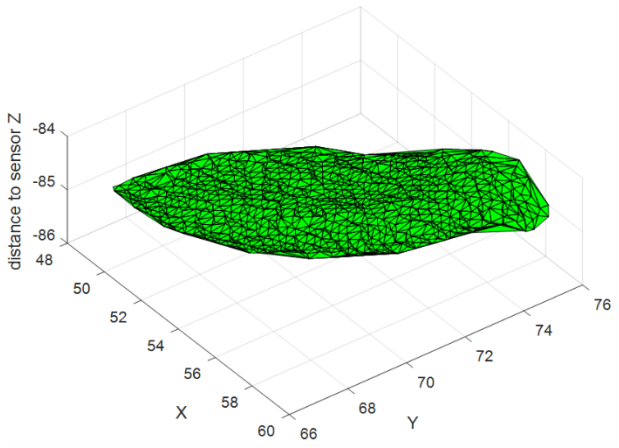

LMS400 leaf PtCloud triangulation

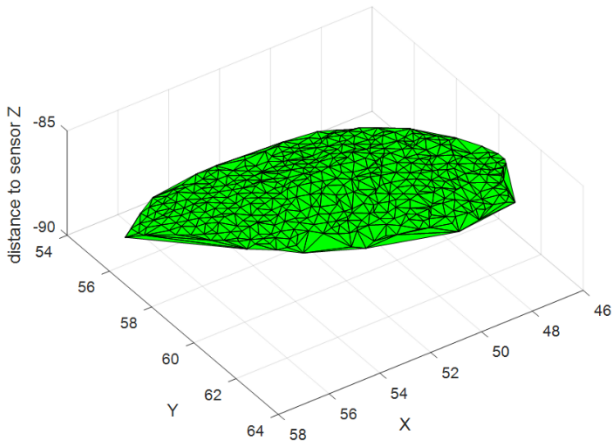

LiDARPheno leaf PtCloud triangulation

[2] https://www.mathworks.com/help/matlab/ref/delaunaytriangulation.html
[3] https://en.wikipedia.org/wiki/Triangle

Figure 5-11: Delaunay triangulation of the leaf point cloud data

$$Area(A,B,C) = \frac{1}{2}\sqrt{\begin{vmatrix} A_x & B_x & C_x \\ A_y & B_y & C_y \\ 1 & 1 & 1 \end{vmatrix}^2 + \begin{vmatrix} A_y & B_y & C_y \\ A_z & B_z & C_z \\ 1 & 1 & 1 \end{vmatrix}^2 + \begin{vmatrix} A_z & B_z & C_z \\ A_x & B_x & C_x \\ 1 & 1 & 1 \end{vmatrix}^2} \quad (5\text{-}8)$$

Area of each triangle generated using Delaunay triangulation are calculated and added to get the final surface area of the leaf.

5.7 Parameters used in post-processing steps.

Post-processing steps on the LiDARPheno data and LMS400 data involves mainly two algorithms, cleaning and segmentation. For cleaning the point cloud data obtained using LiDARPheno, the voxel of 2x2 centimeter and minimum number of neighbors of 5 were chosen with trial-and-error methods and obtained visually appealing results. For LMS400 data, as the point cloud is dense, the parameters voxel size of 1x1 cm and 10 number of neighbors were adequate for filtering the LMS400 acquired data. As the scanning distance was same for all the experiments, the same threshold parameters were used for all the acquired data.

For segmentation algorithm, 1.5 cm was chosen as the distance threshold while the minimum number of neighboring voxels were kept to one. Also, merge threshold of 0.8 cm was applied for checking the overlap between labels as well as merging the nearby labels. The segmentation algorithm first does the rough segmentation and then merges the labels generated. Hence, there were no assumptions made of how many labels will be there in the scene. All the results presented in the chapter 6 are obtained using these threshold and parameters.

Chapter 6

Results and Discussion

This chapter provides the results and comparative analysis of the estimation of the plant leaf traits using LMS400 and LiDARPheno acquired 3D data. Section 6.1 provides the annotated images of the plants used in the experiments. Section 6.2 compares the results of estimation of the traits with the ground truth data. Finally, Section 6.3 discusses the comparison between estimates of the LMS400 and LiDARPheno acquired data and a comparative analysis of the two systems and their utility in the plant phenotyping tasks.

6.1 Leaf Number Annotation

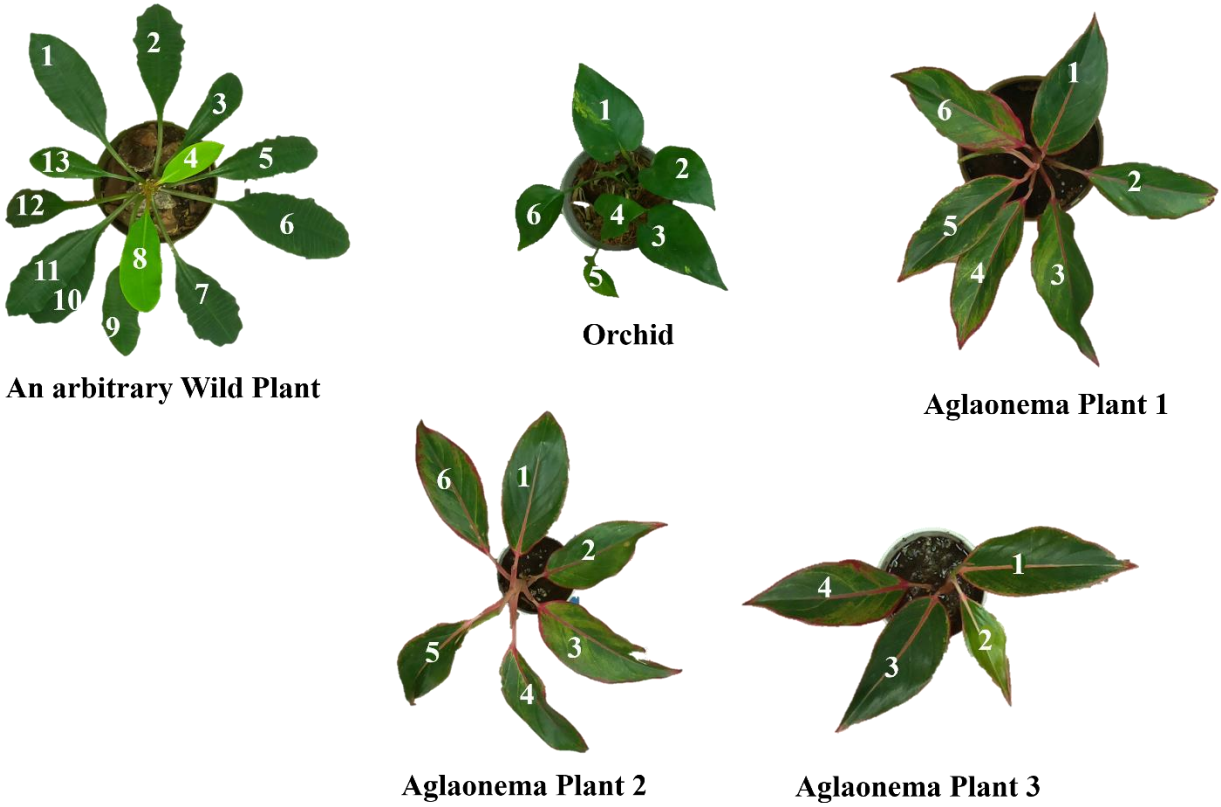

Figure 6-1: Annotated RGB images of the plants for Experiment 1

Figure 6-1 shows the images of the different plants used in experiment 1. These images are used as a reference to represent the leaf in the results section of this thesis. Generally, leaf numbers are given in the clockwise direction. For example, if the result table refers to the leaf 1 of an arbitrary wild plant, the leaf annotated with number 1 is being referred. Also, the annotated leaf number was used in the auto-calculation of the error rate and generate a report in the form of an excel file. Similarly, Figure 6-2 shows the leaf number annotation for the experiment 2 of this study.

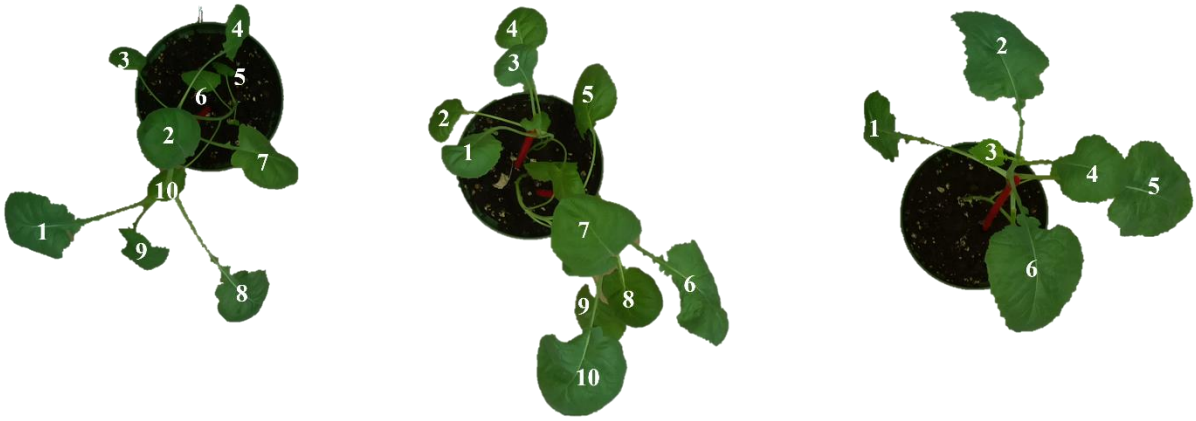

Figure 6-2: Annotated RGB images of the canola for Experiment 2

6.2 Trait Extraction Results

Absolute Percentage Error (APE) is used to evaluate the results of the estimation of the leaf traits (length, width, and area). Two experiments were performed in this work, one is on the indoor plants shown in Figure 6-1 and another, for validation, on canola plants presented in Figure 6-2. Following subsection present the results of the trait estimation using the developed methodologies. Equation (6-1) is used to calculate the percentage error of estimation.

$$APE = \frac{|ActualValue - estimatedValue|}{ActualValue} * 100 \quad (6\text{-}1)$$

6.2.1 Leaf Length Estimation Results

6.2.1.1 Experiment 1 Leaf Length Estimation Results

Experiment 1 consisted of five plants with three different species of indoor plants. Table 6-1 shows the results of the leaf length estimation using LMS400 and LiDARPheno and the error rate of the estimation.

Table 6-1: Leaf length estimation results for an arbitrary wild plant

Leaf #	Ground Truth Length (cm)	LMS400 Estimated Length (cm)	%Error	LiDARPheno Estimated Length (cm)	%Error
1	14.10	12.14	13.90	14.42	2.24
2	16.90	17.53	3.71	11.88	29.70
3	11.10	10.26	7.57	10.16	8.45
4	7.80	7.18	8.00	8.58	10.05
5	14.40	13.98	2.91	13.04	9.43
6	17.00	18.11	6.52	15.81	6.97
7	14.00	14.26	1.85	10.85	22.52
8	11.40	11.62	1.91	11.67	2.33
9	14.00	13.07	6.63	*N/A*[4]	*N/A*
10	15.20	15.04	1.03	*N/A*	*N/A*
11	14.60	14.83	1.56	12.85	11.97
12	14.90	11.20	24.82	*N/A*	*N/A*
13	9.40	6.78	27.83	8.00	14.93
Mean %Error:			**8.33**		**11.86**
Minimum %Error:			**1.03**		**2.24**
Maximum %Error:			**27.83**		**29.70**

[4] N/A: Not detected in the segmentation process

It is evident from the Table 6-1 that leaf length estimations using the developed LiDARPheno system data are reasonably comparable to the one acquired using the LMS400 commercial LiDAR. However, the LiDARPheno acquired point cloud is not as dense and due to the density of the point cloud, some of the leaves are not detected or filtered out in the filtering algorithm. These leaves in an arbitrary wild plant are leaf numbers 9, 10 and 12. If looked carefully in Figure 6-1, those leaves are occluded by another leave, or they are inclined, i.e., due to the inclination angle, LiDARPheno was not able to capture enough number of points to be considered by algorithms to be an object.

The mean (average) error rate for the LiDARPheno and LMS400 are quite similar, LMS400's mean error rate for estimation of the leaf length is 8.33% while that of the LiDARPheno is 11.86%. The maximum error rate for the leaf length estimation using the LiDARPheno data was 29.7% while for the LMS400 it was 27.83%. The minimum error rate of estimating the leaf length is about 1.03% for the LMS400 data, and 2.24% for the LiDARPheno acquired data. Table 6-2 shows the results of the estimation for the remaining plants in experiment 1. It can be seen from the table that results for length estimation on the orchid plant are similar for LiDARPheno and LMS400. However, the mean error rate remains below 25%.

Table 6-2: Leaf length estimation results for the Experiment 1

	Orchid		**Aglaonema Plant 1**		**Aglaonema Plant 2**		**Aglaonema Plant 3**	
%Error	**LMS-400**	**LiDAR-Pheno**	**LMS-400**	**LiDAR-Pheno**	**LMS-400**	**LiDAR-Pheno**	**LMS-400**	**LiDAR-Pheno**
Mean:	22.85	20.75	9.08	18.43	10.52	23.24	3.75	11.16
Minimum:	0.08	5.44	0.58	5.19	2.65	8.52	0.87	5.47
Maximum:	37.54	35.03	29.30	38.45	36.10	35.61	8.37	18.22
Not detected:	*Leaf #5*	*Leaf #5*						

6.2.1.2 Experiment 2 Leaf Length Estimation Results

Experiment 2 consists of two parts and three canola plants. The data for experiment 2 – part "a" were acquired on June3rd, 2018 and for part "b" of the experiment on June 17th, 2018. In part "a" of the experiment, data from two canola plant pots, one with only canola and other with two canola plants in it, were acquired. An RGB image of the two pots for part "a" of the experiment are shown in Figure 6-2 as "Canola Plant 1" and "Canola Plant 2". Results of experiment 2 on canola plants are presented in Table 6-3.

Table 6-3: Results of leaf length estimation on Canola plants.

	Canola Plant 1		**Canola Plant 2**	
	LMS400	**LiDARPheno**	**LMS400**	**LiDARPheno**
Mean %Error:	23.56	28.97	11.36	14.73
Minimum %Error:	0.14	7.99	0.32	0.51
Maximum %Error:	39.77	50.70	30.22	39.40
Non-detected Leaves:	*Leaf #5, 10*	*Leaf #2,4,5,10*	*Leaf #9*	*Leaf #2,3,8*

The results presented indicate that the leaf length of the canola plant estimated using LMS400 and LiDARPheno remains similar, but the number of leaves that remain undetected has increased. This is due to the shape and size of the canola plants used in the experiment. The average length of the leaf for both canola pots was around 5 cm, and the shape was circular. This leads to the less number of points being acquired from the plant object, i.e., leaves. Furthermore, the number of points being acquired also depends on the distance of the LiDAR sensor to the plant as the less distance mean the small area being scanned and high resolution between two points acquired.

The impact of the distance to LiDAR on the performance was evaluated. Part "b" of experiment 2 was performed while keeping the plant distance to LiDAR at approximately 80 cm, 60 cm, and 40 cm, respectively. However, the LMS400 was not moved due to its limitation of the distance where it can acquire data (70 cm minimum distance to object). Only LiDARPheno was used to acquire data at different distances mentioned above and only one data acquisition with

LMS400. The canola plant used for this part of the experiment is shown in Figure 6-2 as "Canola Plant 3". Results of the leaf length estimation when data were acquired with different distance to the sensor are presented in Table 6-4.

Table 6-4: Results of experiment 2 – part "b" on Canola Plant 3

	Canola Plant 3			
	LMS400	**LiDARPheno at ~80cm**	**LiDARPheno at ~60cm**	**LiDARPheno at ~40cm**
Mean %Error:	23.57	29.61	54.92	20.83
Minimum %Error	3.88	8.07	4.74	3.89
Maximum %Error:	57.49	63.45	190.75	59.57
Non-detected Leaves:		*Leaf #1,5*	*Leaf #1,5*	

The error rate for the canola 3 reduces, and all the leaves of were detected when the plant was kept approximately 40cm away from the LiDARPheno during data acquisition. Hence, the distance of the device to plant is a critical parameter in data acquisition. The distance to the object being scanned using the LiDARPheno device is also responsible for the distance between two points when converted to the Cartesian coordinate system. Results of experiment 2 – part "b" have proven the theory of dependency of the point cloud and the estimation accuracy or the error rate.

6.2.1.3 Estimation and Ground Truth Leaf Length Relation

The relation between the ground truth and estimation results can be best represented using the linear correlation plot. In this work, the Root Mean Square Error (RMSE) and coefficient of determination (r^2) are used to represent the relationship between the ground truth data acquired using the manual measurement of the leaf length and the estimated leaf length using the LMS400 data. Figure 6-3 shows the relation between the estimation using LMS400 data and the ground truth leaf length. RMSE was calculated using the equation (6-2).

$$RMSE = \sqrt{\frac{\sum_{i=1}^{n}(groundTruth_i - estimate_i)^2}{n}} \quad (6\text{-}2)$$

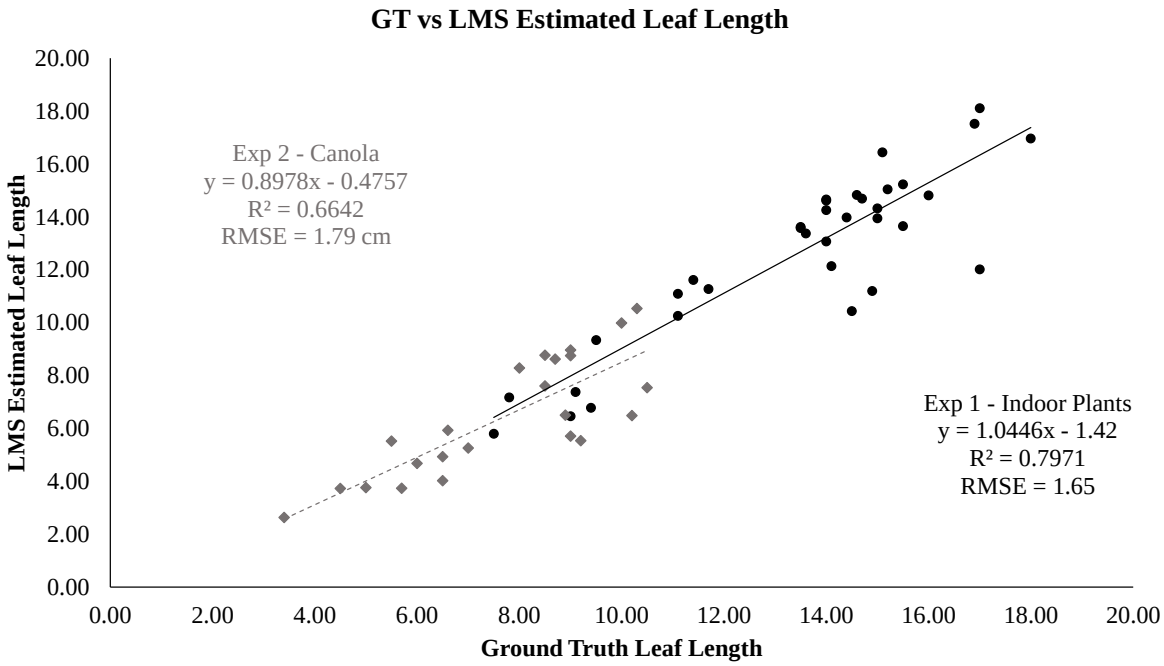

Figure 6-3: Relation between estimation with LMS400 data and ground truth leaf length

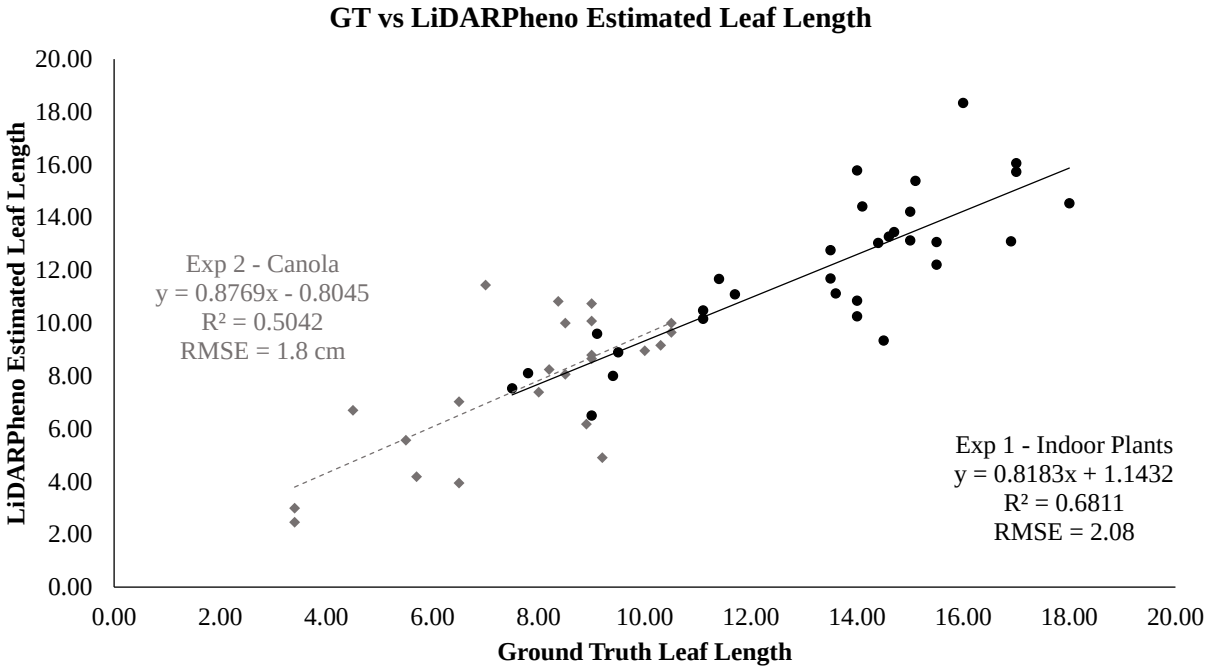

Figure 6-4: Relation between LiDARPheno estimated leaf length and ground truth

The data acquired with LMS400 for experiment 1 on indoor plants show a good relationship between the two with $r^2 = 0.7971$ and RMSE of 1.65 cm. Experiment 2 on the canola plants, however, has an $r^2 = 0.6642$ and RMSE = 1.79 cm.

On the other hand, the estimate for the leaf length from the LiDARPheno data indicates RMSE of 2.08 and 1.8 cm for experiment 1 and experiment 2 respectively. Moreover, the coefficient of determination for experiment 1 and experiment 2 is $r^2 = 0.6811$ and $r^2 = 0.5042$, respectively.

6.2.2 Leaf Width Estimation Results

6.2.2.1 Results for Leaf Width Extraction

Similar to the leaf length estimation, the leaf width estimation is done using the curve fitting method described in section 5.6. Results of the leaf width extraction done on experiment 1, experiment 2 – part "a" and experiment 2 – part "b" are represented in Table 6-5, Table 6-6 and Table 6-7, respectively.

Table 6-5: Leaf width estimation results using LiDARPheno (LP) and LMS400 (LMS)

	Arbitrary Wild plant		**Orchid**		**Aglaonema Plant 1**		**Aglaonema Plant 2**		**Aglaonema Plant 3**	
%Error	**LMS**	**LP**	**LMS**	**LP**	**LMS**	**LP**	**LMS**	**LP**	**LMS**	**LP**
Mean:	17.82	10.77	13.61	17.81	19.21	37.73	11.37	16.24	8.67	15.35
Min:	2.21	0.93	3.27	5.12	6.05	0.27	1.60	3.07	7	5.21
Max:	42.14	28.35	27.30	36.09	58.69	90.37	22.10	39.45	10.65	33.99

The leaf width estimation for the data acquired in experiment 1 is shown in Table 6-5. From the table, it can be interpreted that the estimation of the width with the LMS400 acquired data and the LiDARPheno data are quite similar, except for the Aglaonema plant. The reason for the error increase in the Aglaonema plant might be the plant itself. However, in this study, the reason for the increase in error is not explored. The best distinguishable feature is the leaf color,

which is reddish around the edge of the leaf, which might be a potential reason for increased error for the LiDARPheno data.

Table 6-6: Results of Leaf width estimation on canola plants – experiment 2

	Canola Plant 1		Canola Plant 2	
	LMS400	**LiDARPheno**	**LMS400**	**LiDARPheno**
Mean %Error:	27.32	35.23	21.14	30.59
Minimum %Error:	8.98	10.53	2.88	14.03
Maximum %Error:	52.63	45.00	42.78	65.59

Table 6-7 : Results of leaf width estimation at a different height

	Canola Plant 3			
	LMS400	**LiDARPheno at ~80cm**	**LiDARPheno at ~60cm**	**LiDARPheno at ~40cm**
Mean %Error:	19.83	4.67	31.46	18.26
Minimum %Error	3.48	0.14	20.34	3.33
Maximum %Error:	58.21	7.87	54.82	52.03

Experiment 2 with two parts and different distance for the second part of the experiment shows the similar results. In Table 6-7, it can be seen that LiDARPheno at the distance of 80 cm performs best for width estimation. However, the number of leaves detected in the data acquired at 80 cm were just a few and hence the overall estimation for leaf width are better. Moreover, it can be seen that the estimation results when the data was acquired while keeping the distance around 40 cm are similar to that of the LMS400. Overall, the width estimation also depends on the density of the point cloud, highly dense point cloud exhibits the better estimations.

6.2.2.2 Estimation and Ground Truth Leaf Width Relation

The relationship between the ground truth data and the estimated leaf width with LMS400 and LiDARPheno data is shown in Figure 6-5 and Figure 6-6.

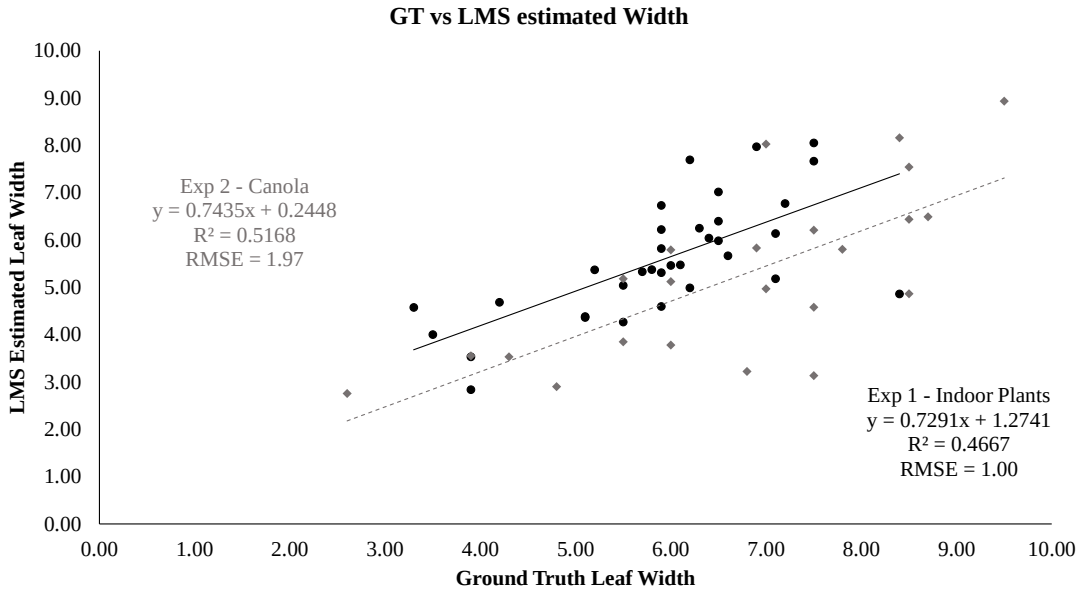

Figure 6-5: Correlation plot for estimated width using LMS400 and ground truth

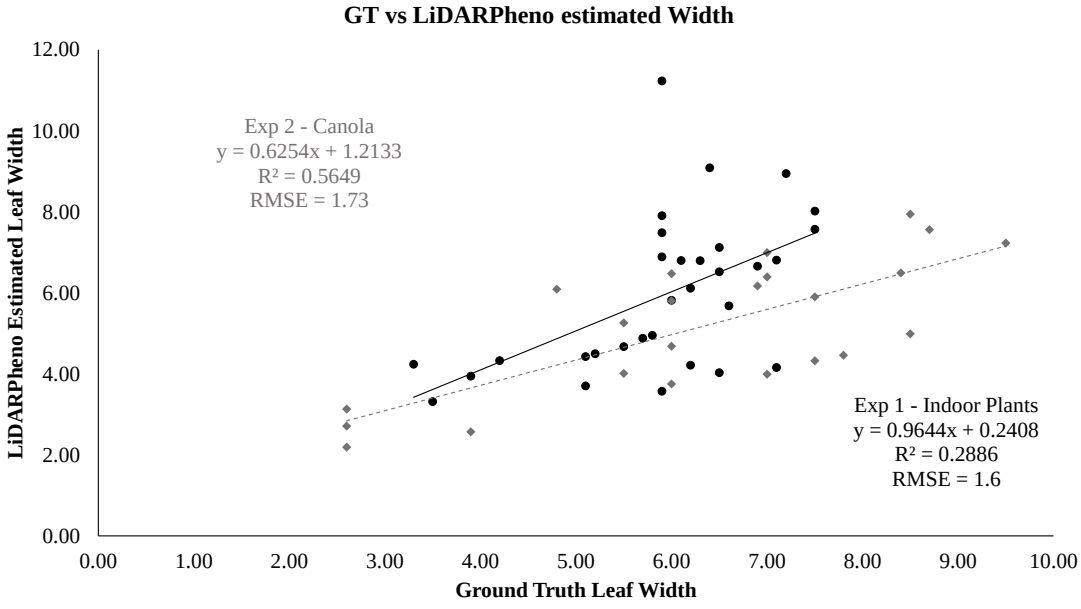

Figure 6-6: Correlation plot for estimated width using LiDARPheno and ground truth

The estimation of the leaf width using LMS400 data has RMSE of 1 cm in experiment 1 and RMSE = 1.97 cm for experiment 2. Coefficient of determination $r^2 = 0.47$ and $r^2 = 0.5168$ was achieved for experiment 1 and experiment 2, respectively.

On the other hand, estimation of the width using LiDARPheno data have RMSE = 1.6 cm for plants in experiment 1 and RMSE = 1.73 cm for plants in experiment 2. The correlation coefficients r^2 are 0.29 and 0.56 for experiment 1 and experiment 2, respectively.

6.2.3 Leaf Area Estimation Results

6.2.3.1 Results for Leaf Area Estimation

Results for the area estimation using the triangulation method on point cloud data is shown in Table 6-8, Table 6-9, and Table 6-10 for experiment 1, experiment 2 – part "a", and experiment 2 – part "b", respectively.

Table 6-8: Leaf Area estimation results using LiDARPheno (LP) and LMS400 (LMS)

	Arbitrary Wild plant		**Orchid**		**Aglaonema Plant 1**		**Aglaonema Plant 2**		**Aglaonema Plant 3**	
%Error	**LMS**	**LP**	**LMS**	**LP**	**LMS**	**LP**	**LMS**	**LP**	**LMS**	**LP**
Mean:	34.37	27.5	26.51	21.82	26.16	42.00	23.41	42.44	16.57	11.16
Min:	11.84	3.30	9.55	12.26	12.02	2.10	10.45	28.34	1.46	3.31
Max:	62.70	52.84	44.78	39.97	49.44	68.27	49.79	58.29	32.11	20.86

In the above table, the error rate for the estimation of the leaf area using the point cloud is provided. The estimation of leaf area for the wild plant outperforms the results for the LMS400. The wild plant's most leaves are facing straight at the scanning system, which can be seen in Figure 6-1. Due to the better exposure of leaves to the scanning system, most of the area of the leaves is captured by the scanning system. However, due to the loss near the edge of the leaves and inclination angle of the leave, some of the points belonging to the leaf gets discarded and results in the erroneous estimation of the area of the leaves.

Table 6-9: Results of leaf area estimation on canola plants – experiment 2

	Canola Plant 1		Canola Plant 2	
	LMS400	**LiDARPheno**	**LMS400**	**LiDARPheno**
Mean %Error:	49.93	44.75	40.76	48.20
Minimum %Error:	27.92	4.20	13.43	30.30
Maximum %Error:	62.71	75.95	62.97	71.63

Results of the estimation of the leaf area in canola plants (experiment 2) are represented in Table 6-9. The error rates for the leaf area estimation are disappointing, but the canola plants tend to have curvy surface and to get all the points belonging to the leaf is difficult with the scan performed using the only top view. Hence, an alternate method to capture the whole 3D point from a different view angle is necessary.

Table 6-10: Results of leaf area estimation at a different height

	Canola Plant 3			
	LMS400	**LiDARPheno at ~80cm**	**LiDARPheno at ~60cm**	**LiDARPheno at ~40cm**
Mean %Error:	28.5	43.04	22.80	44.54
Minimum %Error	2.16	16.54	11.35	9.34
Maximum %Error:	78.07	65.56	35.91	91.86

Error rate results for the canola, while keeping the LiDARPheno at different distances, are presented in Table 6-10. When the distance between the canola plant and LiDARPheno was about 40 cm, all of the leaves of the canola plant can be detected. However, leaf number 1, 3 and 5 produces the most error (more than 40%). The reason behind this substantial error rates is the inclination angle, overlapping leaves, and size of the leave. Leaf number 1 is profoundly declined and obtaining all the points belonging to that leaf is nearly impossible with just a top view scan.

Leaf number 3 is relatively small (~ 5 cm^2), which does not provide enough points to be processed. Leaf 4 and 5 are overlapping and are at the same height as well as leaf number 5 is a curved leaf. These reasons make the estimation process erroneous. However, leaf numbers 2, 4 and 6 are providing a relatively accurate estimation of the leaf area (below 25%) for both LMS400 and LiDARPheno.

6.2.3.2 Estimation and Ground Truth Leaf Area Relation

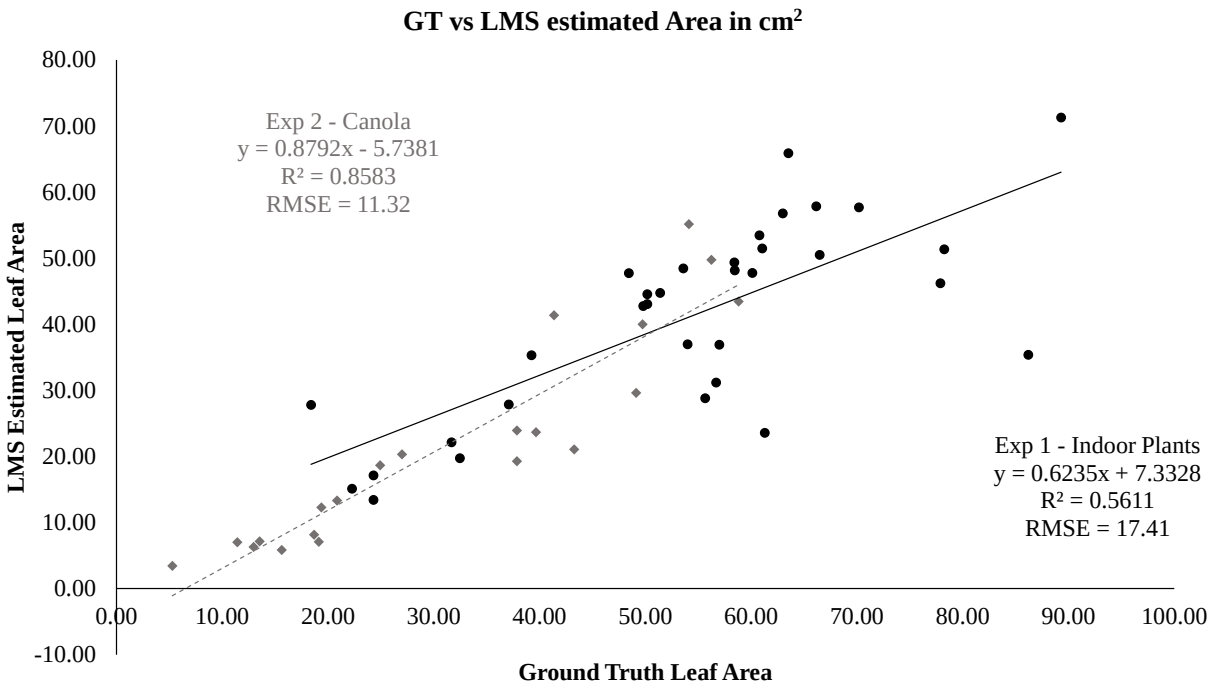

Figure 6-7: LMS400 Estimate area and ground truth area relation

The relation between LMS400 estimated area and ground truth leaf area us shown in the plot of Figure 6-7. For the experiment 1, the coefficient of the determination r^2 is 0.5611 and RMSE of 17.41 cm^2. The experiment 2 on canola plants shows a better correlation with the ground truth leaf area with r^2 = 0.8583 and RMSE of 11.32 cm^2. This suggests the LMS400 is able to correctly estimate the leaf area for the values below 60 cm^2 and more than that it fails to estimate the leaf area correctly. However, the quality of data acquisition is also dependent on the plant material. For example, the better reflection is necessary for any LiDAR sensor to correctly estimate the distance to that plant, which results in the point cloud.

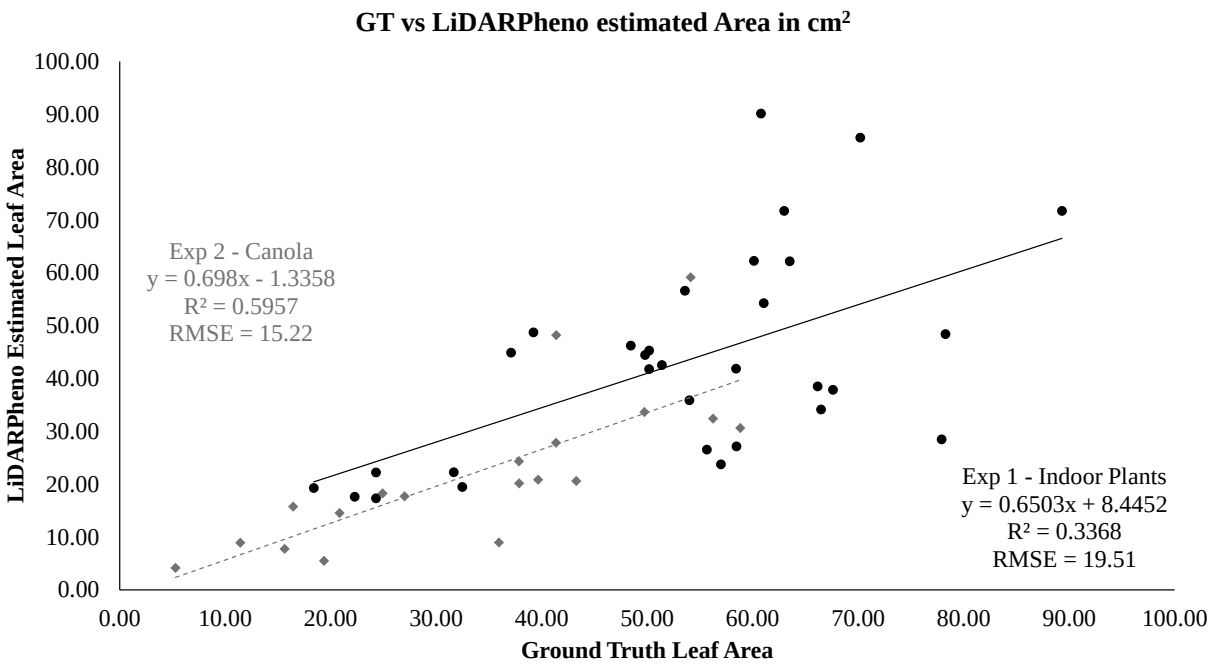

Figure 6-8: LiDARPheno estimated leaf area and ground truth relation.

The leaf area computed using the LiDARPheno point cloud data, and ground truth are related using the scatter plot and linear regression in Figure 6-8. Experiment 1 on the various plants of three different species has an RMSE of 19.51 cm^2 when compared to the ground truth leaf area while $r^2 = 0.3368$. For experiment 2 on the canola plants, the leaf area estimation results using the LiDARPheno data are compared to the ground truth, and the RMSE of 15.22 cm^2 is achieved. Moreover, the r^2 of 0.5957 shows good relation to ground truth data.

6.3 Comparing LiDARPheno and LMS400 Derived Results

The comparisons of the results derived with two different systems, LiDARPheno and LMS400, are presented using the correlation plots of the trait estimation data. Figure 6-9 shows the comparison of the LMS400 and LiDARPheno derived leaf length; Figure 6-10 shows the comparison of the leaf width extraction using two different data, and the relation between the leaf areas estimated using the two systems is presented in Figure 6-11. The relation can be determined using the coefficient of determination (r^2) and RMSE between two results.

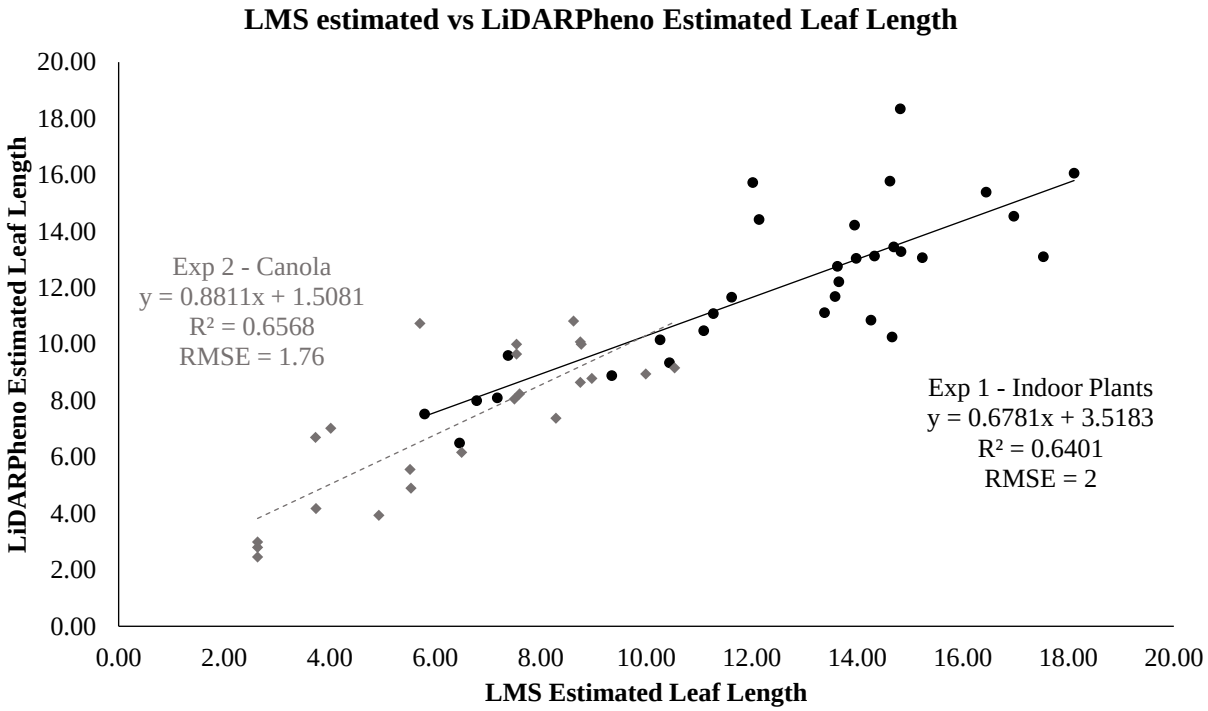

Figure 6-9: Relationships between LiDARPheno-derived and LMS400-derived leaf lengths

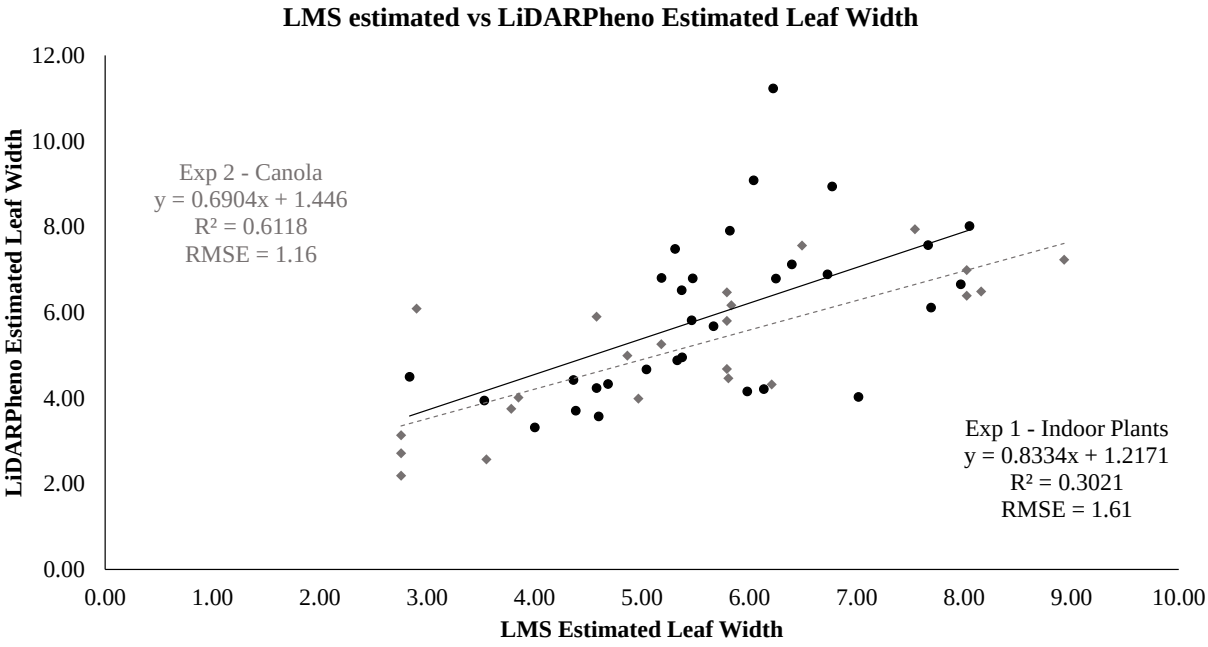

Figure 6-10: Relationships between LiDARPheno-derived and LMS400-derived leaf widths

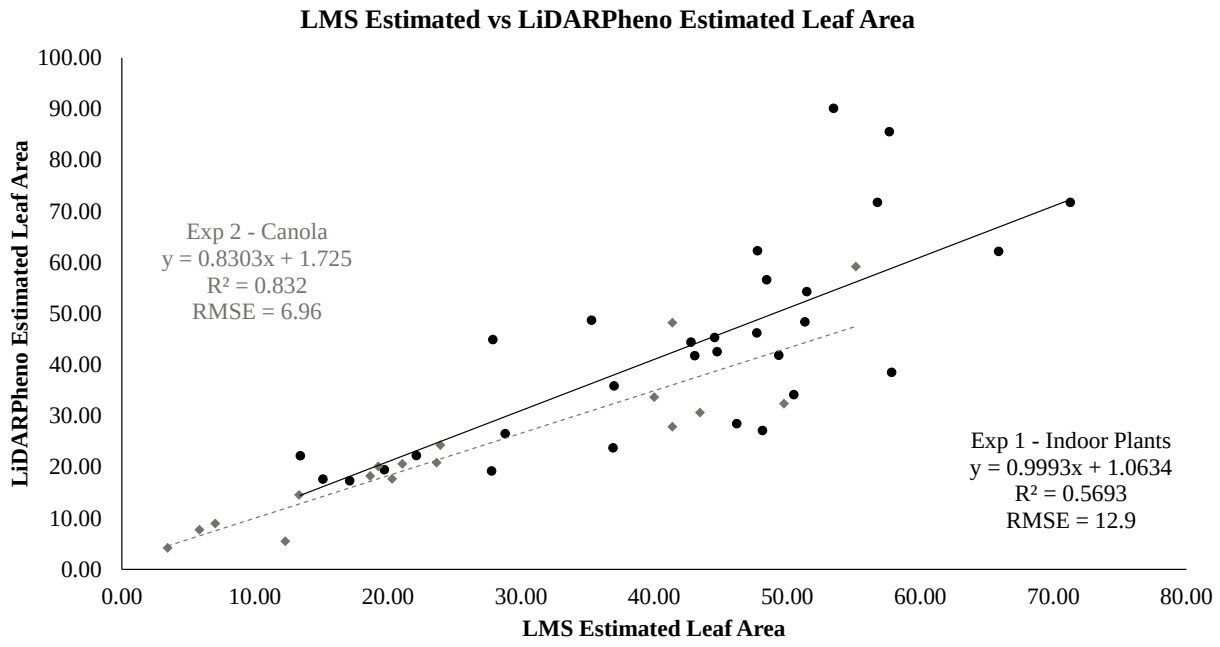

Figure 6-11: Relationships between LiDARPheno-derived and LMS400-derived leaf areas

The leaf length estimation using the commercial LiDAR system LMS400 and LiDARPheno data has a good correlation with the r^2 of 0.64 and 0.66 for experiment 1 and experiment 2, respectively. Moreover, the RMSE of 2 cm in experiment 1 and 1.76 cm in experiment 2 was achieved. The leaf length measurements relation between LMS400-derived and LiDARPheno-derived results indicate that there is a reasonable level of agreement between results estimated using two different data obtained with two different LiDAR sensors.

In Figure 6-10, the relationships between the leaf width measurements using the LMS400 and LiDARPheno data is compared using the linear regression plot. The RMSE of 1.61 cm for experiment 1 and 1.16 cm for experiment 2 indicates the error of estimation in cm. However, the correlation between the two is r^2=0.3021, and r^2=0.6118 for experiment 1 and experiment 2 are presented. This indicates the feasibility of the developed LiDARPheno system to compete with the commercial LiDAR system. The agreement in results of experiment 2, where relatively small canola leaves were scanned, is more satisfactory than the leaf length.

The leaf area measurement agreement between the two LiDAR-based systems is shown in Figure 6-11. The leaf area measurements with both the systems show a functional relationship between the two LiDAR data. For the experiment on indoor plants, the r^2=0.5693 and RMSE of

12.9 cm^2 are achieved, and experiment on canola plants show r^2=0.832 and RMSE = 6.96 cm^2. The relation of the estimating the leaf area using the 3D point cloud data is entirely satisfactory. The results on a canola show excellent agreement for leaf area extraction using LMS400 and LiDARPheno.

Table 6-11: Comparison of the LMS400-based system with LiDARPheno

	LMS400–based system	**LiDARPheno**
Material Cost	~ $10,000	**~ $400**
Scan ready?	No (Requires external setup to hold the LiDAR and move it along scan direction)	**Yes** (The LiDARPheno is designed to work independently of any external requirements)
Setup	Bulky (~1.5kg for LMS400)	**Light-weight** (Less than 500 grams)
Battery Powered?	Could be (Requires large battery)	**Yes** (can run for up to 5 hours on 7.4V 2Ah LiPo battery)
Scan time (for 1x1 m^2)	**~ 5 seconds**	~ 16 minutes
File Size (for 1x1 m^2)	~10 Mbytes	**~ 300 Kbytes**
Point cloud density (for 1x1 m^2)	**~ 2.4 Million points**	~ 40,000 points
Post-processing computational complexity	Highly complex (due to dense point cloud)	**Relatively simple**
Do-it-yourself (DIY)?	No (Sound technical knowledge is required to acquire data)	**Yes** (The system can be bilt by anyone with little technical knowledge)
Other external equipment?	Yes (an external computer is required to acquire the data)	**No** (the system itself has a mini-computer in the design)

Table 6-11 shows the comparison of the developed LiDARPheno system with the LMS400-based 3D scanning system. The first and most important parameter in comparison is the cost of the system. The cost to build LiDARPheno is almost 96% less than the LMS400 device itself. Moreover, the LMS400-based system requires external setup to acquire the 3D point cloud data, while LiDARPheno is an independent system. The LiDARPheno system is much more lightweight than the LMS400-based setup for data acquisition. The power requirement for LMS400 is 25 Watts compared to about 3 watts for LiDARPheno, and hence the small rechargeable LiPo battery can power the LiDARPheno system. LiDARPheno, due to its low-resolution, acquires relatively fewer points and hence, has small file-size. Consequently, the post-processing of the LiDARPheno data is faster compared to the LMS400-based system. The LiDARPheno is designed so that anyone with a little or no technical knowledge can build it using the widely available off-the-shelf components used in the system.

On the other hand, even though LiDARPheno has many benefits, the LiDARPheno is a slow system due to use of two servo motors and the LiDAR sensor used itself. Hence, the LiDARPheno may take up to 16 minutes for the scan of 1 m^2 area, while the LMS400-based system can scan the same area in about 5 seconds. Moreover, the density of the acquired point cloud using LiDARPheno does not permit the analysis of the smaller areas of the object. Also, availability of the reflectance information from the LMS400 device can be used in many cases which are not provided by the LiDARPheno.

Overall, the LiDARPheno system is an excellent combination of cost-feature trade-off. With just a fraction of the cost for a commercial LiDAR-based scanning system, the LiDARPheno enables to monitor some of the critical characteristics of the plants while losing some details. The combination of multiple LiDARPheno systems might prove beneficial and may surpass the results of the commercial LiDAR-based systems.

Chapter 7
Conclusion and Recommendations for the Future Work

7.1 Conclusion

Increasing world population is raising concerns regarding the global food security including producing enough good quality food to feed the ever-rising population. Improving the current farming practices is the key to meeting the demand for the quality food. The improvement process involves increasing the ability of crop plants to produce more food produces and creating new crops with higher resistance to the environmental changes and diseases. The improved gene modification and sequencing technologies have provided opportunities to change the genetic information to make crops more resistive to the disease and environmental stress. However, the advances in phenotyping technologies are a bottleneck in the fast-paced development of the new and modified crops. The available technologies are expensive, inaccessible and need significant improvements.

In this thesis, the new low-cost, accessible LiDAR-based technology is developed. A miniature version of the "LiDARPheno" is designed and developed with low-cost, off-the-shelf components and modules. A detailed design keeping in mind the low-cost, portability, remote accessibility, and low power consumption is described in detail. Moreover, the design included the use of the wireless communication for the actual remote operation of the device with the feasibility of deploying the device in the greenhouse as well as field environment. Use of the existing libraries and APIs provide the feasibility for non-technical users to build and operate a system.

The experimental setup consisting the commercial LiDAR was presented, and a low-cost ground-truth leaf area acquisition method was thought and developed. Moreover, naming convention suggestions were made to maintain the consistency of identifying the data including time, data and type of the data. A method of conversion from raw LiDAR data to the Cartesian coordinates to generate a point cloud was discussed. Simple algorithms for cleaning and segmenting the point clouds were developed and presented. The simple operation of the algorithms

helps the user in developing the software for analysis. The high correlation between the estimates of leaf traits with commercial LiDAR and the developed LiDARPheno system was achieved. Moreover, the estimation of the leaf traits using the developed methods shows considerable accuracy. Performance analysis for the developed system and methodologies were carried out in this work to provide the utility of the low-cost system in plant phenotyping tasks.

The main contribution of this thesis work is in the arrangement of the hardware components to develop a 3D scanning system capable of extracting plant traits. The use of consumer grade LiDAR Lite v3 to develop a system should be seen as the low-cost approach to extraction of phenotypic traits. Moreover, this work contributes to a relatively simple LiDAR data analysis and provides a base for development of the more complex (with added constraints) algorithms for achieving higher accuracies and may be utilizing the developed device in the controlled environment. The section 7.2 will provide insights into recommended future exploration and challenges needed to be handled while utilizing the developed system in the field.

Finally, this work shows the utility of low-cost LiDAR device in the plant phenotyping tasks. The leaf length, width, and area were estimated using the developed methods for the traits characterization. Research objectives for this master's thesis were met by designing, developing and testing the LiDARPheno system for the in-laboratory experiment. This work also compared the performance of the developed system with commonly used LiDAR sensor for phenotyping. The developed prototype shows the utility and advantages of the low-cost devices in the plant phenotyping research. Devices developed with the aim of the low-cost system can help fill the gap of the plant phenotyping research and provide opportunities for the researchers in the field to explore the possibilities to 3D imaging and may lead to findings that are entirely novel.

7.2 Recommendations for the Future Work

Despite having many benefits, the developed system and methodologies have considerable opportunities to explore the possibilities and improving the methods. Some of the suggestions for the exploration are given below:

- For the hardware part of the system, with the proven methodologies in this thesis, an effort can be put into exploring other low-cost, high-speed LiDAR sensors to meet the demand of high-throughput.

- Alternate arrangements for the scanning setup, other than mentioned in this work, can be explored. For example, use of high-speed servo motors, use of rotating mirror with high-speed DC motor or use of the moving setup as was used in the LMS400 setup.
- Exploring the potential sources of errors, whether the sensor itself has a significant error or the algorithms and correcting the data accordingly.
- The segmentation algorithm used here is a modified region-grow algorithm and in 3D graphics or gaming graphics field might have many better algorithms for processing the point cloud. However, the field of computer graphics is a vast field, and extensive review and experimentation might be required to explore the possibilities of the low-cost device fully.
- The algorithms developed for data analysis are the simplest possible workflow of the LiDAR data analysis and does not consider all the possible corner cases. The algorithms are the simple base idea of how the data can be processed. By adding more constraints and optimizations, it might provide better processing speed as well as accuracy.
- Experiments with a different view angle and combining the data to generate a fully 3-dimensional model of the objects may prove to be the better approach for exploring different phenotypic information extraction.
- Exploration and extraction of other phenotypic information such as biomass estimation using the point cloud data, leaf angle, plant angle with respect to ground, or leaf length, width, or area's relationship to photosynthetic rate as well as biomass. However, the experiments to explore the potential match for biomass and photosynthetic rate estimations will need extensive collaboration with plant scientists and breeders.

7.2.1 Limitations and improvement suggestions:

This thesis work might provide satisfactory performance while the plants are in early growth stage. However, it will be interesting to see the performance in the challenging field conditions. The potential challenges for in-field application could be:

- Blowing wind may create movements in the plant, consequently making the scanning difficult. Hence, exploring the effects and mitigating the error caused by that may be of interest.
- Overlapping leaves might not be captured just by taking a scan from the top. Hence, scans from multiple view angle may be required to construct a full 3D model of the plant and extract traits from that model.
- Canopy size and lodging in canola may create difficulties in segmentation and leaf identification. So, individual plant identification methods and then leaf segmentation might be an area to explore for mitigating these challenges.
- The scanning speed is relatively large in terms of time it take and might not be acceptable in field environment conditions if there is plant movement due to wind. However, sunlight does not affect the performance of the LiDARPheno system and it has been simulated in the lab using 3 halogen lights giving about 3000 lx intensity. Hence, improvements in scanning speed might overcome the problem and may make the LiDARPheno usable in the field.

With the above-mentioned suggestions, there may be the higher potential of exploring the phenotypic information as well as establishing new phenotypes with the use of 3D models. Consequently, the technological advancements in phenotyping will help in meeting the tomorrow's food demand.

References

[1] H. C. J. Godfray *et al.*, “Food Security: The Challenge of Feeding 9 Billion People,” *Science (80-.).*, vol. 327, no. 5967, pp. 812–818, Feb. 2010.

[2] Food and Agriculture Organization of the United Nations, “The future of food and agriculture: Trends and challenges,” 2017.

[3] D. Tilman, C. Balzer, J. Hill, and B. L. Befort, “Global food demand and the sustainable intensification of agriculture,” *Proc. Natl. Acad. Sci.*, vol. 108, no. 50, pp. 20260–20264, Dec. 2011.

[4] N. J. Baltes, J. Gil-Humanes, and D. F. Voytas, “Genome Engineering and Agriculture: Opportunities and Challenges,” in *Progress in Molecular Biology and Translational Science*, vol. 149, Academic Press, 2017, pp. 1–26.

[5] I. Herskowitz, *Principles of Genetics*. New York: Macmillan, 1973.

[6] M. Yano and R. Tuberosa, “Genome studies and molecular genetics—from sequence to crops: genomics comes of age,” *Curr. Opin. Plant Biol.*, vol. 12, no. 2, pp. 103–106, Apr. 2009.

[7] F. Fiorani and U. Schurr, “Future Scenarios for Plant Phenotyping,” *Annu. Rev. Plant Biol.*, vol. 64, no. 1, pp. 267–291, Apr. 2013.

[8] K. Schneeberger and D. Weigel, “Fast-forward genetics enabled by new sequencing technologies,” *Trends Plant Sci.*, vol. 16, no. 5, pp. 282–288, May 2011.

[9] A. Walter, F. Liebisch, and A. Hund, “Plant phenotyping: from bean weighing to image analysis,” *Plant Methods*, vol. 11, no. 1, p. 14, Mar. 2015.

[10] “Plant Phenotyping and Imaging Research Centre - U of S Plant Phenotyping and Imaging Research Centre - University of Saskatchewan.” [Online]. Available: https://p2irc.usask.ca/. [Accessed: 07-Jul-2018].

[11] “IPPN Home.” [Online]. Available: https://www.plant-phenotyping.org/. [Accessed: 07-Jul-2018].

[12] “Australian Plant Phenomics Facility. Plant phenotyping tools and research.” [Online]. Available: https://www.plantphenomics.org.au/. [Accessed: 07-Jul-2018].

[13] “North American Plant Phenotyping Network.” [Online]. Available: http://nappn.plant-phenotyping.org/. [Accessed: 07-Jul-2018].

[14] N. Fahlgren, M. A. Gehan, and I. Baxter, “Lights, camera, action: high-throughput plant phenotyping is ready for a close-up,” *Curr. Opin. Plant Biol.*, vol. 24, pp. 93–99, Apr. 2015.

[15] R. T. Furbank and M. Tester, “Phenomics – technologies to relieve the phenotyping bottleneck,” *Trends Plant Sci.*, vol. 16, no. 12, pp. 635–644, Dec. 2011.

[16] L. Li, Q. Zhang, and D. Huang, “A Review of Imaging Techniques for Plant Phenotyping,” *Sensors*, vol. 14, no. 11, pp. 20078–20111, Oct. 2014.

[17] W. H. Stuppy, J. A. Maisano, M. W. Colbert, P. J. Rudall, and T. B. Rowe, “Three-dimensional analysis of plant structure using high-resolution X-ray computed tomography,” *Trends Plant Sci.*, vol. 8, no. 1, pp. 2–6, Jan. 2003.

[18] H. Van As and J. van Duynhoven, “MRI of plants and foods,” *J. Magn. Reson.*, vol. 229, pp. 25–34, Apr. 2013.

[19] P. B. Reich, D. S. Ellsworth, and M. B. Walters, “Leaf structure (specific leaf area) modulates photosynthesis-nitrogen relations: evidence from within and across species and functional groups,” *Funct. Ecol.*, vol. 12, no. 6, pp. 948–958, Dec. 1998.

[20] W. Johannsen, “The Genotype Conception of Heredity,” *Am. Nat.*, vol. 45, no. 531, pp. 129–159, Mar. 1911.

[21] B. Govaerts and N. Verhulst, *The normalized difference vegetation index (NDVI) Greenseeker(TM) handheld sensor : toward the integrated evaluation of crop management part A : concepts and case studies*. Mexico: CIMMYT, 2010.

[22] L. Winterhalter, B. Mistele, and U. Schmidhalter, “Evaluation of active and passive sensor systems in the field to phenotype maize hybrids with high-throughput,” *F. Crop. Res.*, vol. 154, pp. 236–245, Dec. 2013.

[23] O. S. Walsh, A. R. Klatt, J. B. Solie, C. B. Godsey, and W. R. Raun, “Use of soil moisture data for refined GreenSeeker sensor based nitrogen recommendations in winter wheat (Triticum aestivum L.),” *Precis. Agric.*, vol. 14, no. 3, pp. 343–356, Jun. 2013.

[24] T. Truong, A. Dinh, and K. Wahid, “An IoT environmental data collection system for fungal detection in crop fields,” in *2017 IEEE 30th Canadian Conference on Electrical and Computer Engineering (CCECE)*, 2017, pp. 1–4.

[25] H. Scharr *et al.*, “Leaf segmentation in plant phenotyping: a collation study,” *Mach. Vis. Appl.*, vol. 27, no. 4, pp. 585–606, May 2016.

[26] J. M. Pape and C. Klukas, “3-d histogram-based segmentation and leaf detection for rosette

plants," in *Lecture Notes in Computer Science (including subseries Lecture Notes in Artificial Intelligence and Lecture Notes in Bioinformatics)*, 2015, vol. 8928, pp. 61–74.

[27] M. R. Golzarian *et al.*, "Accurate inference of shoot biomass from high-throughput images of cereal plants," *Plant Methods*, vol. 7, no. 1, p. 2, Feb. 2011.

[28] S. Arvidsson, P. Pérez-Rodríguez, and B. Mueller-Roeber, "A growth phenotyping pipeline for Arabidopsis thaliana integrating image analysis and rosette area modeling for robust quantification of genotype effects," *New Phytol.*, vol. 191, no. 3, pp. 895–907, Aug. 2011.

[29] V. Hoyos-Villegas, J. H. Houx, S. K. Singh, and F. B. Fritschi, "Ground-Based Digital Imaging as a Tool to Assess Soybean Growth and Yield," *Crop Sci.*, vol. 54, no. 4, p. 1756, 2014.

[30] R. T. Clark *et al.*, "Three-Dimensional Root Phenotyping with a Novel Imaging and Software Platform," *PLANT Physiol.*, vol. 156, no. 2, pp. 455–465, Jun. 2011.

[31] A. S. Iyer-Pascuzzi *et al.*, "Imaging and Analysis Platform for Automatic Phenotyping and Trait Ranking of Plant Root Systems," *PLANT Physiol.*, vol. 152, no. 3, pp. 1148–1157, Mar. 2010.

[32] M. Minervini, M. V. Giuffrida, P. Perata, and S. A. Tsaftaris, "Phenotiki: an open software and hardware platform for affordable and easy image-based phenotyping of rosette-shaped plants," *Plant J.*, vol. 90, no. 1, pp. 204–216, Apr. 2017.

[33] A. Hartmann, T. Czauderna, R. Hoffmann, N. Stein, and F. Schreiber, "HTPheno: An image analysis pipeline for high-throughput plant phenotyping," *BMC Bioinformatics*, vol. 12, no. 1, p. 148, May 2011.

[34] S. Aich and I. Stavness, "Leaf Counting with Deep Convolutional and Deconvolutional Networks," Aug. 2017.

[35] S. Aich *et al.*, "DeepWheat: Estimating Phenotypic Traits from Crop Images with Deep Learning," in *2018 IEEE Winter Conference on Applications of Computer Vision (WACV)*, 2018, pp. 323–332.

[36] J. Ubbens, M. Cieslak, P. Prusinkiewicz, and I. Stavness, "The use of plant models in deep learning: an application to leaf counting in rosette plants," *Plant Methods*, vol. 14, no. 1, p. 6, Dec. 2018.

[37] H. G. Jones, R. Serraj, B. R. Loveys, L. Xiong, A. Wheaton, and A. H. Price, "Thermal infrared imaging of crop canopies for the remote diagnosis and quantification of plant

responses to water stress in the field," *Funct. Plant Biol.*, vol. 36, no. 11, p. 978, Nov. 2009.

[38] R. Munns, R. A. James, X. R. R. Sirault, R. T. Furbank, and H. G. Jones, "New phenotyping methods for screening wheat and barley for beneficial responses to water deficit," *J. Exp. Bot.*, vol. 61, no. 13, pp. 3499–3507, Aug. 2010.

[39] S. Zia *et al.*, "Infrared Thermal Imaging as a Rapid Tool for Identifying Water-Stress Tolerant Maize Genotypes of Different Phenology," *J. Agron. Crop Sci.*, vol. 199, no. 2, pp. 75–84, Apr. 2013.

[40] E. B. Knipling, "Physical and physiological basis for the reflectance of visible and near-infrared radiation from vegetation," *Remote Sens. Environ.*, vol. 1, no. 3, pp. 155–159, Jun. 1970.

[41] M. R. Schlemmer, D. D. Francis, J. F. Shanahan, and J. S. Schepers, "Remotely Measuring Chlorophyll Content in Corn Leaves with Differing Nitrogen Levels and Relative Water Content," *Agron. J.*, vol. 97, no. 1, p. 106, 2005.

[42] F. Remondino, L. Barazzetti, F. Nex, M. Scaioni, and D. Sarazzi, "UAV PHOTOGRAMMETRY FOR MAPPING AND 3D MODELING – CURRENT STATUS AND FUTURE PERSPECTIVES," *ISPRS - Int. Arch. Photogramm. Remote Sens. Spat. Inf. Sci.*, vol. XXXVIII-1/, no. C22, pp. 25–31, 2012.

[43] M. P. Pound, A. P. French, E. H. Murchie, and T. P. Pridmore, "Automated Recovery of Three-Dimensional Models of Plant Shoots from Multiple Color Images," *PLANT Physiol.*, vol. 166, no. 4, pp. 1688–1698, Dec. 2014.

[44] R. P. de M. Frasson and W. F. Krajewski, "Three-dimensional digital model of a maize plant," *Agric. For. Meteorol.*, vol. 150, no. 3, pp. 478–488, Mar. 2010.

[45] W. Kazmi, S. Foix, G. Alenyà, and H. J. Andersen, "Indoor and outdoor depth imaging of leaves with time-of-flight and stereo vision sensors: Analysis and comparison," *ISPRS J. Photogramm. Remote Sens.*, vol. 88, pp. 128–146, Feb. 2014.

[46] Y. Song, C. A. Glasbey, G. W. A. M. van der Heijden, G. Polder, and J. A. Dieleman, "Combining Stereo and Time-of-Flight Images with Application to Automatic Plant Phenotyping," Springer, Berlin, Heidelberg, 2011, pp. 467–478.

[47] J. Li and L. Tang, "Developing a low-cost 3D plant morphological traits characterization system," *Comput. Electron. Agric.*, vol. 143, pp. 1–13, Dec. 2017.

[48] National Oceanic and Atmospheric Administration, "What is LIDAR," *National Ocean*

Service website, 2014. [Online]. Available: https://oceanservice.noaa.gov/facts/lidar.html. [Accessed: 11-Jul-2018].

[49] J. R. Rosell *et al.*, "Obtaining the three-dimensional structure of tree orchards from remote 2D terrestrial LIDAR scanning," *Agric. For. Meteorol.*, vol. 149, no. 9, pp. 1505–1515, Sep. 2009.

[50] M. Bietresato, G. Carabin, R. Vidoni, A. Gasparetto, and F. Mazzetto, "Evaluation of a LiDAR-based 3D-stereoscopic vision system for crop-monitoring applications," *Comput. Electron. Agric.*, vol. 124, pp. 1–13, Jun. 2016.

[51] S. Sun, C. Li, and A. Paterson, "In-Field High-Throughput Phenotyping of Cotton Plant Height Using LiDAR," *Remote Sens.*, vol. 9, no. 4, p. 377, Apr. 2017.

[52] D. Deery, J. Jimenez-Berni, H. Jones, X. Sirault, and R. Furbank, "Proximal Remote Sensing Buggies and Potential Applications for Field-Based Phenotyping," *Agronomy*, vol. 4, no. 3, pp. 349–379, Jul. 2014.

[53] N. Tilly *et al.*, "EVALUATION OF TERRESTRIAL LASER SCANNING FOR RICE GROWTH MONITORING," *ISPRS - Int. Arch. Photogramm. Remote Sens. Spat. Inf. Sci.*, vol. XXXIX-B7, pp. 351–356, Aug. 2012.

[54] K. Omasa, F. Hosoi, and A. Konishi, "3D lidar imaging for detecting and understanding plant responses and canopy structure," *J. Exp. Bot.*, vol. 58, no. 4, pp. 881–898, Nov. 2006.

[55] F. Hosoi and K. Omasa, "Estimating vertical plant area density profile and growth parameters of a wheat canopy at different growth stages using three-dimensional portable lidar imaging," *ISPRS J. Photogramm. Remote Sens.*, vol. 64, no. 2, pp. 151–158, Mar. 2009.

[56] J. A. Jimenez-Berni *et al.*, "High Throughput Determination of Plant Height, Ground Cover, and Above-Ground Biomass in Wheat with LiDAR," *Front. Plant Sci.*, vol. 9, p. 237, Feb. 2018.

[57] M. Herrero-Huerta, R. Lindenbergh, and W. Gard, "Leaf Movements of Indoor Plants Monitored by Terrestrial LiDAR," *Front. Plant Sci.*, vol. 9, p. 189, Feb. 2018.

[58] S. Sun *et al.*, "In-field High Throughput Phenotyping and Cotton Plant Growth Analysis Using LiDAR," *Front. Plant Sci.*, vol. 9, p. 16, Jan. 2018.

[59] Australian Plant Phenomics Facility, "Phenotyping Technology." [Online]. Available: https://www.plantphenomics.org.au/technology/#tab-bb6f781109c0bda571f. [Accessed:

14-Jul-2018].

[60] “Field Phenotyping Systems | LemnaTec.” [Online]. Available: https://www.lemnatec.com/products/field-phenotyping/. [Accessed: 14-Jul-2018].

[61] “The Digital Phenotype - KeyGene.” [Online]. Available: https://www.keygene.com/technology/2-the-digital-phenotype/. [Accessed: 14-Jul-2018].

[62] Phenospex, “PlantEye F500 - Multispectral 3D laser scanner for plant phenotyping,” 2017. [Online]. Available: https://phenospex.com/products/plant-phenotyping/science-planteye-3d-laser-scanner/planteye-f500-multispectral-3d-laser-scanner/. [Accessed: 14-Jul-2018].

[63] G. J. Rebetzke, J. Jimenez-Berni, R. A. Fischer, D. M. Deery, and D. J. Smith, “Review: High-throughput phenotyping to enhance the use of crop genetic resources,” *Plant Sci.*, Jun. 2018.

[64] Garmin Ltd., “Lidar Lite v3 Operation Manual and Technical Specifications Laser Safety.” Garmin Ltd., p. 14, 2016.

[65] HITEC RCD USA, “HS-85BB Premium Micro Servo | HITEC RCD USA.” [Online]. Available: http://hitecrcd.com/products/servos/micro-and-mini-servos/analog-micro-and-mini-servos/hs-85bb-premium-micro-servo/product. [Accessed: 04-Jul-2018].

[66] Arduino, “Arduino - Home,” 2018. [Online]. Available: https://www.arduino.cc/.

[67] Garmin International, “LIDARLite_Arduino_Library,” *GitHub repository*. GitHub.

[68] RASPBERRY PI FOUNDATION, “Raspberry Pi 3 Model B.” [Online]. Available: https://www.raspberrypi.org/products/raspberry-pi-3-model-b/.

[69] Omnivision, “OV5647 datasheet,” 2009.

[70] RobotShop, “Step-down DC-DC Power Converter 25W - RobotShop.” [Online]. Available: https://www.robotshop.com/ca/en/step-down-dc-dc-power-converter-25w.html. [Accessed: 14-Jul-2018].

[71] RobotShop Inc., “7.4V, 2000mAh, 5C LiPo Battery.” [Online]. Available: https://www.robotshop.com/ca/en/74v-2000mah-5c-lipo-battery.html.

[72] Arduino, “Arduino - Libraries.” [Online]. Available: https://www.arduino.cc/en/Reference/Libraries.

[73] Python Software Foundation, “Python™.” [Online]. Available: https://www.python.org/.

[74] A. Fabrizi, “Dropbox Uploader,” *GitHub repository*. GitHub, 2016.

[75] A. Chatzinikos, T. A. Gemtos, and S. Fountas, “The use of a laser scanner for measuring

crop properties in three different crops in Central Greece," in *Precision agriculture '13*, 2013, pp. 129–136.

[76] J. Digne and C. de Franchis, "The Bilateral Filter for Point Clouds," *Image Process. Line*, vol. 7, pp. 278–287, Oct. 2017.

[77] B. Delaunay, "Sur la sphere vide," *Bull. l'Académie des Sci. l'URSS*, 1934.